DOCTOR OF PHILOSOPHY

Molecular and transcriptional characterisation of Phytophthora capsici – host interactions

Jupe, Julietta

Award date:
2014

DOCTOR OF PHILOSOPHY

Molecular and transcriptional characterisation of Phytophthora capsici – host interactions

Julietta Jupe

2014

University of Dundee

Molecular and transcriptional characterisation of *Phytophthora capsici* – host interactions

Julietta Jupe, Dipl. Ing. (FH)

Doctor of Philosophy

The University of Dundee

College of Life Sciences

Division of Plant Sciences

January 2014

Declaration

The following presented results in this PhD thesis are conducted by myself. All work other than my own is clearly stated by adequate references and publications. I hereby declare that I am the author of this thesis and that the work has not been previously accepted for any higher degree.

Julietta Jupe

I do certify that Julietta Jupe has fulfilled all conditions of the relevant Ordinance and Regulations of the University and is qualified to submit this thesis for the degree of Doctor of Philosophy.

Dr Edgar Huitema
College of Life Sciences
University of Dundee

Abstract

Pathogen-host interactions feature a dynamic interplay between defence signalling cascades and specialized pathogen machineries that can subvert immunity. Plant pathogens secrete effector molecules that enable parasitic infection and reproduction and thus determine the success of the interaction with the host. The *Phytophthora* species *P. capsici,* a hemi-biotrophic oomycete*,* affects a wide range of members of important crop families such as cucurbits and solanaceae worldwide. Despite the presence of diverse effector repertoires, *P. capsici* shares a number of RXLR proteins with other *Phytophthora* species in this genus. To better understand the interaction between *Phytophthora* and its hosts on the molecular level, the infection process of *P. capsici* was explored on four plant species and compared to phenotypic observations. A model infection system was established to characterise the hemi-biotrophic life-style using a set of three marker genes that determine the three steps during the *P. capsici* life cycle: biotrophy, necrotrophy and sporulation. Using a unique microarray approach that combined pathogen and tomato genomes on one array, important insights were gained into the transcriptional changes during disease development. While a large number of *P. capsici* genes were differentially regulated during the biotrophic phase, a number of genes including some RXLR effectors were found to be upregulated only during the necrotrophic phase. Analysis of tomato gene expression identified two distinct transcriptional responses to *P. capsici* infection.

It is hypothesised that conserved effectors play important roles in virulence and form attractive targets to disable pathogenesis. The *P. capsici* effector *Pc03192* was identified as the putative ortholog to the well studied *P. infestans Pi03192* that is known to interact with two potato NAC transcription factors. For *Pc03192* and the orthologous tomato NACs *SlNAC1* and *SlNAC2*, a yeast-two-hybrid screen could confirm weak protein interaction, and confocal microscopy provided evidence for a co-localisation of the putative interactors to the endoplasmatic reticulum.

Results gained in this Thesis open the door towards comparative transcriptomics that should help unravel pathogen infection strategies and exploit host basal defence responses, as well as enable future studies into conserved *Phytophthora* effector proteins.

Table of Contents

List of Figures

List of Tables

Digital Files

File 1
List of expressed *P. capsici* genes specific to *N. benthamiana* or pepper
Gene lists extracted from the Venn diagram with ontology analyses as shown in Figure 2.9

File 2
***P. capsici* genes encoding putative secreted proteins found expressed in microarray experiments**
Gene identifiers and SignalP HMM probabilities are given for all genes expressed during infectious stages as well as an overview with genes sorted per time point that they are expressed.

File 3
***PcHmp1*, *PcNPP1* and *PcCdc14* co-regulated genes**
Overview of genes found to be co-regulated with marker genes in *P. capsici*. Gene identifiers and normalized expression values are given.

File 4
Significantly enriched ontologies coregulated with marker genes
Overview of gene ontologies that are significantly enriched in the fractions that are specifically co-regulated with *P. capsici* marker genes as shown in Figure 3.3 C. GO terms, p-values and False Discovery Rates (FDR) are given as well as query and reference sample sizes.

File 5
***P. capsici* candidate RXLR genes expressed in microarray experiments**
Overview of RxLR effector genes found to be upregulated during specific life cycle stages in *P. capsici*. Gene identifiers and normalized expression values are given.

File 6
Annotation and expression of tomato genes differentially expressed in pairwise comparisons
Overview of genes found to be differentially expressed between timepoints during *P. capsici* infection. Gene identifiers, normalized expression values and GO annotations are given.

File 7
Tomato genes differentially expressed in each pairwise comparison
Overview of genes found to be differentially expressed during *P. capsici* infection in pairwise comparisons between two timepoints. Gene identifiers and normalized expression values are given.

File 8
Genes corresponding to enriched GOs in pairwise comparisons
Overview of gene ontologies that are significantly enriched in the fractions that are specifically up or down regulated between two time points as shown in Figure 3.6. GOs, p-value and FDR as well as query and reference sample sizes are given.

File 9
Tomato genes with possible roles in PAMP perception and signaling, differentially expressed during *P. capsici* infection
Overview of candidate PAMP signaling and transcription factor genes found to be differentially expressed during *P. capsici* infection. Gene identifiers, normalized expression values and annotations are given. Genes are grouped based on their expression patterns as shown in Figure 3.7 and 3.8 respectively.

File 10
Putative RxLR effectors used in this study
Overview of putative RxLR effectors. Gene names, probe ID and sequences are given for each gene.

Publications Arising From This Work

Lamour, K.H., Stam, R., **Jupe, J.**, and Huitema, E. (2011). The oomycete broad-host-range pathogen *Phytophthora capsici*. Molecular Plant Pathology 13, 329-337.

Stam, R., **Jupe, J.**, Howden, A.J.M., Morris, J.A., Boevink, P.C., Hedley, P.E., and Huitema, E. (2013). Identification and characterisation CRN effectors in *Phytophthora capsici* shows modularity and functional diversity. PLoS ONE 8, e59517.

Jupe, J., Stam,R., Howden,J.A.M., Morris,J.A., Zhang,R., Hedley, P.E. and Huitema,E. (2013). *Phytophthora capsici*-tomato interaction features dramatic shifts in gene expression associated with a hemi-biotrophic lifestyle. Genome Biology 14.

Abbreviations

At	*Arabidopsis thaliana*
AVR	Avirulence
BLAST	Basic Local Alignment Search Tool
cDNA	Complementary DNA
CRN	Crinkler
DNA	Deoxyribonucleic Acid
ER	Endoplasmatic Reticulum
EST	Expressed Sequence Tag
ETI	Effector Triggered Immunity
ETS	Effector Triggered Susceptibility
Flg22	22 amino acid section of bacterial flagellin with PAMP activity
GC	Germinating Cysts
gDNA	Genomic DNA
GFP	Green Fluorescent Protein
HMP1	Haustorium-specific Membrane Protein 1
Hp	*Hyaloperonospora parasitica*
HR	Hypersensitive Response
INF1	Elicitin Infestin 1
ITS	Internal Transcribed Spacer
MAMPs	Microbe Associated Molecular Patterns
Mbp	Million Base Pair
MYC	Mycelia
Nb	*Nicotiana benthamiana*
NLP	Nep 1-like Proteins
NPP1	Necrosis-inducing *Phytophthora* Protein 1
OD	Optical Density
PAMPs	Pathogen Associated Molecular Patterns
PCD	Programmed Cell Death
PCR	Polymerase Chain Reaction
Pc	*Phytophthora capsici*
Pi	*Phytophthora infestans*
Pme	Pectin Methylesterase
PRRs	Pattern Recognition Receptors
PTI	PAMP-Triggered Immunity
R	Resistance
RNA	Ribonucleic Acid
Sl	*Solanum lycopersicum*
Sp	*Saprolegnia parasitica*
Spor	Sporangia/Zoospores samples
TF	Transcription Factor
T3SS	Type-III Secretion System
Y2H	Yeast-Two Hybrid assay

Acknowledgements

I would like to thank Dr Edgar Huitema, Prof John Brown, Prof Paul Birch and the division of Plant Sciences for arranging this PhD project and to the BBSRC for providing the financial support. Special thanks go to my supervisor Dr Edgar Huitema and my committee members Prof Paul Birch, Prof Andy Flavell, Dr Gordon Simpson and Dr Steve Hubbard for supporting and advising me throughout my whole PhD time.

A big Thank you to Prof Paul Birch and his group for all the resources I could use and providing support for my PhD project. Special Thanks go to Pete Hedley and Jenny Morris for the major help with the microarrays and the great collaboration, as well as to Petra Boevink, Alison Roberts, Kath Wright and Sean Chapman for good help with the confocal microscopy.
Thank you to all my other colleagues who have been involved directly in the work presented in this thesis and also to all colleagues from the University of Dundee and the James Hutton Institute, who always had some good advice for me and kept me smiling along the way. Special Thanks to Dr Andrew Howden, for being such a great lab mate, for all the fun but also for the good guidance and proof-reading this thesis and other manuscripts. And thanks for your help at work especially during my time of pregnancy. I couldn't have a better colleague and friend.

I would like to thank of course my family for the good support during all the years being in Scotland, and my dad for the design of figures, posters and presentations. Thanks for all the advice in good and in bad times.

Last but not least my very special Thanks go to my husband, Florian, for being there for me at all times and giving me enough motivation to keep going. Thanks for proof-reading this thesis and the refreshing and mind refocusing discussions.

Thanks also to my little daughter, who gave me a lot of joy and happiness during my last PhD year and all the writing.

1 Introduction

Plants are sessile organisms that are constantly threatened by pests and pathogens that are soil-borne, water- or wind-dispersed or mechanically transmitted. The use of mono-culture crop production systems in fields or under glass has further increased disease pressure on plants and causes major problems in modern agriculture. The farmer is able to control most diseases to a certain degree using chemical agents, however wild plants have had to defend themselves since millions of years. The fact that plants are not constantly sick proves that they must have evolved some kind of an immune system. Only the advances in molecular biology and genetics over the last decades have enabled a deeper insight into the strategies of plants and pathogens, and how they cause disease or counter the attack. The studies of these host-microbe interactions have shown that, in contrast to mammals, plants lack an adaptive immune system and hence mobile defender cells, but they have evolved over time a multi-layered defence system against pathogens and pests. This thesis aims to shed some light onto the molecular interactions between the devastating pathogen *Phytophthora capsici* and a variety of host plant species.

1.1 Molecular plant-pathogen interactions

Plants are continually bombarded by microbes, many of which form serious disease threats. To fend off potential pathogens, plants feature robust preformed barriers and chemical defences to infection as well as an inducible immune system. Given that plants form a wide range of associations with microbes that are either symbionts, commensals or parasites, suggests that host-microbe interactions feature dynamic processes that are driven by signalling interplay. Indeed, studies on genetic, molecular and biochemical aspects of both plant immunity and pathogen biology have unveiled a wide range of processes that underpin plant-microbe associations. Collectively, these studies have led to a number of important conceptual advances that have helped us understand the basis of disease and resistance to pests and pathogens.

Plants are exposed to an array of abiotic as well as biotic stresses and rely on diverse mechanisms of an innate immunity, which reveals a basal preformed layer of defence, including waxy cuticles and strong cell walls that prevent penetration of pathogens [1-3].

Plant physiology and morphology form a physical barrier against most of these stress conditions, however, some pests and pathogens have developed specialized strategies to interplay with host defence mechanisms in order to disarm immunity [1, 4].

1.1.1 Pathogen-associated molecular pattern (PAMP)-triggered immunity (PTI)

Plants are sources of nutrients and water, and are therefore challenged as hosts to many diverse microbes. Innate immunity to most microbes is achieved by deployment of surface exposed Pattern Recognition Receptors (PRRs) that detect the presence of a given microbial threat [5, 6]. These PRRs recognize Microbe or Pathogen-Associated Molecular Patterns (MAMPs or PAMPs) and are able to initiate an effective first layer of active defence responses, termed PAMP-triggered immunity (PTI). This early response against a broad range of potential pathogens [2, 4, 7, 8] is ensured by the presence of highly conserved microbial components that play fundamental biological roles in these organisms, but are absent in the host. Classical examples of MAMPs or PAMPs are bacterial flagellin, elongation factor TU, lipopolysaccharides, fungal chitin or oomycete β-glucans [4, 9-11]. In this first layer of defence, PRRs activate, amongst others, protein kinase cascades, the production of reactive oxygen species or chitinases, or pathogenesis related defence genes that are often regulated by transcription factors [12], ultimately leading to immunity of the plant. The first evidence, and most studied example for PRR-mediated PTI, was shown for a 22 amino acid-long, conserved domain of bacterial flagellin, termed flg22, that is recognised by the receptor like kinase FLS2 in *Arabidopsis* [13]. Upon interaction of flg22 with the PRR FLS2, internalization of the receptor occurs via endocytosis [14]. *Arabidopsis* mutants that lack FLS2 showed an increased susceptibility to virulent bacteria [15, 16]. Another well studied PAMP is the abundantly secreted *Phytophthora infestans* elicitin Infestin 1 (INF1). The recognition of INF1 results in a localised plant cell death (hypersensitive response (HR)) in e.g. *Nicotiana benthamiana* and prevents the pathogen from growth by diminishing the nutritional supply [9, 17-19]. An HR is therefore thought to be a very effective response against obligate biotrophs or hemi-biotrophic pathogens that depend on living host tissue to reproduce.

1.1.2 Effector-triggered susceptibility (ETS)

The adapted pathogen is able to interfere with PTI responses by secreting an arsenal of proteins, so called effector molecules, into the host where they either accumulate in the apoplast (extracellular effectors) or travel across the cell membrane into the cytoplasm (intracellular effectors). The cytoplasmic effectors modify, for example, cellular targets to suppress PTI and enable parasitic infection, access to nutrients, growth and reproduction [2, 20, 18]. While most bacteria secrete their effectors through a Type-III secretion system (TTSS) into the cell [22], aphids and nematodes deliver the effectors with their saliva through stylets [23, 24]. These effector proteins are thus key features of the pathogen and might have arisen during co-evolution of the pathogen with its host(s) [9]. Effectors interfere with the signalling pathways and processes that lead to PTI after PAMP recognition. When this interference is successful, the susceptibility of the plant is restored and this state is known as Effector-Triggered Susceptibility (ETS). One large class of effector molecules known from oomycete pathogens share a conserved motif near the N-terminus, known as the RXLR (arginine, any amino-acid, leucine, arginine) motif [25], which was shown to be required for effector translocation inside host cells [26]. Effectors that are recognised by the plant defence system are then called avirulence (AVR) proteins. Well studied examples for AVR proteins are the *P. infestans* RXLR effector Avr3a, that mediates intracellular suppression of INF1 induced cell death [19, 27] or the extracellular protein Avr4 from *Cladosporium fulvum* which inhibits plant chitinases and therefore prevents hydrolysis of its fungal cell wall [28].
Overall, successful pathogens use their effector repertoire to subvert PRR-dependent responses for nutrient uptake, growth and dispersal.

1.1.3 Plant disease resistance and effector-triggered immunity (ETI)

In plants that have adapted to a certain pathogen lineage, specific effectors or their activities can be recognized either directly or indirectly by plant disease resistance (R) proteins, which induce a defence pathway accompanied by an HR. This second layer of activated defence is called Effector-Triggered Immunity (ETI), and is the next step in the co-evolutionary arms race of the pathogen and host, in which the pathogen attempts to evade

host recognition. The plant in turn evolves new *R* genes that recognize the pathogen again to be able to restrict its growth [2, 4, 9].These R proteins typically belong to the large NB-LRR gene family present in all plants, named after their central nucleotide-binding domain followed by a C-terminal leucine-rich repeat region [4]. Two major classes are defined by their N-terminal extension, TIR-NB-LRR and CC-NB-LRR, with all oomycete resistance genes identified so far to the latter class [4, 29]. Most examples studied to date have identified an indirect interaction, in which the plant *R* gene senses conformational changes of specific host proteins that are induced by the pathogen effector. The indirect interaction can be explained by the guard model [1] and has since been proposed to include the "decoy" model [30]. The models describe how the effector modifies an accessory protein that is its potential virulence target (guard model) or a structural mimic of the original target (decoy model). The modified accessory protein is then recognized by the NB-LRR receptor. The above mentioned *P. infestans* effector *Avr3a* for example, is recognised indirectly in the plant cell. The *R* gene *R3a* relocates from the cytoplasm to endosomal compartments when coexpressed with the recognized form *Avr3a-KI*. *Avr3a-KI* also relocalizes to the endosomes in the presence of *R3a* [31, 32].

Further well characterised examples for effector proteins and their corresponding *R* gene are the *Pseudomonas syringae* effectors *AvrRpm1* and *AvrB* that are detected by the *R* gene *Rpm1* in *Arabidopsis thaliana* [33], or the tomato *R* gene *Prf* directly recognising the *P. syringae Avr* proteins *AvrPto* and *AvrPtoB* [34, 35]. Both host and pathogen have evolved large repertoires of proteins and regulatory mechanisms to be successful. Co-evolution has led to innovation and the emergence of novel protein classes that are required for host-microbe interactions, many of which are not yet fully understood.

1.2 *Phytophthora capsici* – a pathogen with a broad host range

The oomycete *Phytophthora capsici* is a devastating pathogen for many agricultural crops. Oomycetes, also known as water moulds, are a distinct group of eukaryotic organisms with fungal-like morphology, that are phylogenetically more closely related to photosynthetic algae instead of true fungi [36, 37]. They comprise an array of 800 diverse species that include members of the genus *Phytophthora*, which entail a long history of research due to their importance in past and present agriculture [38]. Members of the oomycete family

cause disease in animals, humans and plants, affecting most dicotyledonous crop species across the globe and generate severe problems not only in agriculture but also in natural environments [39]. Mankind has played a large role in the spread of these diseases. In 1861, *Phytophthora infestans* was reported for the first time by de Bary to cause a plant disease [40]. Ever since, *Phytophthora* and other oomycetes have caused severe damage including the great Irish potato famine caused by *P. infestans* in the 1840s. Although the biology has been studied in great detail, the molecular aspects of the infection process of these very successful plant pathogens remains in the dark. During the last century, a number of resistance genes against *P. infestans* have been identified and used in breeding resistant cultivars, however resistance has in all cases been overcome within a couple of years [41]. In contrast, so far only one functional *R* gene against *P. capsici*, another very important oomycete species within the *Phytophthora*-family, has been identified from a pepper cultivar [42]. *P. capsici* is a highly dynamic and destructive pathogen of various vegetable crops and the occurrence and severity has increased significantly in recent years. Multi-billion dollar losses in crop production are caused every year by *P. infestans* and *P. capsici* [42, 43]. In comparison to *P. infestans*, which infects *Solanaceae* only, *P. capsici* has a broad host range including members of the plant families *Solanaceae*, *Cucurbitaceae* and *Fabaceae*. It causes root, crown, foliar and fruit rot on, for example, tomato, pepper, eggplant, cucumber, pumpkin, and also on snap and lima beans [44-46]. The epidemiology on the population level varies according to the geographical location, and is composed of many unique genotypes in which sexual reproduction is common [42].

During epidemics, farmers fight damage and crop losses by *P. capsici* with chemical treatments. The absence of resistant crop cultivars, the high level of genotypic diversity within *P. capsici* isolates, as well as the threat of sexual recombination in the fields, makes *P. capsici* a worst-case scenario for crop production [42].

Oomycetes feature defined developmental stages in their life cycle that are not found in fungal pathogens and can live as (hemi)-biotrophic or necrotrophic pathogens in association with plants, animals or other microbes. *P. capsici*, the pathogen studied in this Thesis, was first described 1922 by Leon H. Leonian as a pathogen of Chile pepper in Las Cruces, New Mexico [47]. Nowadays, *P. capsici* is widespread throughout the world in warm and wet regions and infects a wide range of hosts including cultivated crops, ornamentals or native plants and the model plant *N. benthamiana*, belonging to diverse plant families [42, 44]. In

Europe, *P. capsici* can be found in the milder Mediterranean climate, however is not yet present in the UK due to environmental conditions.

1.2.1 Taxonomy, identification and diversity

P. capsici belongs to the class oomycetes in the phylum Oomycota and kingdom Chromista [42]. Phylogenetic analyses on a large number of different *Phytophthora* species enabled the classification into 10 major clades, wherein *P. capsici* falls into Clade 2 and the potato late blight pathogen *P. infestans* into Clade 1 [48-50]. A closely related sister species of *P. capsici* is *P. tropicalis*. Both species have similar morphological and physiological attributes, but both can be distinguished on the molecular level [51], as well as by host range. *P. capsici* isolates are generally recovered from annual plants like most vegetables, whereas *P. tropicalis* is more often recovered from woody nursery and perennial crops, such as cacao, papaya or black pepper [42]. Indeed, literature refers to *P. tropicalis* as *P. capsici* due to their morphological similarity, but also because of the deposition of mislabelled internal transcribed spacer (ITS) regions and other DNA sequences into GenBank [42, 52]. The study of *P. capsici* populations in a number of US states and other countries where this pathogen is economically important, such as Peru, Argentina or South Africa, have enabled successful phylogenetic analyses to understand the distribution of genetic variations [53-58]. A recent study from worldwide locations and various hosts of *P. capsici* using hundreds of isolates confirmed the immense genetic diversity amongst *P. capsici* at a global level [55]. Therefore, molecular mechanisms of pathogen-host interactions should be addressed with the help of sequence analysis by identifying and studying proteins that have been found in other *Phytophthora* spp.

1.2.2 Infection cycle

P. capsici can reproduce either sexually or asexually, however the asexual reproduction is responsible for massive outbreaks during the growing season. The pathogen is heterothallic, and thus two mating types (designated as A1 and A2) are required for sexual reproduction [59]. Both mating types can produce antheridia (male) and oogonia (female) gametangia [44]. Meiosis takes place in the gametangia and haploid nuclei are transported via a fertilization tube into the oogonium [42]. The spores of the sexual stage are defined as

oospores that need an indeterminate dormancy period and can survive in the soil for many years due to the thick cell wall, and can thus form a threat for future growing seasons [60]. When crossed *in vitro,* the oospores can produce viable sexual progeny [42]. During germination, oospores produce germ tubes, which branch as hyphae into mycelium, and under adequate environmental conditions (25-30 °C and high humidity) produce high numbers of sporangia on the surface of infected plant tissue. Between 2-3 days after starting infection, asexual sporulation occurs. Mature sporangia are easily dislodged by rain and irrigation, and upon submergence in water about 20-40 biflagellated motile zoospores can be released from each sporangium [42], resulting in the previously mentioned massive outbreaks. The sporangia are limoniform with conoidal endings containing the short-lived zoospores as shown in Figure 1.1.

Figure 1.1: Sporangia and zoospores from the pathogen *Phytophthora capsici*
Microscopic samples of *P. capsici* strain LT1534, grown on V8-Agar medium, dislodged in water
A: Limoniform sporangia with produced zoospores inside their body **B:** Single zoospore released from a sporangium.

After reaching an infection site on the leaf surface, the zoospores shed their flagella, encyst and develop a germ tube. The germinating cyst forms an appressorium, a swollen tip of the cyst germination tube where the cytoplasm becomes concentrated immediately prior to infection, which penetrates the plant cuticle directly to colonize the host tissue. With electron microscopy it could be demonstrated that this direct penetration of the cuticle happens within one hour [46]. Figure 1.2 depicts the various life stages from infections that are caused by a germinated oospore, a directly germinating sporangium or an encysted zoospore by penetrating the plant cuticle. From the point of penetration, hyphae form and

spread between mesophyll cells. From these hyphae, specialized infection structures, termed haustoria, are formed and push into the plant cell, but not the plasma membrane, to interface with the host membrane during the early biotrophic stage [61, 62] (Fig. 1.2). *Phytophthora* spp. are hemi-biotrophic pathogens, a lifestyle that features a biotrophic phase, followed by a switch to necrotrophy [63-65]. This life style is common with other detrimental filamentous plant pathogens like fungi that fall into the genera *Magnaporthe, Colletotrichum* and *Mycosphaerella* [66]. The initial biotrophic phase is crucial for infection and disease establishment including rapid intercellular growth and colonization, but ultimately leading to host cell death where sporulation occurs [67] and a new infection cycle is initiated.

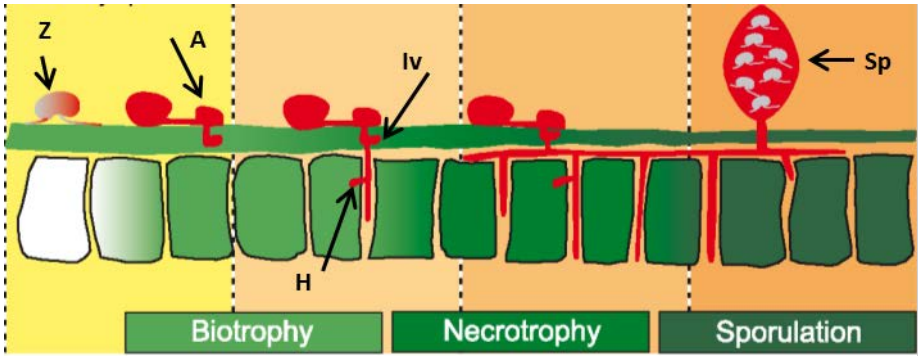

Figure 1.2: Asexual life cycle including three infection phases of *Phytophthora*
(Image adopted from Lamour *et al.* 2011 [42]): Sporangia are spread by wind and water onto the leaf surface of nearby plants. Motile zoospores (Z) are released from sporangia which encyst and form an appressorium (A), followed by an infection vesicle (Iv) to penetrate the leaf cuticle. Hyphae spread throughout the leaf tissue and produce specialized infection structures, termed haustoria (H) that push into the plant cell during biotrophy without penetrating the cell membrane. Those protrusions form a direct host-pathogen interface. Hyphae that grow through stomata outside the leaf in the sporulation phase can produce sporangia (Sp) again and a new infection life cycle starts.

1.2.3 The impact of *P. capsici* on agriculture

Due to the tremendous economic impact *Phytophthora*-host associations have on crop production, it is critical to understand how this group of pathogens manipulate their host and promote damage. Current breeding strategies rely on introgression of resistance (*R*) genes and identification of new *R* gene variants [29, 68, 69], which are however often rapidly overcome by the pathogen [41, 70, 71]. To date, genetic resistance to *P. capsici* isolates has only been identified in one non-commercial pepper variety [72] and in a wild tomato species [73]. It is very difficult to control the pathogen in the field once it has

become established, as chemical control agents and cultural strategies are difficult to implement under pathogen-favourable warm and wet weather conditions [42]. Therefore, of increasing interest to growers as well as breeders and scientists, is knowledge about the mechanisms underpinning infection and disease establishment of *P. capsici.*

1.2.4 Importance of a model infection system for *P. capsici*

Phytophthora capsici is a devastating pathogen of considerable economic and scientific importance. It attacks a broad range of vegetable crops, produces long-lived dormant sexual spores, has an enormous genotypic diversity due to recombination and features a devastating and short asexual disease cycle [42]. Additionally *P. capsici* can successfully infect the model plant *Arabidopsis* and a novel pathosystem was used recently to study various roles in defence against *P. capsici* [74].

Due to its explosive disease cycle, *P. capsici* can kill fields completely within days or weeks. In addition, the oospores persist for a very long time and under harsh conditions in the fields. All those characteristics reflect a worst-case scenario to growers, and therefore it is becoming increasingly important to find novel strategies to control *P. capsici* and other oomycete pathogens to secure food production. *P. capsici* represents a robust model to study, since it infects many plant species, is easy to grow and mate in the laboratory. Recently, a reference genome has become available for the well characterised strain LT1534 [43]. This sequenced strain was initially crossed from two field isolates: the A1 mating type LT51 (recovered from cucumber, Michigan, USA) and A2 mating type LT263 (recovered from pumpkin, Tennessee, USA). From that initial cross, two successive backcrosses to LT263 were executed and the isolate LT1534 (A2 mating type) was chosen from the progeny on a set of characteristics including a massive and spontaneous sporulation on simple V8-juice agar medium, a robust oospore production when crossed with *P. capsici* A1-isolates and abundant zoospore production [43]. The genome size of this *P. capsici* line is 64 Mbp, compared to other genomes within the *Phytophthora* family, *P. infestans*, *P, sojae* or *P. ramorum* at 240, 95 and 65 Mbp, respectively. With 19,805 predicted genes, *P. capsici* has similar gene content to *P. infestans*, *P. sojae* and *P. ramorum* (17,797, 16,988 and 14,451, respectively) [43, 75, 76]. The genome sequence information and genome assemblies are publicly available (http://genome.jgi-psf.org).

1.3 Oomycete effectors

As introduced earlier, pathogen effectors are small molecules that are actively expressed and can be translocated into the host cell to shut down the first layer of disease resistance, or to switch on plant machineries to feed the pathogen. These molecules typically have a modular organization, and in case of *Phytophthora* effectors, have two main functional domains [18, 77]. The N-terminus encodes a signal peptide for secretion and targeting, and in case of cytoplasmic effectors the conserved motifs, RXLR or LXLFLAK (described in more detail below). The C-terminal domain is responsible for the effector function and activity and operates in case of the cytoplasmic effectors inside plant cells [18, 77].

1.3.1 The genomes of *Phytophthora* spp. encode multiple effector classes

Throughout the infection cycle, *Phytophthora* secretes effectors into its host to enable growth and reproduction [2, 78-80]. The *Phytophthora* effector repertoire consists of secreted extracellular proteins (apoplastic effectors) that inhibit or counter defence associated compounds as well as secreted, intracellular proteins (cytoplasmic effectors) that directly traverse the host membrane and target intracellular processes [81]. Several apoplastic effectors interact with extracellular targets and surface receptors, acting as inhibitors of host enzymes, such as proteases and glucanases, which get activated in response to the pathogen infection [82, 83]. In contrast, the biochemical activities of cytoplasmic effectors are less understood. Amongst those intracellular proteins are the RXLRs that will be discussed in more detail later on [26, 77, 84]. *Phytophthora* genomes further encode another large class of intracellular effectors, termed Crinklers. The Crinkler (CRN for CRinkling and Necrosis) protein family was named after a characteristic leaf crinkling phenotype observed upon ectopic expression of *P. infestans* secreted proteins in plants [85]. CRN proteins feature a conserved LXLFLAK motif, which is required for effector translocation and exclusively target the host nucleus upon delivery [62, 76, 86].
In addition to intracellular effectors, other secreted proteins have been implicated as possible virulence factors. Eighteen necrosis-inducing *Phytophthora* proteins (*PcNPP*), also called *NLPs* (Nep 1-like proteins) [87, 88] and nine pectin methylesterase (*PcPme*) coding genes [89] have been identified in *P. capsici* strain SD33. The *NPP* coding genes, which have

been previously identified in other oomycetes, induce cell death *in planta* suggesting a role in host cell perturbation [90-92]. An additional 12 *PcNPP* proteins were found to be expressed during infection and were reported to be involved in the transition from biotrophy to necrotrophy, however their functional roles in *P. capsici* virulence remain elusive. The *PcPme* genes were also found to be expressed during infection and contribute to the virulence process by promoting tissue collapse and successive cell death [89].

1.3.2 The RXLR effector family

A major group of oomycete effectors that are translocated into the host cytoplasm are the RXLR effectors. RXLR effector proteins can be rapidly identified by the characteristic RXLR-dEER-motif in the N-terminal region after the signal peptide [79] and a less conserved C-terminus which is responsible for the effector function [93]. Within the available *P. capsici* genome (strain LT1534), 357 putative RXLR candidates have been identified pointing to an important role in *P. capsici* biology [43]. Subsequent RXLR gene expression analysis revealed biotrophy-associated expression for most RXLR proteins, suggesting a role in virulence [67]. Similar numbers of RXLR genes have been reported for *P. infestans*, with 563 RXLR effectors, 396 for *P. sojae* and 374 for *P. ramorum* [76, 94].
Despite their divergent sequence, Jiang *et al.* (2008) [94] suggest that these RXLR effectors could be all related and presumably evolved from a common ancestor by rapid evolution. RXLR genes are also predicted in the genomes of other oomycetes, such as e.g. 134 RXLR from the obligate downy mildew pathogen *Hyaloperonospora arabidopsidis [95]* or in *Saprolegnia parasitica*, a fish pathogen that causes severe damage to wild and reared fish stocks *[96]*, as well as in the biotrophic oomycete *Albugo candida* [97]. In contrast, RXLR genes are absent as an example in the genome of the necrotrophic pathogen *Pythium ultimum*, suggesting these proteins could be specific to the (hemi-)biotrophic lifestyle of some oomycete species [98].

1.3.3 RXLR effector proteins as avirulence factors and their translocation

In recent years, six functionally characterized oomycete cytoplasmic effectors, for which plant targets are known, have been discovered through their avirulence activity [25, 31, 99-102]. All six proteins share a signal peptide and the conserved RXLR motif within the N-

terminus, followed by a C-terminal domain, associated with a virulence function [103]. There have been other functional avirulence genes found from oomycetes that encode RXLR effectors, such as e.g. *Avr4*, *AvrSmira1* and *AvrSmira2* [104] from *P. infestans* or several genes from *P. sojae* [105-109], but their plant targets are not known yet.

Although it is known for the *P. infestans* RXLR effector *Avr3a*, that translocation occurs after secretion from the haustoria across the cell wall and plasma membrane of the host plant cells [26], the mechanism of translocation remains unclear. The oomycete RXLR motif is similar to a motif found in effectors of the human malaria parasite *Plasmodium falciparum*, which also target the host cells, and is required for the translocation of the effector proteins into the red blood cells of the host [110, 111]. In addition, it was demonstrated that the RXLR-dEER motif of *P. infestans Avr3a* can be replaced with the malaria parasite motif without influencing translocation into the plant cells [112]. Additional examples include the RXLR motifs ATR1 and ATR13 from *H. arabidopsidis* which function in *Phytophthora* for effector delivery into plant cells by replacing the RXLR-domain of *Avr3a* [113]. The RXLR-dEER domain of the *P. sojae* effector *Avr1b* was shown to translocate the full-length effector protein together with a GFP-tag into different plant cell types in the absence of any pathogen-encoded machinery [93]. In addition to *Avr1b*, the signal peptides of the RXLR-dEER domain from *Avh5* and *Avh331* were expressed as fusion proteins to the C-terminus of *Avr1b* and co-bombarded (with GUS) into Rps1b soybean and thus secreted from the leaf cells [93, 114]. The signal peptide presumably directed the protein to the apoplast, where the RXLR-dEER motif promoted the re-entry into the plant cells and was therefore detected by the Rps1b protein.

Another example for a putative RXLR effector comes from the oomycete *S. parasitica*, as mentioned above, that is termed *SpHtp1*. Although this effector contains an RXLR, but no dEER domain, it has been shown to translocate into trout cells via binding tyrosine-*O*-sulphate on the host cell surface [115].

With conflicting results within recent years, the controversy over RXLR effector entry into plant cells has suggested that the RXLR domain is required for microbe-independent entry of proteins into the host and non-host plant or animal cells [116, 117]. In contrast to published data from B. Tyler's group, the groups of P. van West, R. Kahmann and T. Nürnberger support the conclusion that the RXLR domains of *P. infestans* Avr3a and *P. sojae* Avr1b alone are not sufficient to enable microbe-independent entry of those proteins into its hosts

[118]. Also Petre and Kamoun (2014) discussed recent conflicting findings of the mechanisms by which fungal and oomycete effectors enter into plant cells and highlighted different approaches of both parasite and host during infection [119]. Nonetheless, the mechanisms of RXLR effector entry into plant cells remain unclear to date, and therefore more studies on effector host-translocation are still required.

1.3.4 Function of oomycete RXLR effectors

Many plant pathogens use effector proteins to subvert plant immunity and promote susceptibility. Bacterial pathogen species secrete effectors into the cytoplasm of plant cells through the type-III secretion system (T3SS) [22]. Bacterial effectors have been studied in great detail and therefore molecular activity and function are well known [120]. In contrast to bacterial effectors, the understanding of effector functions, in both oomycetes and fungi is still in its infancy [65, 121]. Therefore, there is yet a lot to be learned about the virulence strategies that eukaryote pathogens employ when they infect plants. The best studied example is the previously mentioned *P. infestans* effector *AVR3a*, which targets the E3 ligase CMPG1 within the plant cell during the early stages of infection [19]. It was shown that CMPG1 is important for activation of the plant defence and disease resistance and INF1-mediated cell death, concluding that CMPG1 is a key virulence target [19, 122, 123]. Another *P. infestans* effector *AVR2,* which is up-regulated during infection, accumulates at the site of haustoria formation and is recognized inside the host cells by the potato protein R2 [124]. Further investigations showed, that recognition of the *AVR2* effector by the NB-LRR protein R2 requires the putative phosphatase BSL1 [125]. This reveals that, recognition of such effectors can be mediated via a host protein that interacts with both the effector as well as the NB-LRR immunoreceptor [125]. An additional example is the *P. infestans* effector *Avrblb2* that targets PLCP C14, which is a plant defense protease. *Avrblb2* blocks the C14 protease secretion into the apoplast and therefore points towards a unique counterdefense strategy from the pathogen to neutralize secreted plant defense proteases [78]. Another recently studied effector protein from *P. infestans*, called Pi03192, which interacts with two plant NAC transcription factors at the endoplasmatic reticulum (ER) inside the host cells. The transcription factors are released from the ER to enter the nucleus and are important to restrict disease. Pi03192 prevents re-localisation of the NAC transcription factors from the

ER to the nucleus and promotes disease progression [126], which suggests a novel strategy from the pathogen to enhance host susceptibility.

P. sojae RXLR effectors have also been studied, such as the protein *Avr3b* that carries a Nudix motif that mediates ADP-ribose and NADH pyrophosphorylase activity [127]. Deletion of the *Avr3b* Nudix motif reduced enzyme activity, however mutations in the Nudix motif revealed an importance for *Avr3b* virulence function, but not for the recognition by the corresponding *R* gene *Rps3b* [127]. Nudix hydrolases have been identified as negative regulators of processes required for immunity in plants [127], and therefore *Avr3b* might act as a plant Nudix hydrolase. Other *P. sojae* effectors have been discovered to function as defence suppressors. For example, the strongly expressed *Avh172* from *P. sojae* can suppress the cell death that is triggered by some early effectors, such as Avr4/6 [128]. Observations support the hypothesis that key immediate-early effectors suppress plant defenses triggered by effectors expressed later in infection. That means some isolates of *P. sojae* appear to be less virulent and contain a specific group of effectors that target different stages of the plant immune system [128]. This infection strategy could have been adopted by other oomycete plant pathogens as well.

To give an example of an effector from *H. arabidopsidis*, *HaRxL44*, which is targeting the mediator complex and interacts with the Mediator subunit 19a (MED19a), resulting in the degradation of MED19a in a proteasome-dependent manner [129]. That means, by shifting the gene expression and therefore defence transcription, *HaRxL44* is enhancing susceptibility to its biotrophic host.

1.4 Transcriptomic studies

Transcriptomics, also referred to as expression profiling, examines the expression level of mRNAs in a given cell population, often using high-throughput techniques based on DNA microarray technology or next-generation sequencing of cDNA (RNAseq) (http://gel.berkeley.edu/research/research-methods/transcriptomics/) [130, 131]. Understanding the gene regulatory networks is highly desired, especially during biological phases like disease resistance, and therefore information about transcript levels is required. Prior to the availability of whole genome annotations, expressed sequence tags (EST) provided a reliable set of transcribed elements that have been identified to be expressed in

particular growth conditions, cell types, and developmental stages from e.g. both potato and *P. infestans* as part of the interaction transcriptome [132]. Annotated genome and transcriptome databases are available for many organisms, including *P. capsici* and *P. infestans* as well as their solanaceous host species [43, 76, 133, 134]. These databases enable the creation of precise microarray probes and also provide great references for mapping of RNAseq data. An example for a genome-wide microarray analysis to identify molecular defence responses that are activated after treatment with β-aminobutyric acid (BABA) in potato infected with *P. infestans,* were shown for the reference potato *Solanum tuberosum* group phureja [135]. Results of this transcriptomic study were combined with proteomic studies and identified over 5000 differentially expressed transcripts as well as a massive activation of defence mechanisms after BABA-treatment and suggested new candidates and biomarkers for improved resistance in potato [135]. Several other microarray [136, 137] as well as RNAseq studies [138, 139] describe the transcriptomes of soybean and *P. sojae* during their interactions. More targeted studies were also carried out, for example to study salicylic acid-dependent plant responses in a tomato-aphid interaction [140] or ontogenic resistance genes in the Apple-*Venturia* pathosystem [141]. The global analysis of gene expression has become an important tool to better understand the role of genes and pathways in biological processes.

1.5 Scope of this thesis

Pathogens and pests continue to hamper food production and disrupt the food supply chain on a global level. With important crops, such as wheat, rice, potato and multiple vegetable crops affected by pathogens, disease epidemics can cause major price hikes and thus threaten food security. Hence, there is an urgent need for new disease control strategies that will help to increase crop yields and alleviate demands on food production. An understanding of the molecular mechanisms of both plant and pathogen will be critical to growers, as well as breeders and scientists. Therefore, studies aiming to compare genes are required for infection or defence responses to identify conserved versus species-specific strategies of the pathogens. The tremendous economic impact that *Phytophthora* species have on crop production make an understanding of how this group of pathogens manipulate their host and promote damage, which is a very important scientific target.

Current crop breeding strategies rely on the introgression of resistance genes and the identification of new *R* gene variants [29, 68, 69]. However, history has shown that these are rapidly overcome by the pathogen. Therefore, an increasing interest lies in understanding the mechanisms underpinning infection, disease establishment and epidemics to use the few available resistance genes in an intelligent way.

The primary aim of my thesis is to develop a model interaction system for *P. capsici* to distinguish the different infection phases: the biotrophic and necrotrophic phase, followed by sporulation and host cell death (Chapter 2). When I started this project, there were no studies yet describing infection processes of *P. capsici* on various host species. Infection time course assays were generated to reveal the distinct hemi-biotrophic infection cycle, featuring haustoria formation early during infection, followed by necrotrophy in the late infection stages and phenotypic observations were linked to molecular aspects through the identification of a biological marker gene set that discriminated the three distinct infection phases. Parts of this work were published in *Molecular Plant Pathology* (Lamour,K.H., Stam,R., Jupe,J. and Huitema,E. 2011) [42].

The established corner stones of pathogen development were then deployed in gene expression studies. The literature describes several studies where either host or pathogen gene expression patterns were analysed during the course of infection. These experiments have always deepened the understanding of either the pathogen's infection strategy or the host response to it. In chapter two and three of this thesis, a novel approach describes the simultaneous study of transcriptional changes of *P. capsici* and several important host species. Exploiting the recently reported genome sequences of *P. capsici* and tomato, customized microarray chips were designed to harbour all predicted genes of the host as well as the pathogen. This enabled the identification of essential transcriptional changes that occur in the pathogen during infection, its establishment and transition from biotrophy to necrotrophy. Equally important for understanding disease, however, will be the identification of host processes and signalling pathways that are perturbed by the pathogen whilst progressing through its specific life stages. These unveil a requirement for *Phytophthora* enhanced protein production and metabolism in biotrophy, catabolism during its transition to necrotrophy and the induction of signalling and developmental processes upon sporulation. Chapter 3 is a published manuscript in *Genome Biology* (Jupe,J. *et al.* 2013) [67] and *PLOS One* (Stam,R., Jupe,J. *et al.* 2013) [86].

In a case study, the genome sequences for two *Phytophthora* spp., *P. infestans* and *P. capsici*, two divergent species that both infect tomato, were used to explore whether conserved *Phytophthora* effector protein sequences equal conserved functions and roles in parasitism (Chapter 4). Using BLAST analyses, homologs of selected *P. infestans* RXLR effectors in *P. capsici* were identified and candidate genes were compared to profiles available for *P. infestans*. In addition functional and phenotypic studies were conducted for the biotrophy-stage-specific RXLR gene *Pc03192* (Chapter 4).

Chapter 4 elaborates on this putative *P. capsici* RXLR effector protein Pc03192 for which a potential orthologous sequence has earlier been described from *P. infestans* to interact with two potato NAC transcription factors as demonstrated in McLellan *et al.* (2013) [126].

This work opens the door towards comparative transcriptomics that should help unravel pathogen infection strategies and exploit host basal defence responses.

2 Characterisation of *Phytophthora capsici*-host interactions and the development of a model infection system

2.1 Introduction

Plant pathogenic microbes are specialised organisms that have evolved the ability to infect and cause disease on host plants. Interestingly, pathogen host range can vary significantly with pathogens causing disease on only a single host, and some that affect a wide range of plant species, suggesting that the latter group must have evolved the ability to overcome diverse immune systems. The host range between members of the oomycete genus *Phytophthora* varies significantly. While *P. capsici*, *P. ramorum*, *P. cinnamomi* and *P. parasitica* have a broad host range, others such as *P. infestans* or *P. sojae* only affect few crops [42, 142-144]. In several cases the host range also overlaps, and a good example is *P. capsici*, which shares tomato as a host with *P. infestans*.

As previously introduced in Chapter 1, plant pathogens secrete effector molecules that enable parasitic infection and reproduction [2, 18, 20] and thus determine the success for the interaction with the host. The observed differences in host range as well as the occurrence of divergent *Phytophthora* spp. on the same host should therefore be underpinned by effector complements that are effective in a variety of plants, or that determine specialisation. Identification of genes that encode secreted proteins from the available *P. infestans* and *P. capsici* genomes have shown that they possess comparable numbers of effectors that harbour either an RXLR or LXLFLAK domain. These observations combined, raises the questions as to whether effectors function in different host species, or whether their expression is determined by the host or more generally, whether the infection progress is regulated in a similar way on various hosts?

The aim of the work presented in this chapter was to assess whether *P. capsici* infection and disease development is changing dependent on the host. For this purpose, a combination of semi quantitative RT-PCR, confocal microscopy and microarray analyses was deployed to characterize a model infection system for the broad host range pathogen *P. capsici*. The infection process was compared between four host plant species in a variety of time course inoculation experiments on detached leaves phenotypically and by assessing gene expression during the course of infection using PCR analyses. The studies were carried out

on three *Solanaceae* and one *Cucurbitaceae* host plant: *Nicotiana benthamiana* as model plant, and *Solanum lycopersicum* (tomato), *Capsicum annuum* (pepper) and *Cucumis sativus* (cucumber) as important agricultural crops.

The hemibiotrophic life-style of *P. capsici* features three distinct stages, biotrophy, necrotrophy and sporulation (as introduced in Chapter 1). In this chapter, the distinct phases of infection were studied on the cell biology and molecular level. Using confocal microscopy experiments the formation of haustoria during biotrophy was observed, providing evidence for a close interaction between pathogen and host. A set of three biological marker genes was developed, enabling the observation of the molecular switch between the distinct stages using semi-quantitative PCR. The design of a microarray, harbouring all predicted *P. capsici* gene models, enabled the study of genes that are regulated during the interaction with three of the tested hosts, *N. benthamiana*, pepper and tomato. This experiment has shown that the majority of genes are host-independent, but expression of a group of genes is host dependent during infection. This study provides important insights into the molecular basis underlying the host range of *Phytophthora* spp. Results from this chapter allowed the establishment of a model system that is a starting point towards understanding molecular host specificity and defence suppression in *P. capsici*.

2.2 Material and Methods

Plant material

The following plant species were used in the experiments described here: *Nicotiana benthamiana* 'Sainsbury', the transgenic line *Nicotiana benthamiana* 'CB28' (expressing GFP in the ER), *Solanum lycopersicum* 'Moneymaker', *Capsicum annuum* 'ECW123' and 'California Wonder' and *Cucumis sativus* 'Venlo'. Plants were grown in a greenhouse at 22 °C and 16 h light. For all detached leaf infection assays, young fully expanded leaves, and single leaflets in case of tomato, from at least four to six week old plants were placed upside down in humid transparent plastic trays at room temperature (approximately 20 °C). Leaf discs of infected lesion centres and non-infected tissue were harvested using a cork borer (ϕ 7 mm). The leaf material was collected in 1.5 ml-microcentrifuge tubes, frozen in liquid nitrogen and stored at -80 °C until further use.

Phytophthora capsici inoculation and *in vitro* samples

Phytophthora capsici wild type strain LT1534 was grown on V8 agar medium [146] in a dark incubator at 25 °C for three days and for two days under bright light at 25 °C. To induce zoospore release, plates were flooded with ice-cold distilled water and spores were harvested from sporulating mycelia by dislodging the sporangia with a sterile glass spreader. Sporangial suspensions were collected and incubated at room temperature under bright light conditions. Release of zoospores was followed and the zoospores were counted under the microscope using a haemocytometer and adjusted to $1x10^5$ ml. The detached leaves were inoculated with four droplets (each 20 µl) of the zoospore solution. In addition to the infectious stages, two *in vitro* samples were taken: sporangia/zoospores (Spor) and germinating cysts (GC) grown *in vitro* and sampled at various time points. Samples of Spor and GC were taken from the same inoculum/sporangial suspension. These samples were collected from 10 ml of the sporangial suspension after an incubation time of 1 h for the Spor-sample and 8, 16 or 24 h for GC at room temperature. To produce genomic DNA (gDNA) from *P. capsici* strain LT1534 as a positive control sample, mycelia was grown in 1 ml pea broth (according to http://www.plantpath.cornell.edu/Fry/Protocols-Culture.html), inoculated with 20 µl of inoculum (sporangia and zoospores mixed) and placed at 25 °C. After 48 hpi the mycelium mat was harvested and distributed into 10ml-tubes. All samples were harvested by centrifugation for 2 min at 1500 relative centrifugal force (rcf x g). After taking off the supernatant, the pellets were collected and frozen in liquid nitrogen. The mycelium was ground in liquid nitrogen to disrupt the cell walls, and DNA was further extracted using the protocol supplied with the DNeasy Plant Mini Kit (QIAGEN).

RNA extraction and cDNA synthesis

RNA was isolated from frozen leaf tissue/*in vitro* samples following the protocol supplied with the RNeasy Plant Mini Kit (QIAGEN) and treated afterwards with DNAse (DNA-free™ DNA Removal Kit (DNaseI), Ambion/Life Technologies) to remove genomic DNA contamination according to the manufacturer's instructions. To test for gDNA contamination, a PCR with primers specific for *PcTubulin* (see in table 1) was performed on the extracted RNA using GOTAQ polymerase at an annealing temperature of 57 °C. The cDNA was then synthesized from 500 ng RNA using the SuperScript TMII RT cDNA synthesis kit (INVITROGEN) following the manufacturer's protocol.

Semi quantitative and quantitative RT-PCR to analyse gene expression

Tissue was harvested from all four host plant species as described above and samples were taken at 0, 8, 24, 30, 48, 54, 72 and 78 hours post inoculation (hpi) for the detached leaf assay and a semi-quantitative PCR. For the quantitative RT-PCR time course experiment, leaf tissue was harvested at 0, 18, 42, 66 and 90 hpi.

Semi quantitative RT-PCRs were performed in 50-µl reaction volumes with 1 µl of cDNA as template using a 1:5 dilution of cDNA. The GoTaq® Flexi DNA Polymerase from Promega was used with all components according to the manufacturer's protocol. Thermocycling conditions of the PCR were: 94 °C for 2 minutes, followed by 30 or 35 cycles at 94 °C for 30 sec, 57 or 58 °C for 30 sec and 72 °C for 2:30 or 1:30 minutes. Extension was finalized at 72 °C for 10 minutes to allow filling of incomplete polymerizations. Two controls (H_2O and gDNA from the wild type *P. capsici* strain LT1534, as described above) were included in each PCR. For the relative quantification of the gene *PcHmp1*, a quantitative RT-PCR assay was carried out in 25-µl reaction volumes with 2 µl of cDNA template using a 1:40 dilution of cDNA. The SYBR® Green Master Mix (QIAGEN) according to the manufacturer's protocol was used with 40 cycles as described in Avrova *et al.* (2003) [147] with minor changes to the amplification. The samples were denatured at 95 °C for 15 minutes, followed by 95 °C for 15 sec, 59 °C for 30 sec and 72 °C for 30 sec. The primers (see in table 2.1) were designed in the programs Primer3 and NetPrimer and optimized afterwards with two final concentrations (300 nM and 900 nM) for Forward- and Reverse-primer according to the protocol for Real-Time qRT-PCR (TaqMan probe and primer design, assay optimisation, Applied Biosystems). The cDNA was tested in combination with the different primer concentrations in a dilution series of 1:5, 1:10, 1:20 and 1:40 with the same program settings as above prior the actual experiment. The optimization and experiment was conducted on a Chromo4 qRT-PCR machine from BIO-RAD. The standard curve for the primers and cDNA was calculated as reference for the CT-value in terms of ng of template that is present in each sample. Statistical analyses on the quantitative RT-PCR approaches were then performed using the comparative Ct method (ΔΔCt) and "Formula of the line method" in Microsoft Excel. The *P. capsici* gene *PcTubulin* was used as a constitutively expressed endogenous control [67] and the relative expression was normalized against expression levels of sporangia, which was set to a value of 1.0 for statistical analyses, as previously described [148].

Table 2.1: Primer sequences used for quantitative Real Time PCR

Primer	Sequence (5' to 3')	Concentration in nM
qPcTubulin-F	CTCCCAAGGGTCTGAAGATG	300
qPcTubulin-R	CCTGAATGGCAGTCGAGTTA	300
qPcHmp1-F	CTTGCTGTTGTGTCGGCTAT	300
qPcHmp1-R	GAGGCTGATGGTGTCACTGT	900

Marker gene sequences

For all marker genes, the original *P. infestans* sequences were retrieved from NCBI (http://www.ncbi.nlm.nih.gov/guide/) using the published accession numbers (*PiHmp1:* EU680858.1 *; PiNPP1*: AF356840.1; *PiCDC14:* AY204881.1). The sequences were then applied in a tBLASTn and BLASTp [149] search with the program setting for sequences to expect 1.0E-5 against the *P. capsici*-genome version 11 (http://genome.jgipsf.org/Phyca11/Phyca11.home.html;2011) to get the corresponding homologous *P. capsici* sequences from which the primer pairs (see in table 2.2) have been designed. Amplicons from cDNA were Sanger sequenced and derived sequences were aligned to *P. infestans* reference sequences using the program ClustalW Multiple Sequence Alignment [150] to investigate the levels of sequence similarity.

Identification of the *Pc*RXLR complement

Analysis of previously published *P. capsici* RXLRs [43] revealed that the present database was incomplete. Therefore a new identification strategy was implemented by Remco Stam (University of Dundee, UK) whereby RXLRs were sought using previously published methods [26, 103, 151]. All output was collated and compared to the previously predicted *P. capsici* RXLR complement using BLASTN. Redundancies were removed, and in case of differences in predicted ORF length, sequences were compared with known *P. infestans* RXLR sequences and manually curated. This yielded a set of 516 RXLR candidates which were used for further analyses.

Expression profiling of *P. capsici* genes

For the semi-quantitative PCR gene expression analysis, the following *P. capsici* genes were chosen: *PcTubulin, PcHmp1, PcNPP1, PcCdc14* and the three RXLR effector genes *Pc03192, Pc16737* and *Pc08599.* Primers (Table 2.2) for the effector genes were designed with the software Primer3 and NetPrimer to amplify the coding sequence after the signal peptide, except for *Pc08599*, the primers were designed to amplify the whole gene including the signal peptide.

Table 2.2: Primer sequences used for semiquantitative PCR

Primer	Sequence (5' to 3')
PcTubulin-F	GACTCGGTGCTTGATGTTGTC
PcTubulin-R	CCATCTCATCCATACCCTCGCCAG
PcHmp1-F	CATGATGGCAGTCATGGTCGGTGAAG
PcHmp1-R	TTAGCTAACATTGAGGCGGGCATGCAG
PcNPP1-F	CAGCTCCACATCACCAACGGCT
PcNPP1-R	CTCTTCCCGTTCAAATAGTTC
PcCdc14-F	GGAAGCGATTGAGTTCTTGC
PcCdc14-R	TTCTCCACACGCTCAAAGTG
Pc03192-F	AAAAAGGATCCCCAAGACTTCCGTTACGGTGAACAC
Pc03192-R	AAAAAGAATTCCTATCTTCTCCCCCAGACC
Pc16737-F	AAAAAGGATCCCCGCATCCAAAGACTCGAAGCTGATG
Pc16737-R	AAAAAGAATTCTTACTTCCTGACGGGTGGGCCAGGAC
Pc08599-F	ATGGCGACCGACAAGCA
Pc08599-R	CTAGGCTTCGACCTTCAGC

Microarray experiment

A custom 60-mer oligonucleotide microarray was designed from predicted transcripts of the *P. capsici* (LT1534 v11.0, [43]) and *S. lycopersicum* (ITAG 2.3,) genomes using eArray software (Agilent Technologies, USA) as described in Stam *et al*. [86] and Jupe *et al.* [67] with the difference of a fluorescent two-colour labeling of the RNA. The two-colour labeling was applied as recommended (Agilent Two-Colour Microarray-Based Gene Expression Analysis (Low Input Quick Amp Cy3- and Cy5-Labeling) version 6.5) using 8×60k format slides. RNA labeling and microarray hybridisation procedures (see protocol in appendix 1) were performed at Genome Technology, at the James Hutton Institute, UK.

The three different host species (*Nicotiana benthamiana*, *Solanum lycopersicum* 'Moneymaker', *Capsicum annuum* 'ECW123'/'California Wonder') of *P. capsici* were compared in this approach with an infection sampled at 24 hpi and 72 hpi using detached leaves from two biological replicates. Datasets were quantile-normalized as described in Jupe *et al.* [67] , as well as in more detail in Chapter 3 (Material and Methods; Microarray design and analysis) and loaded into Genespring (version 7.3, Agilent Technologies, USA). To generate lists of expressed *P. capsici* genes for each time point and each individual host species, probes were selected with a signal >100 after the fold change was compared to the median values across the samples in both replicates. In addition the criteria of genes that were not expressed anywhere in the tomato timecourse-experiment was used for the analysis. Unique and overlapping expressed gene lists were identified between individual hosts using Venn diagrams with the program Genespring. To investigate specific gene ontologies, GO-term annotations were used to specify molecular functions, biological processes or cellular components. For confirmation of the four exclusive RXLR genes found by the Venn diagram, primers were designed as described above to the coding sequences after removing the signal peptides and semi-quantitative PCR analyses were conducted on cDNA from whole time course experiments on *N. benthamiana*, tomato and pepper, as described before.

Confocal imaging

Zoospores ($1x10^5$ ml; extracted with the same method as described above) of transformed *P. capsici* LT1534:tdTOMATO (transgenic strain was kindly provided by Ariane Kemen, Jonathan Jones-Lab, The Sainsbury Laboratory, Norwich, UK) were inoculated in 30 µl

droplets onto leaves of transgenic *N. benthamiana* plants, expressing GFP in the endoplasmatic reticulum (ER), *Solanum lycopersicum* 'Moneymaker' and *Capsicum annuum* 'California Wonder'. The plants were incubated in a small climate controlled chamber to keep humidity and maintained at 20 °C for 20 hrs to allow *P. capsici* to penetrate the host cells and form hyphae with haustoria. All GFP (488 nm excitation; emission 500-530 nm) and tdTOMATO (561 nm excitation; emission 590-630 nm) imaging was conducted on a Leica TCS-SP2 AOBS confocal microscope using HC PL FLUOTAR 63×0.9 or HCX APO LUVI 40×0.8 water dipping lenses.

2.3 Results

2.3.1 Phenotypic observations of disease progression on four host species

To assess *P. capsici* disease progression, a first infection time course assay was performed on detached leaves of the Solanaceous model plant *N. benthamiana.* The aim of this experiment was to establish an adequate model system for infection assays and to find suitable time points for subsequent analyses. Photographs were taken at 0, 18, 42, 66 and 90 hours post inoculation (hpi) as shown in Figure 2.1 (This Thesis and [42]) and plant tissue was harvested from the infection lesion centre for every time point for further RNA extractions.

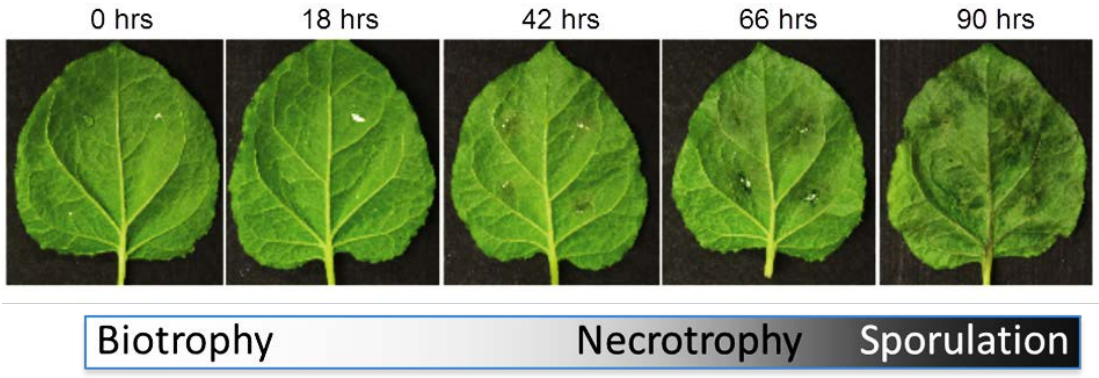

Figure 2.1: *Phytophthora capsici*-host interaction study on the Solanaceous model *Nicotiana benthamiana*
Infection time course assay performed on detached *N. benthamiana* leaves and photographs were taken at the time points indicated. The infection features an initial biotrophic phase (0-18 hrs), onset of necrosis (necrotrophic phase) > 42 hrs with lesion darkening and further tissue collapse and sporulation (66-90 hrs). Figure is also shown in Lamour *et al.* (2011) [42].

A second time course assay was conducted on *C. annuum* 'ECW123' (pepper), *S. lycopersicum* (tomato) and *N. benthamiana* as control, with closer time-points at 0, 8, 24, 30, 48, 54, 72 and 78 hpi to identify differences in host phenotypes (Figure 2.2 and 2.3). In addition, the infection phases of the pathogen were determined visually from the observed phenotypes as described below and demonstrated in Figure 2.2.

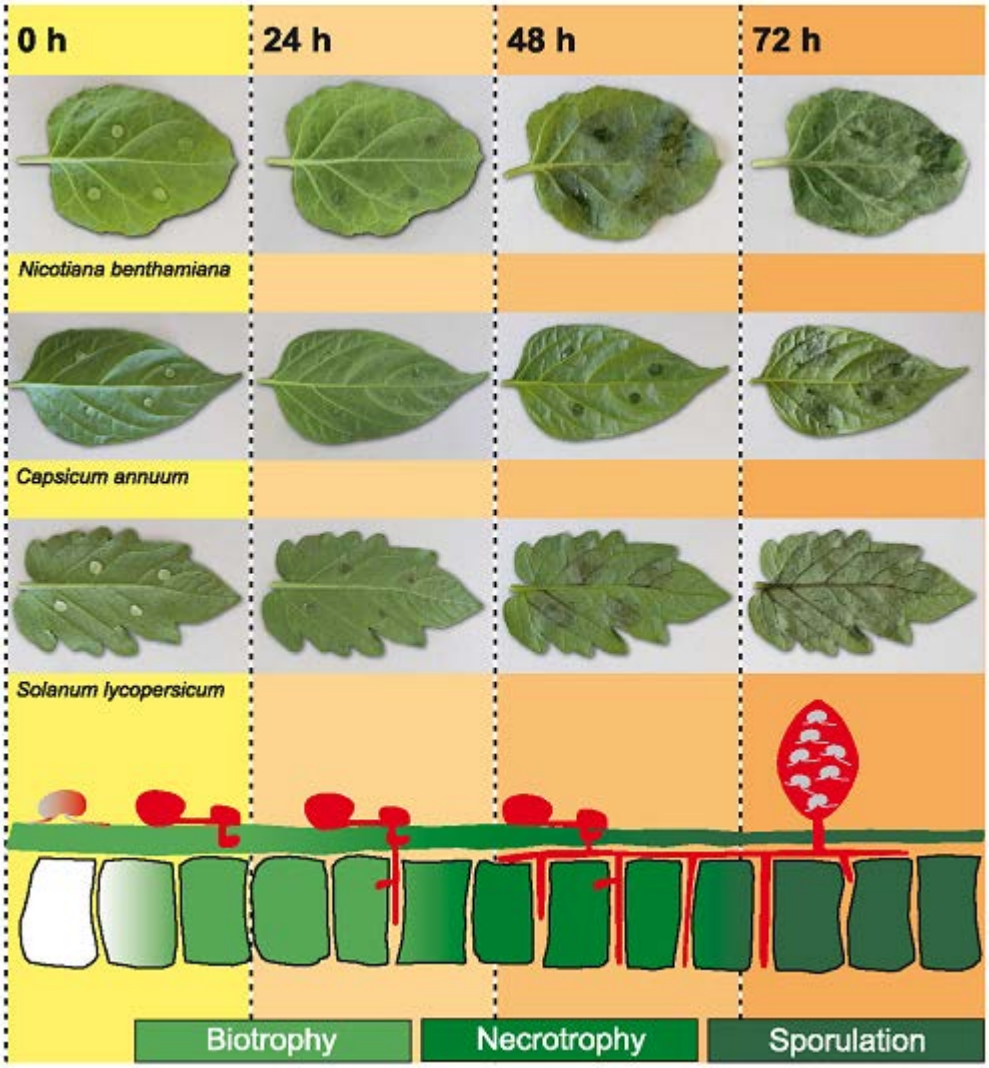

Figure 2.2: Phenotypic characterization of the infection progress of *P. capsici* on *N. benthamiana*, *C. annuum* 'ECW123' and *S. lycopersicum*
Detached leaves in a parallel time course experiment (as part from the time course shown in figure 2.3); *P. capsici* disease progression, showing the inoculation points at 0 hours, 24, 48, 72 and 78 hrs post infection (hpi). The time course experiment revealed the presence of a biotrophic stage (0-24 hpi), onset of necrosis (necrotrophic phase) > 24 hpi and further tissue collapse and sporulation (>72 hpi), independent of the host. The three infection phases of *P. capsici* are demonstrated and adopted from Lamour *et. al* (2011)[42]: zoospores encyst and penetrate the leaf cuticle. Hyphae grow throughout the leaf tissue and produce haustoria that push into plant cells during biotrophy and necrotrophy. In the sporulation phase, sporangia are produced, containing new spores again for the next infection life cycle.

In all further time course experiments on detached leaves, the susceptible pepper variety 'Californian Wonder' was used and the host species *Cucumis sativus* (cucumber) was included as representative cucurbit host of *P. capsici.* All phenotypic assessments of infection sites were conducted at 0, 8, 24, 30, 48, 54, 72 and 78 hpi (Figure 2.2 (partly) and 2.3). The photographs were taken from the same leaf throughout the whole time course experiment and leaf tissue was harvested from the infection lesion centre for every time point for subsequent RNA extractions.

Phenotypic analyses showed that during the early phase of infection (0-24 hours), tissue remained healthy with limited water soaking and tissue darkening, whereas after 24 hours, infection rapidly progressed with the formation of dark and necrotic lesions at the sites of the inoculation in all tested plant species (Figure 2.3). This indicates a switch from the biotrophic phase to necrotrophy; *P. capsici* is causing widespread cell death, resulting in tissue collapse in the host and spore production in the pathogen, ultimately resulting in dispersal of spores/sporangia, completing the infection cycle [42]. Lesion development was accompanied by lateral *P. capsici* growth and colonization of leaves in the later stages (>72 hpi) (Figure 2.2 and 2.3). Importantly, the timing of infection and subsequent development of disease symptoms was nearly identical on each host. Although on cucumber the infection development seemed visually slightly delayed, the different infection phases were still visible. The observed three distinct phases of infection (biotrophy, necrotrophy and sporulation) are shown in Figures 2.1-2.3. Taken together, *P. capsici* infects all tested host species in the same aggressive way with tissue collapse and sporulation taking place at 72hpi.

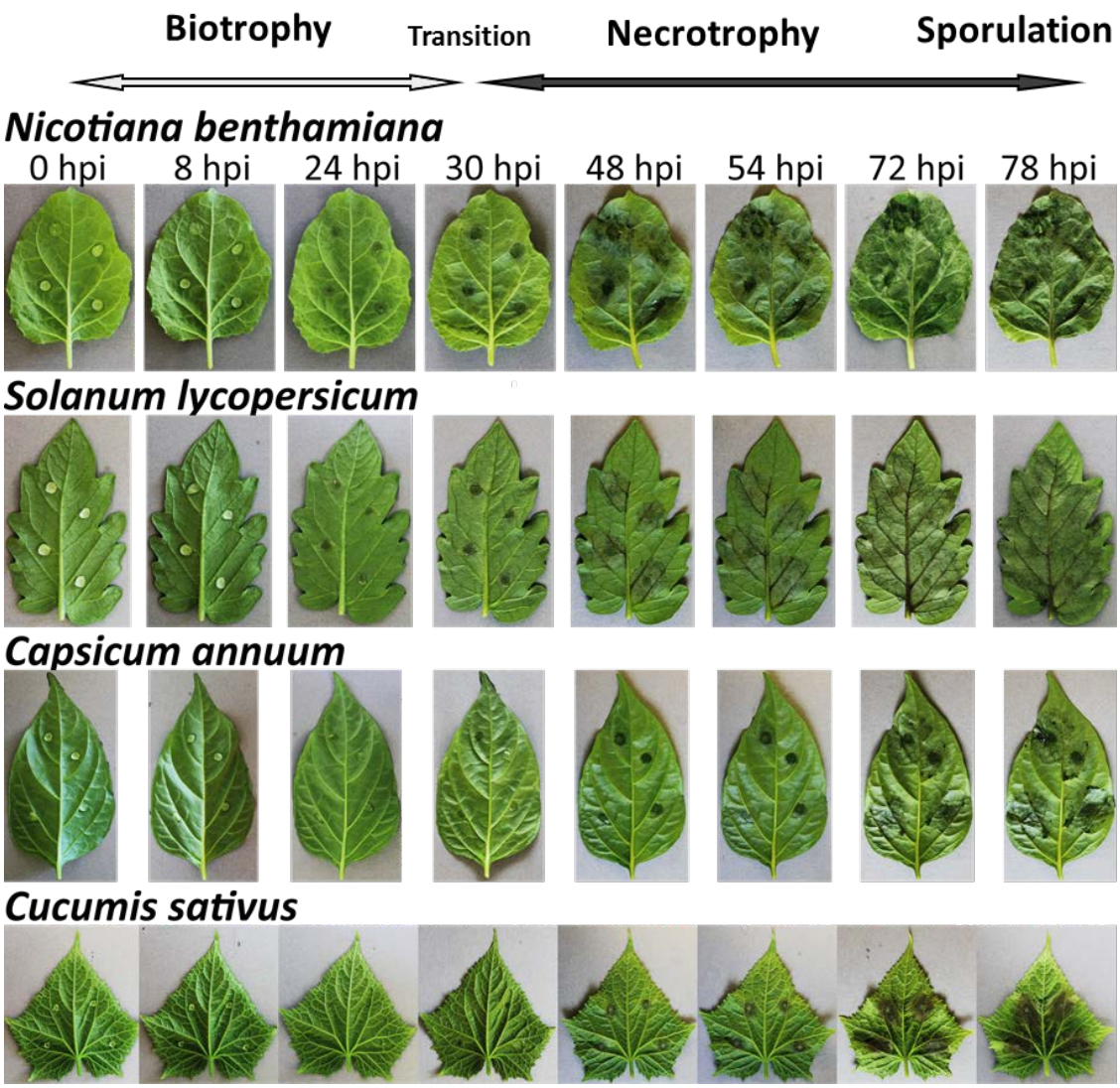

Figure 2.3: Phenotypic characterization of the infection progress of *P. capsici* on *N. benthamiana*, *S. lycopersicum, C. annuum* and *C. cucumis*
Detached leaves in a parallel time course experiment; *P. capsici* disease progression, showing the inoculation points at all time points at 0, 8, 24, 30, 48, 54, 72 and 78 hrs post infection (hpi). This time course experiment demonstrates in detail the presence of a biotrophic stage (0-24 hpi), onset of necrosis (necrotrophic phase) after 24 hpi and further tissue collapse and sporulation (>72 hpi), independent of the host.

2.3.2 Formation of haustoria shows intimate associations of *P. capsici* and host plants

Inoculations followed by phenotypic analyses across time points suggested that during the early stages of infection (up to 24 hpi), *P. capsici* ingress features a biotrophic phase during which the host tissue appears healthy and unaffected (Figure 2.1-2.3). These results are consistent with the observation that members of the *Phytophthora* genus form close associations with their hosts through haustoria, specialized infection structures that form the principal site of RXLR effector secretion and translocation into host cells [26].

Considering the obvious importance for successful infection, it was investigated whether *P. capsici* forms haustoria *in planta* in the three solanaceous hosts used in this study. Transgenic *N. benthamiana* plants carrying a GFP fluorescent marker of the endoplasmic reticulum (ER-GFP), standard tomato as well as pepper plants were inoculated with zoospores derived from a transgenic *P. capsici* strain, expressing the tdTomato fluorescent protein-coding gene. Colonization of leaf tissue was evidenced by growth of red fluorescent *P. capsici* hyphae in all three inoculated host tissues, and formation of haustoria, seen as red fluorescent bulbous pathogen structures that are encapsulated by GFP labelled endoplasmic reticulum (ER) from the host (*N. benthamiana* CB28 only), was assessed 24 hours after inoculation by confocal microscopy (Figure 2.4 and 2.5). These results are consistent with a biotrophic interaction and confirm the presence of the distinct infection vesicles.

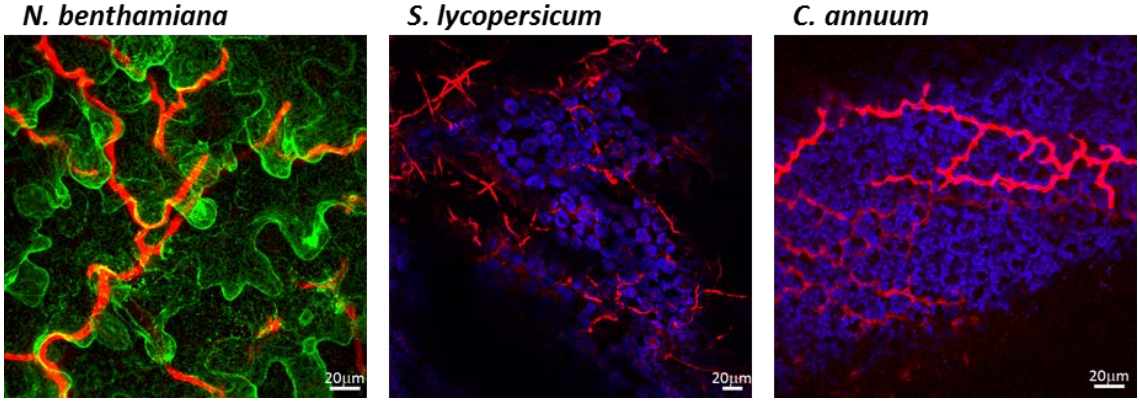

Figure 2.4: Confocal microscopy images show colonization by growth of mycelia from the pathogen *P. capsici*
Strain LT1534tdTomato (red), on three different host species: *N. benthamiana,* tomato (*S. lycopersicum*) and pepper (*C. annuum*). The infection was monitored at 24 hpi. Plants of *N. benthamiana* are expressing GFP in the ER (green) and the auto fluorescence of the chloroplasts is shown blue in the tomato and pepper plants.

A

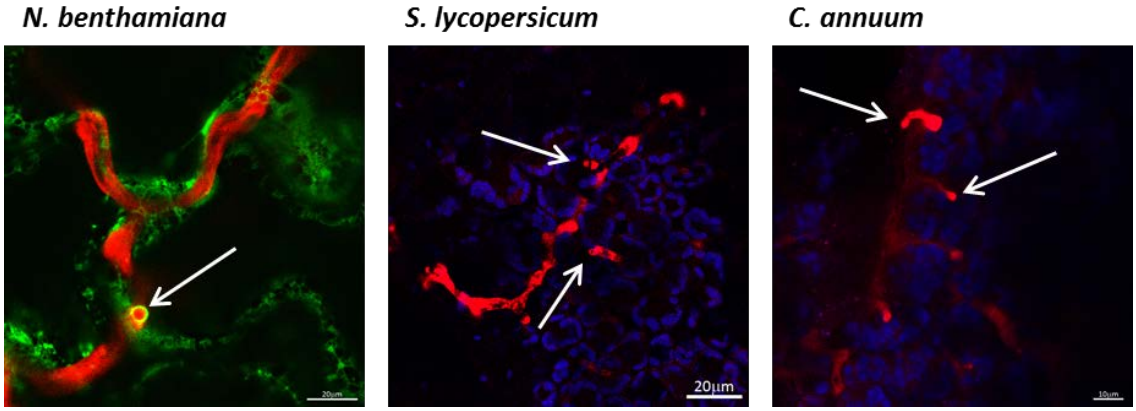

B

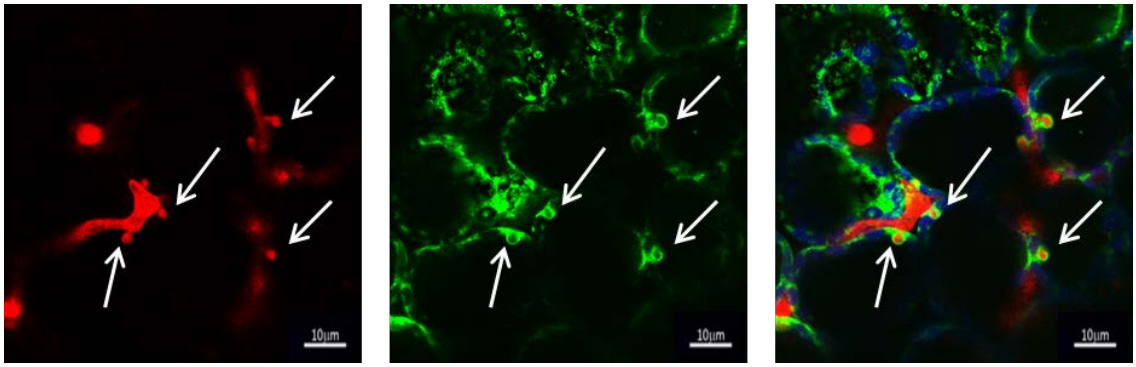

Figure 2.5: Confocal microscopy images show formation of haustorial structures of the pathogen *P. capsici* (indicated by arrows):
P. capsici strain LT1534tdTomato (red) was used for infection and imaged at 24 hpi, on three different host species: *N. benthamiana,* tomato (*S. lycopersicum*) and pepper (*C. annuum*). **A:** Haustorium in *N. benthamiana* nicely shown as bulbous GFP labelled structure encapsulating the red fluorescent pathogen (left image). Plants of *N. benthamiana* are expressing GFP in the ER (green) and the auto fluorescence of the chloroplasts is shown blue in the tomato and pepper plants. **B:** *P. capsici* haustoria formation in *N. benthamiana* (red, left image) and haustorial structures that push into the plant cell (green, middle image) demonstrated in single scan pictures. The right image shows the overlay of pathogen and host. The presence of the haustoria proves an interaction between the pathogen *P. capsici* and its host plants.

2.3.3 Development of a *P. capsici* marker gene set suited to tracking disease progression

To determine which specific time points represent the biotrophic, necrotrophic and sporulation stages, the *P. capsici* genome was mined to identify marker gene homologs for which pre-existing information from the literature was available. Using known *Phytophthora* marker gene sequences, BLAST searches were performed against the *P. capsici* gene model set to identify homologs in *P. capsici*. These searches with the *P. infestans* haustorium-specific membrane protein *Hmp1*, a biotrophic marker gene [152], *NPP1* for necrotrophy [90] and *Cdc14* as sporulation marker [153, 154] led to the identification of *PcHmp1*, *PcNPP1*

and *PcCdc14,* respectively. The marker genes were highly similar to those identified in *P. infestans* with a similarity at the protein level of 77% for *Hmp1*, 77% for *NPP1* and 88% for *CDC14*.

A quantitative Reverse-Transcription PCR (qRT-PCR) analysis of the biotrophy associated gene *PcHmp1* (Fig. 2.6) was conducted on *N. benthamiana* cDNA of the first time course experiment (0, 18, 42, 66, 90 hpi time points). Expression of the marker gene peaked at 18 hpi and was strongly reduced after the onset of the necrotic phase at 42 hpi (Fig.2.6). This result suggests that *P. capsici* infection features a distinct biotrophic stage early on (18 hpi) in infection of *N. benthamiana*, which is similar to results found for the *P. infestans Hmp1*-gene [152].

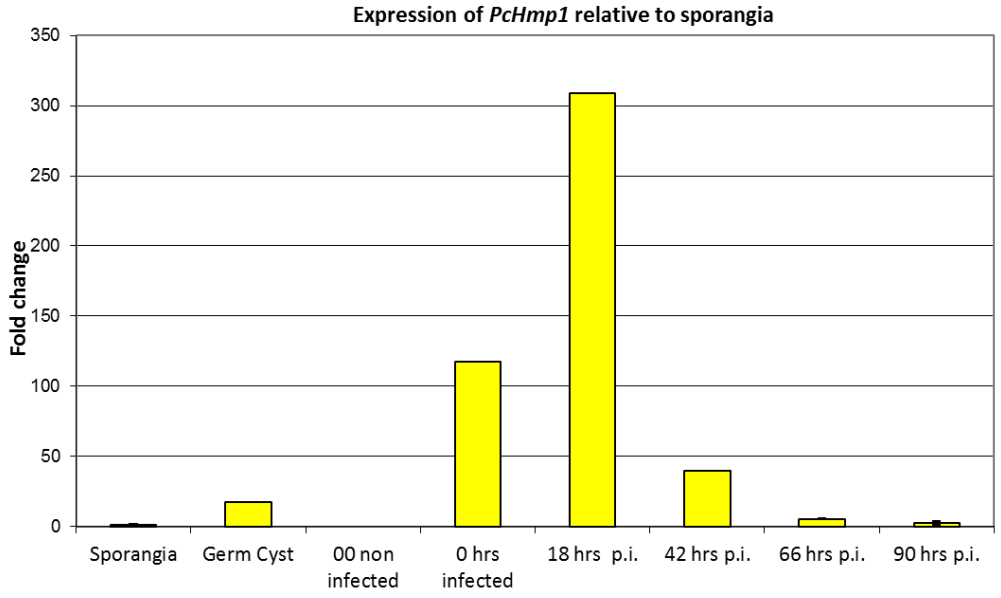

Figure 2.6: Molecular characterization of the biotrophy marker gene *PcHmp1*
Using quantitative RT-PCR of the infection stages on *N. benthamiana* at 0, 18, 42, 66 and 90 hpi (the infection time course assay is shown in Figure 2.1). In addition two *in vitro* samples (sporangia (0 hpi) and germinating cyst (24 hpi) were taken, directly derived from the inoculum and a non-infected leaf tissue as negative control. The gene expression of *PcHmp1* is highly upregulated at 18 hpi in the early stage of infection, demonstrating a distinct biotrophic phase. Fold difference of expression was compared to the sporangia sample. The error bars, which can be seen only in the three samples Sporangia, 66 hpi and 90 hpi due to small errors only, indicate three technical replicates.

The marker gene for biotrophy was also tested in semi-quantitative PCRs on the expanded time course series of *N. benthamiana* (see Figure 2.2 and 2.3) and was clearly upregulated during the biotrophic phase from 8-30 hpi, as it is shown in Figure 2.7 and 2.8. In all PCR

experiments on the infection time course experiments involving the three host species tomato, pepper and cucumber, *PcHmp1* was, compared with the consitutively expressed *PcTubulin*, highly expressed during the early phase of infection (Figure 2.8).
In *P. sojae*, the secreted Nep1 like protein PsojNIP is encoded by a gene whose expression coincides with transition to necrotrophy [90, 155]. *PcNPP1* was tested for suitability as a marker for this transition during *P. capsici* infection of *N. benthamiana*. Therefore gene expression was assessed on the second time course series (0, 8, 24, 30, 48, 54, 72 and 78 hpi time points, see Figure 2.2 and 2.3) using semi-quantitative PCR (Fig. 2.7). Interestingly, *PcNPP1* gene expression was first detected at 24 hpi, corresponding to the late biotrophic phase. Expression peaked at 30-48 hpi and was strongly reduced after the onset of the necrotic phase. PcCdc14 expression showed high upregulation at 0 hpi and after 72 hpi, coinciding with sporulation (Figure 2.7). In addition, this gene was expressed in the *in vitro* samples taken from sporangia/spores and germinating cysts.

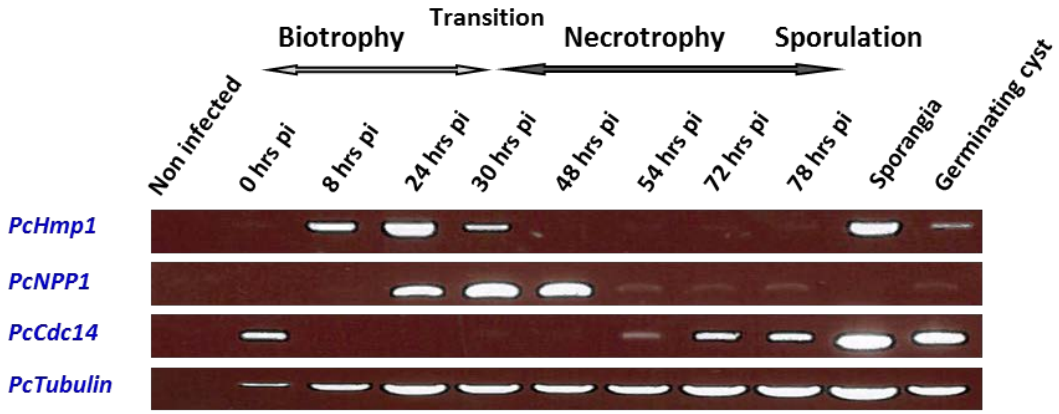

Figure 2.7: Molecular characterization of *P. capsici* infection on the model plant *N. benthamiana* (from detached leaves):
Semi-quantitative PCR on selected developmental stages demonstrates the three infection phases biotrophy, necrotrophy and sporulation using a defined set of *Phytophthora* markers and *PcTubulin* as control gene for constitutive expression.

2.3.4 Gene expression analysis

The infection assays revealed almost identical development of disease symptoms in all hosts (Figure 2.2 and 2.3), suggesting that the disease progression is not host dependent. To assess whether the timing of transition between developmental stages were affected by host species, semi-quantitative PCR experiments were conducted (Figure 2.8) and the same

time course and marker set as shown in Figure 2.7 was used for comparison. The established marker genes showed consistent expression patterns over the distinct infection phases on all four hosts, indicating a host-independent upregulation of 'stage specific' *P. capsici* genes. The constitutive control gene *PcTubulin* was lower expressed on pepper, which could be due to the cDNA synthesis procedure. Expression analyses on *P. capsici* infected cucumber leaves revealed an extended biotrophic phase with detectable *PcHmp1* expression extending to 48 hours after infection (Figure 2.8). In addition to *PcHmp1*, *PcNPP1* seems to be induced at a later timepoint, which also suggests that the biotrophic phase is extended; therefore no sporulation could be detected by the marker gene *Cdc14* at 72 or 78 hpi, but in the zoospore inoculum at 0 hpi the spores are present and detectable. Although the infection seems to be slightly delayed on cucumber, all marker genes are upregulated for the distinct infection phases and can distinguish biotrophy, necrotrophy and sporulation. In addition another sample derived at 8 hpi from the zoospore/sporangia inoculum was included to test whether the *in vitro* sampled germinating cysts show a difference in gene expression by harvesting after 8 hpi or 24 hpi. A clear difference was only visible for the gene *PcHmp1* with a higher expression in germinating cysts at 8 hpi in comparison to 24 hpi. In addition, the time point of expression of three known *P. capsici* RXLR effector genes, *Pc03192, Pc16737* and *Pc08599,* was compared to the marker set. Both *Pc03192* and *Pc16737* were upregulated together with the marker gene *PcHmp1* in all four host species, whereas *Pc08599* was co-regulated with the necrotrophy marker *PcNPP1* (Figure 2.8).

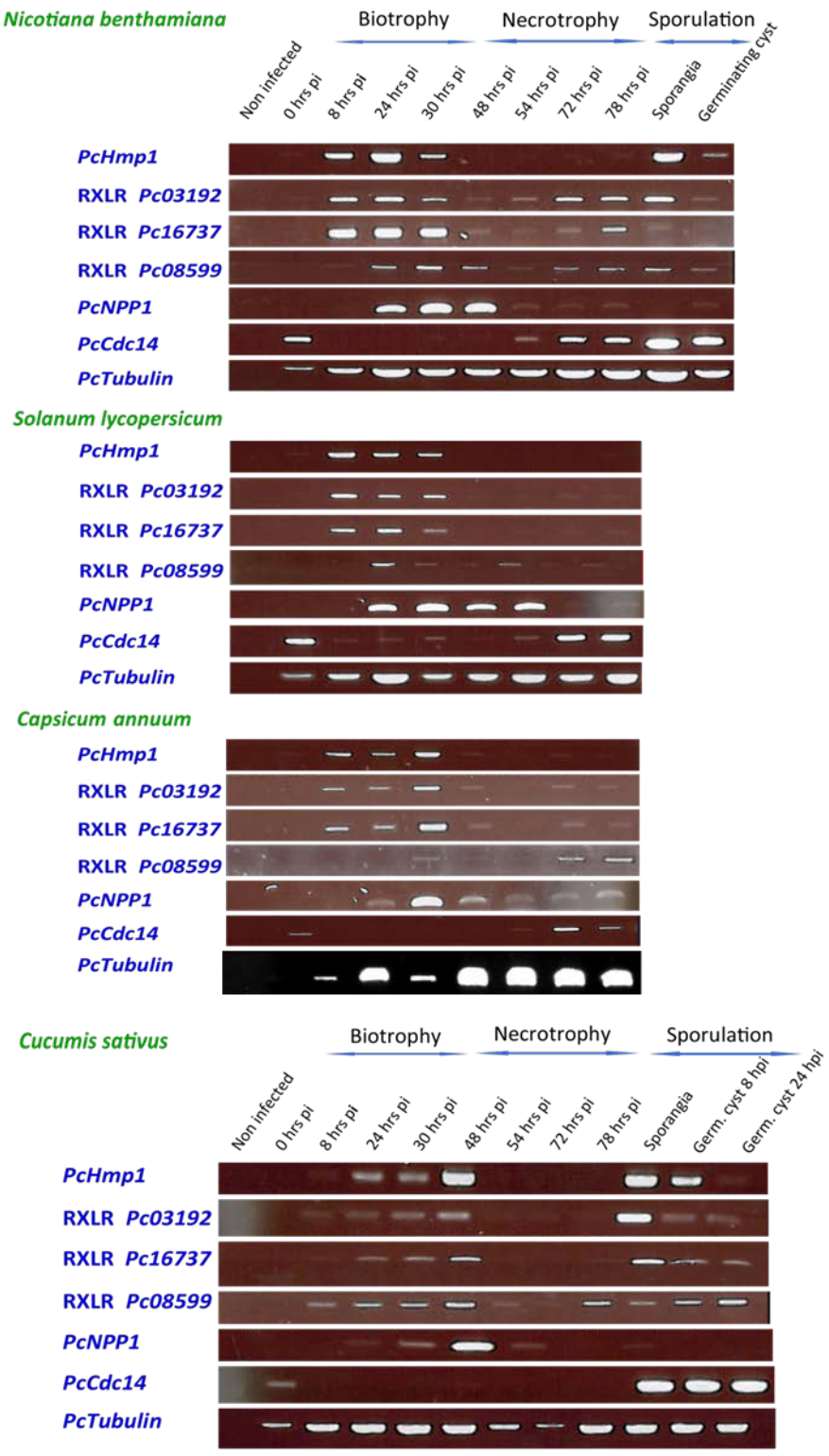

Figure 2.8: Molecular characterization of the marker gene set and three selected *P. capsici* RXLR genes on four host species

Semi-quantitative PCR assays show marker genes (same experiment for *N. benthamiana* as shown in Figure 2.7) for the three infection phases biotrophy, necrotrophy and sporulation, along with *PcTubulin*, which is a constitutive control gene. Both RXLR genes *Pc03192* and *Pc16737* were upregulated during the biotrophic phase, correlating with the marker gene *PcHmp1* in all four host species, whereas *Pc08599* was co-regulated with the necrotrophy marker *PcNPP1*. All marker genes showed similar expression patterns for all four hosts. On cucumber the infection was slightly delayed.

2.3.5 Transcriptome-wide comparison of *P. capsici* gene expression on *N. benthamiana*, tomato and pepper

In order to comparatively study *P. capsici* infection on the three host species *N. benthamiana*, *C. annuum* and *S. lycopersicum*, a microarray experiment was conducted. The aim was to gain knowledge of gene expression during biotrophy and necrotrophy, and whether a host dependent expression of *P. capsici* genes could be observed. Infection strategy and microarray design are in principle as described in Stam *et al.* (2012) [86] and Jupe *et al.* (2013) [67], but with fluorescent two-colour labelling of the RNA samples and only two biological replicates. To assess differences in *P. capsici* gene expression between hosts, PCR expression data on the markers were used to select equivalent infection stages from each host. Two samples per time course were chosen: one reflecting the biotrophic phase at 24 hpi and the second reflecting the necrotrophic phase at 72 hpi. Plant material from two independent time course assays were applied as the two replicates.
The probes were selected with the signal >100 after the fold change was compared to the median values across the samples in both replicates and the tomato time course array from Jupe *et al.* (2013) [67] was used as known data for the analysis. Lists of expressed *P. capsici* genes were generated for each time point and each individual host species which are presented in Figure 2.9 and 2.10 (Digital file 1). The *P. capsici* gene expression analyses revealed that from 20,530 gene models represented on the array [67], 67% of the genes were expressed in the *in planta* stages of tomato, whereas 33% were not expressed in tomato at all, based on the microarray explained in chapter three. Those 33% of *P. capsici* genes, that were not expressed during the tomato infection were used to create Venn diagrams and the number of expressed genes specific to *N. benthamiana* and pepper was compared between the two infection time points during biotrophy (24 hpi) and necrotrophy (72 hpi). Genes that were switched on or off on each given host were identified by this approach. These analyses revealed that during biotrophy, 14 genes are exclusively expressed on *N. benthamiana* and seven on pepper, while the expression of four genes is shared between both hosts (Figure 2.9 A and Table 2.3). During necrotrophy 11 genes are only expressed on *N. benthamiana* and 42 on pepper while two genes are shared (Fig 2.9 B and Table 2.3).

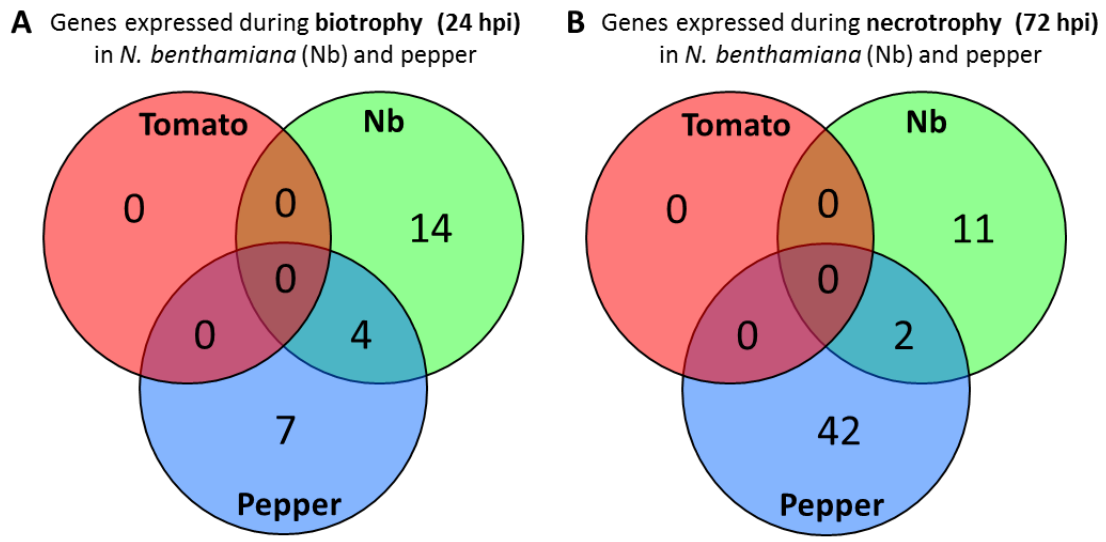

Figure 2.9: Host specific genes of *P. capsici* during biotrophy and necrotrophy
The Venn diagram shows host comparison in an infection assay of *P. capsici* during biotrophy (24 hpi) (A) and necrotrophy (72 hpi) (B) between *N. benthamiana* (Nb), *S. lycopersicum* (tomato) and *C. annuum* (pepper). For *N. benthamiana* (green) 18 genes are expressed during biotrophy at 24 hpi (left image), 13 during necrotrophy (right image) and for pepper (blue) 11 genes during biotrophy and 44 during necrotrophy. The red circle demonstrates that none of those genes specific for the two hosts are expressed anywhere in tomato *in planta* stages. Additionally the Venn diagram demonstrates the overlapping genes that are expressed in both plant species.

The identified host specific genes were further classified based on available gene annotation and their corresponding biological processes proposed using Gene Ontology (GO) annotation. No information was available for 45 of 80 genes (Table 2.3 and Digital file 1). Enrichment of GO annotations was only found for three annotations for *P. capsici* protein-binding genes (GO:0005515) in *N. benthamiana* and pepper during necrotrophy, however none during biotrophy. Further, only single genes for biological processes or cellular components could be detected (Table 2.3 and Digital file 1). Among those host specific genes identified during biotrophy were three RXLR encoding genes (RXLR_1, _3, _4; see Table 2.4) (Figure 2.10 A) that are exclusively expressed on *N. benthamiana* and one (RXLR_2, Table 2.4) on pepper. RXLR_2 expression is shared between both hosts. During necrotrophy (Fig 2.10 B) only one RXLR effector gene (RXLR_1, Table 2.4) is expressed exclusively on *N. benthamiana*. RXLR_1 in Figure 2.10 B was identified to be the same gene as RXLR_1 in Figure 2.10 A and is thus interestingly expressed at both time points of 24 and 72 hpi.

Table 2.3: Expressed *P. capsici* genes at 24 and 72 hpi specific to *N. benthamiana* and pepper with their corresponding biological processes proposed using Gene Ontology (GO) annotation

Timepoint 24 hpi	Plant species	GO ID	annotation	type	GO-term
Phyca11_129550	Peppper	3838	nucleus	cellular_component	GO:0005634
Phyca11_52244	Nb	-	-	-	-
PHYCAscaffold_10	Nb	-	-	-	-
PHYCAscaffold_12	Nb	-	-	-	-
Phyca11_62197	Nb	-	-	-	-
PHYCAscaffold_10	Nb	-	-	-	-
Phyca11_126085	Nb + Pepper	2682	serine-type endopeptidase activity	molecular_function	GO:0004252
Phyca11_13253	Nb	2176	DNA binding	molecular_function	GO:0003677
Phyca11_21093	Pepper	-	-	-	-
Phyca11_546107	Pepper	5830	metabolic process	biological_process	GO:0008152
		13916	cysteine desulfurase activity	molecular_function	GO:0031071
Phyca11_9359	Nb	3824	cell wall	cellular_component	GO:0005618
		13460	pectinesterase activity	molecular_function	GO:0030599
Phyca11_42479	Nb	-	-	-	-
Phyca11_21968	Pepper	-	-	-	-
Phyca11_22034	Nb	-	-	-	-
Phyca11_71166	Pepper	-	-	-	-
Phyca11_73434	Nb	2176	DNA binding	molecular_function	GO:0003677
		8441	DNA integration	biological_process	GO:0015074
		2175	nucleic acid binding	molecular_function	GO:0003676
Phyca11_113017	Pepper	2216	RNA binding	molecular_function	GO:0003723
		2417	RNA-directed DNA polymerase activity	molecular_function	GO:0003964
		4437	RNA-dependent DNA replication	biological_process	GO:0006278
Phyca11_20211	Nb + Pepper	-	-	-	-
Phyca11_6218	Nb + Pepper	3736	ATP binding	molecular_function	GO:0005524
		10082	ATPase activity	molecular_function	GO:0016887
		162	nucleotide binding	molecular_function	GO:0000166
		10269	nucleoside-triphosphatase activity	molecular_function	GO:0017111
PHYCAscaffold_92	Nb + Pepper	-	-	-	-

Table 2.3 continued

Timepoint 24 hpi	**Plant species**	**GO ID**	**annotation**	**type**	**GO-term**
Phyca11_71903	Nb	-	-	-	-
PHYCAscaffold_52	Nb	-	-	-	-
Phyca11_63212	Pepper	-	-	-	-
Phyca11_132351	Nb	-	-	-	-
Phyca11_570443	Nb	-	-	-	-
Timepoint 72 hpi	**Plant species**	**GO ID**	**annotation**	**type**	**GO-term**
Phyca11_541093	Pepper	-	-	-	-
Phyca11_540846	Pepper	2290	catalytic activity	molecular_function	GO:0003824
		5830	metabolic process	biological_process	GO:0008152
		6286	phospholipid biosynthetic process	biological_process	GO:0008654
		9978	phosphotransferase activity, for other substituted phosphate groups	molecular_function	GO:0016780
		2348		molecular_function	GO:0003882
Phyca11_12671	Pepper	-	-	-	-
Phyca11_82258	Pepper	586	chromatin	cellular_component	GO:0000785
		2180	chromatin binding	molecular_function	GO:0003682
		3838	nucleus	cellular_component	GO:0005634
		4483	chromatin assembly or disassembly	biological_process	GO:0006333
Phyca11_535833	Pepper	-	-	-	-
Phyca11_133087	Pepper	-	-	-	-
Phyca11_100476	Nb	3708	binding	molecular_function	GO:0005488
Phyca11_547601	Nb	3727	protein binding	molecular_function	GO:0005515
Phyca11_12462	Pepper	-	-	-	-
Phyca11_507679	Pepper	-	-	-	-
Phyca11_125172	Pepper	-	-	-	-
Phyca11_130611	Pepper	-	-	-	-
Phyca11_83749	Nb	2175	nucleic acid binding	molecular_function	GO:0003676
		5846	methyltransferase activity	molecular_function	GO:0008168
		15094	methylation	biological_process	GO:0032259
Phyca11_541703	Nb	3724	calcium ion binding	molecular_function	GO:0005509

Table 2.3 continued

Timepoint 72 hpi	Plant species	GO ID	annotation	type	GO-term
Phyca11_555829	Pepper	2196	transcription factor activity	molecular_function	GO:0003700
		3838	nucleus	cellular_component	GO:0005634
		4504	regulation of transcription, DNA-dependent	biological_process	GO:0006355
		19030	sequence-specific DNA binding	molecular_function	GO:0043565
Phyca11_560972	Pepper	-	-	-	-
Phyca11_125614	Pepper	-	-	-	-
scaffold_83_90[129822-130205]	Pepper	-	-	-	-
Phyca11_544803	Pepper	9320	membrane	cellular_component	GO:0016020
Phyca11_560975	Pepper	-	-	-	-
Phyca11_559520	Pepper	3727	protein binding	molecular_function	GO:0005515
Phyca11_108526	Pepper	9985	hydrolase activity	molecular_function	GO:0016787
Phyca11_96894	Pepper	3724	calcium ion binding	molecular_function	GO:0005509
Phyca11_509786	Pepper	2175	nucleic acid binding	molecular_function	GO:0003676
		3827	intracellular	cellular_component	GO:0005622
		5939	zinc ion binding	molecular_function	GO:0008270
Phyca11_16798	Pepper	-	-	-	-
Phyca11_103792	Pepper	-	-	-	-
Phyca11_109274	Nb	5939	zinc ion binding	molecular_function	GO:0008270
Phyca11_66715	Pepper	3043	protein kinase activity	molecular_function	GO:0004672
		3736	ATP binding	molecular_function	GO:0005524
		4602	protein amino acid phosphorylation	biological_process	GO:0006468
		3079	protein-tyrosine kinase activity	molecular_function	GO:0004713
		3045	protein serine/threonine kinase activity	molecular_function	GO:0004674
Phyca11_72076	Pepper	-	-	-	-
Phyca11_106663	Pepper	-	-	-	-
Phyca11_9893	Nb + Pepper	9320	membrane	cellular_component	GO:0016020
		12906	metal ion transport	biological_process	GO:0030001
		21296	metal ion transmembrane transporter activity	molecular_function	GO:0046873

Table 2.3 continued

Timepoint 72 hpi	Plant species	GO ID	annotation	type	GO-term
Phyca11_58463	Nb	2628	aspartic-type endopeptidase activity	molecular_function	GO:0004190
		4639	proteolysis	biological_process	GO:0006508
Phyca11_503749	Pepper	2290	catalytic activity	molecular_function	GO:0003824
		3708	binding	molecular_function	GO:0005488
		5830	metabolic process	biological_process	GO:0008152
		2413	NADPH:quinone reductase activity	molecular_function	GO:0003960
Phyca11_133363	Pepper	2628	aspartic-type endopeptidase activity	molecular_function	GO:0004190
		4639	proteolysis	biological_process	GO:0006508
Phyca11_71166	Pepper	-	-	-	-
Phyca11_533182	Pepper	4650	amino acid metabolic process	biological_process	GO:0006520
		9710	oxidoreductase activity	molecular_function	GO:0016491
		2290	catalytic activity	molecular_function	GO:0003824
		3708	binding	molecular_function	GO:0005488
		5830	metabolic process	biological_process	GO:0008152
		2758	glutamate dehydrogenase activity	molecular_function	GO:0004352
Phyca11_133850	Pepper	2216	RNA binding	molecular_function	GO:0003723
		2417	RNA-directed DNA polymerase activity	molecular_function	GO:0003964
		4437	RNA-dependent DNA replication	biological_process	GO:0006278
Phyca11_552962	Pepper	-	-	-	-
Phyca11_109480	Nb	9946	transferase activity, transferring groups other than amino-acyl groups	molecular_function	GO:0016747
Phyca11_102150	Pepper	-	-	-	-
Phyca11_20211	Nb	-	-	-	-
Phyca11_544502	Pepper	3727	protein binding	molecular_function	GO:0005515
Phyca11_6218	Nb + Pepper	3736	ATP binding	molecular_function	GO:0005524
		10082	ATPase activity	molecular_function	GO:0016887
		162	nucleotide binding	molecular_function	GO:0000166
		10269	nucleoside-triphosphatase activity	molecular_function	GO:0017111

Table 2.3 continued

Timepoint 72 hpi	Plant species	GO ID	annotation	type	GO-term
PHYCAscaffold_92_f_4945_5391_1	Nb	-	-	-	-
Phyca11_50941	Pepper	-	-	-	-
Phyca11_63510	Pepper	-	-	-	-
Phyca11_75944	Nb	3043	protein kinase activity	molecular_function	GO:0004672
		3736	ATP binding	molecular_function	GO:0005524
		4602	protein amino acid phosphorylation	biological_process	GO:0006468
		3079	protein-tyrosine kinase activity	molecular_function	GO:0004713
Phyca11_52807	Pepper	9320	membrane	cellular_component	GO:0016020
Phyca11_132351	Nb	-	-	-	-
Phyca11_577733	Pepper	6387	UDP-N-acetylmuramoylalanyl-D-glutamyl-2,6-diaminopimelate-D-alanyl-D-alanine ligase activity	molecular_function	GO:0008766
		10509	ribosomal S6-glutamic acid ligase activity	molecular_function	GO:0018169
		19237	coenzyme F420-0 gamma-glutamyl ligase activity	molecular_function	GO:0043773
		19238	coenzyme F420-2 alpha-glutamyl ligase activity	molecular_function	GO:0043774
Phyca11_53569	Pepper	-	-	-	-
Phyca11_129051	Pepper	-	-	-	-
Phyca11_82350	Pepper	-	-	-	-
Phyca11_133234	Pepper	-	-	-	-
Phyca11_565320	Pepper	3046	transmembrane receptor protein serine/threonine kinase activity	molecular_function	GO:0004675
		3047	3-phosphoinositide-dependent protein kinase activity	molecular_function	GO:0004676
		3048	DNA-dependent protein kinase activity	molecular_function	GO:0004677
		3049	AMP-activated protein kinase activity	molecular_function	GO:0004679
		3050	casein kinase activity	molecular_function	GO:0004680
		3051	casein kinase I activity	molecular_function	GO:0004681
		3057	cyclic nucleotide-dependent protein kinase activity	molecular_function	GO:0004690

Table 2.3 continued

Timepoint 72 hpi	Plant species	GO ID	annotation	type	GO-term
		3061	eukaryotic translation initiation factor 2alpha kinase activity	molecular_function	GO:0004694
		3062	galactosyltransferase-associated kinase activity	molecular_function	GO:0004695
		3063	glycogen synthase kinase 3 activity	molecular_function	GO:0004696
		3065	calcium-dependent protein kinase C activity	molecular_function	GO:0004698
		3067	atypical protein kinase C activity	molecular_function	GO:0004700
		3068	receptor signaling protein serine/threonine kinase activity	molecular_function	GO:0004702
		3070	NF-kappaB-inducing kinase activity	molecular_function	GO:0004704
		3071	JUN kinase activity	molecular_function	GO:0004705
		3072	JUN kinase kinase kinase activity	molecular_function	GO:0004706
		3074	MAP kinase kinase activity	molecular_function	GO:0004708
		3076	MAP/ERK kinase kinase activity	molecular_function	GO:0004710
		3077	ribosomal protein S6 kinase activity	molecular_function	GO:0004711
		3084	Janus kinase activity	molecular_function	GO:0004718
		6004	MAP kinase 1 activity	molecular_function	GO:0008338
		6005	MP kinase activity	molecular_function	GO:0008339
		6015	MAP kinase kinase kinase kinase activity	molecular_function	GO:0008349
		6196	JUN kinase kinase activity	molecular_function	GO:0008545
		10102	MAP kinase 2 activity	molecular_function	GO:0016908
		10103	SAP kinase activity	molecular_function	GO:0016909
		11472	transmembrane receptor protein kinase activity	molecular_function	GO:0019199
		12154	cyclin-dependent protein kinase activating kinase activity	molecular_function	GO:0019912
		17037	GTP-dependent protein kinase activity	molecular_function	GO:0034211

Table 2.4: Expressed RXLR effector genes of *P. capsici* between *N. benthamiana* and pepper

RXLR gene	Gene name: Primary accession	Signal peptide	Length in aa	Microarray expressed hpi	PCR expressed hpi
RXLR_1	PHYCAscaffold_92_f_4945_5391_1	MRFSQVLVVAAVSLLFASETAA	148	24/72	8/78
RXLR_2	PHYCAscaffold_10_r_709287_708784_5	MRLSVILLVVAAFAVA	167	24	8-48
RXLR_3	PHYCAscaffold_52_r_440859_440521_6	MRICFALLLAVTALTAVVSG	112	24	-
RXLR_4	PHYCAscaffold_12_r_646417_645890_4	MRLSYFVLVAAVCIFACCEQVAA	175	24	24-30/72-78

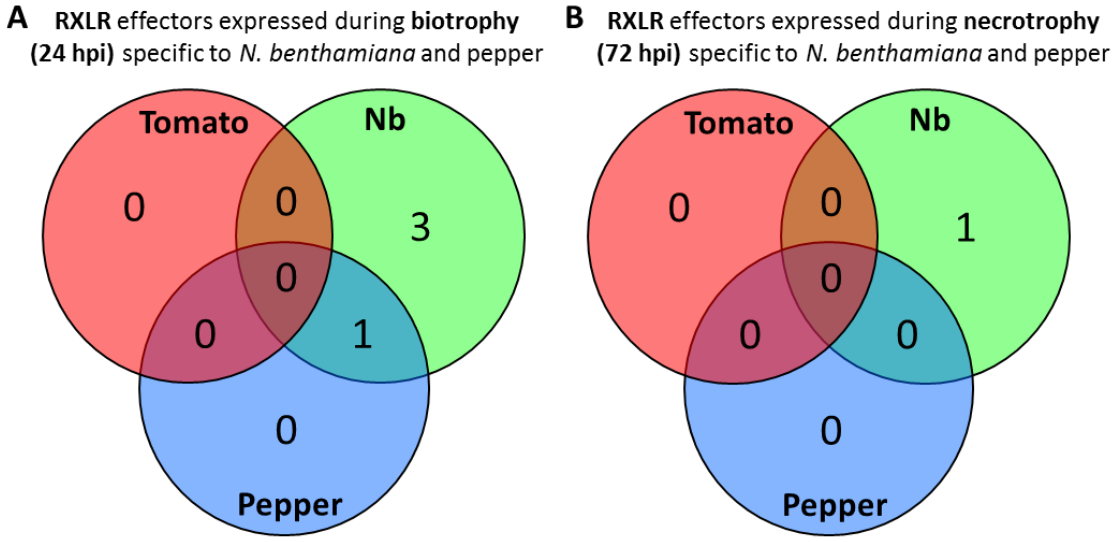

Figure 2.10: Host specific RXLR genes of *P. capsici* during biotrophy and necrotrophy
Venn diagram shows host comparison in an infection assay of *P. capsici* RXLR effector genes during biotrophy (24 hpi) (A) and necrotrophy (72 hpi) (B) between *N. benthamiana* (Nb), *S. lycopersicum* (tomato) and *C. annuum* (pepper). For *N. benthamiana* (green) four genes are expressed during biotrophy at 24 hpi (left image), one gene during necrotrophy (right image) and for pepper (blue) one gene during biotrophy and none during necrotrophy. The red circle demonstrates that none of those RXLR effectors specific for the two hosts are expressed anywhere in tomato *in planta* stages. Additionally the Venn diagram demonstrates the overlapping genes that are expressed in both plant species.

To confirm the expression of the four RXLR genes that could be identified (Table 2.4), primers were designed on the sequences encoding mature effector proteins (after the signal peptides) for semi-quantitative PCR analysis on cDNA from both time course experiments. RXLR_3 (Table 2.4) could not be detected in any of the PCR analyses. As presented in Figure 2.11 A, expression could be shown on *N. benthamiana* at 8 hpi (RXLR_1 and _2) and 24 hpi

(RXLR_2 and _4). No such expression could be found on the other two hosts pepper or tomato, using cDNA from the first microarray time course replicate (Fig. 2.2). Using cDNA from the second replicate (time course Figure 2.3 and Figure 2.11 B), expression could be shown on *N. benthamiana* at 8 hpi (RXLR 1 and 2), 24 hpi (RXLR_1, _2, _4), 30 hpi (RXLR_2 and _4), 48 hpi (RXLR_2) and 78 hpi (RXLR_1). On tomato, a very faint band is visible at 8 hpi (RXLR_1) and on pepper expression was detected at 30 and 72-78 hpi (RXLR_4).

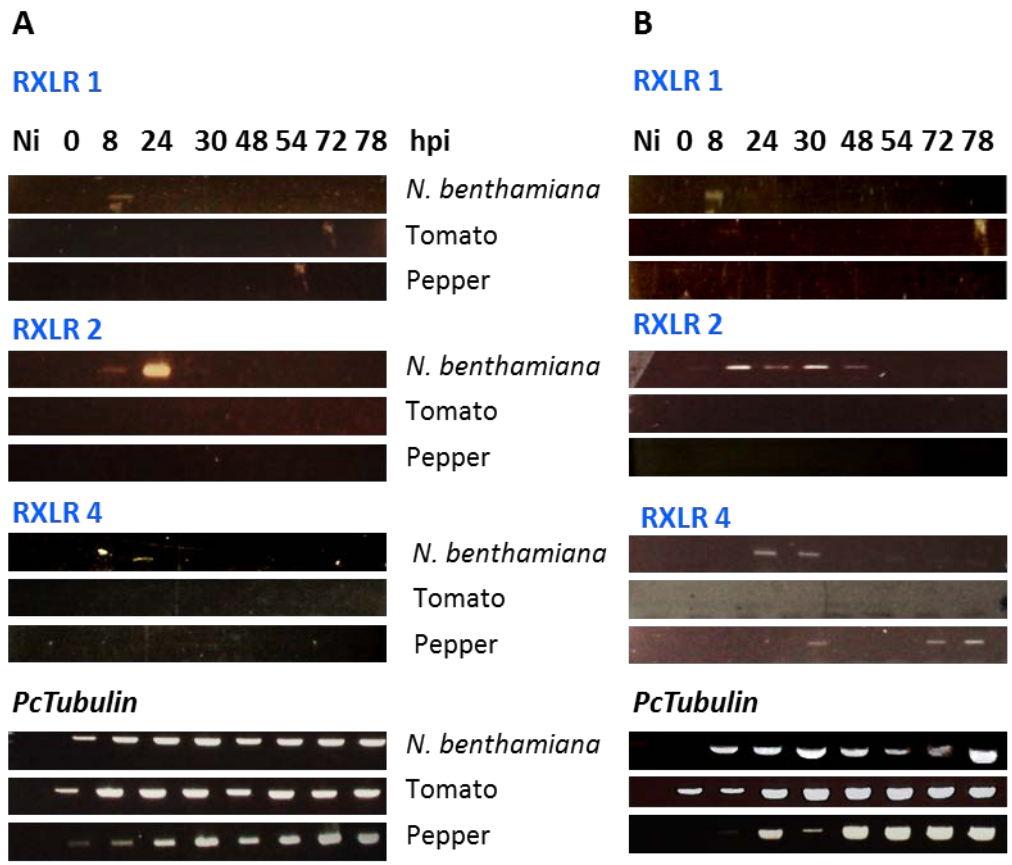

Figure 2.11: Confirmation of *P. capsici* RXLR effector genes on three host species by semi-quantitative PCR analyses
(A) First replicate of microarray time course: Expression is shown on *N. benthamiana* for RXLR1 at 8 hpi, for RXLR2 at 8 and 24 hpi, and for RXLR4 at 24 hpi. No upregulation could be detected on pepper or tomato within this series. **(B)** Second replicate of microarray time course: Expression is shown on *N. benthamiana* for RXLR1 at 8 and 78 hpi, for RXLR2 at 8-48 hpi, and for RXLR4 at 24 and 30 hpi. In addition expression is detected on pepper for RXLR4 at 30 and 72-78 hpi. Low expression could be also found on tomato for RXLR1 at 8hpi. *PcTubulin* is shown along on all three host species as constitutive control gene.

Conclusively, the arrays agree only with the PCR-analyses for RXLR_1, which was shown to be expressed at both time points (24 and 72 hpi). In contrast RXLR_2 was found to be expressed on the array in both hosts, *N. benthamiana* and pepper (Figure 2.10 A, Table 2.4),

but could only be detected in the PCR analyses on *N. benthamiana* (Figure 2.11), whereas RXLR_4 was detected in the PCRs, but not on the array as being expressed in pepper. Unfortunately for RXLR_2 and RXLR_4 the results have been inconclusive, therefore a quantitative PCR would be necessary to validate the gene expression of those effectors. For none of the four RXLR effector genes (Table 2.4), could any molecular function or biological process be found within the GO annotation terms.

2.4 Discussion

In this chapter, a *P. capsici*-host interaction model system was created for four different plant host species that will allow more detailed and targeted molecular analyses of the *P. capsici* lifestyle. To distinguish the distinct life stages during the infection process, a set of pathogen specific genes was defined that can be used as molecular markers for disease progression in PCR based assays. This set is based on existing literature and sequence information of the draft genomes from *P. capsici* and *P. infestans*, and consists of three *Phytophthora* marker genes that could inform on disease progression and development after infection. The haustorial membrane protein *Pi*HMP1 from *P. infestans* was described to be expressed during biotrophy and to accumulate around haustoria. Consistent with its expression and localisation patterns, it was found to be essential for host colonization [152]. PcNPP1 is a member of the large family of necrosis-inducing Nep1-like proteins (NLPs), as described previously [67]. NLPs have been identified in bacteria, fungi and oomycetes [90]. Expression analyses revealed that this gene is also upregulated during the transition from biotrophy to necrotrophy at 24, 30 and 48 hrs post inoculation. *PcNPP1* can thus not only be used as a marker for necrotrophy, but as marker for the transition phase, because its upregulation overlaps with *PcHmp1* expression at 24 and 30 hrs, as discussed in Kanneganti *et al.* (2006) [90] for *P. infestans*.

Presence and expression of the genes *PcHmp1*, *PcNpp1* and *PcCdc14* during the *P. capsici* infection cycle confirm a hemibiotrophic life cycle. Hemibiotrophs switch their mode of action from non-killers to killers at different stages of their life cycle [156]. The marker gene set presented here can thus not only be used in analysis of gene expression in semi-quantitative and quantitative RT-PCRs, but also as guides to cluster genes specific for the different infection stages in microarray or RNAseq experiments.

Using confocal microscopy, a partly biotrophic life-style was also confirmed by the formation of haustorial structures into host cells (Figure 2.3 and 2.4). These structures are evidence for the very close physical interaction between pathogen and host and require the pathogen to keep the host cell alive. These structures are known from a wide range of oomycetes, fungi or even parasitic plants with biotrophic and hemi-biotrophic life-styles, including the model pathogens *Hyaloperonospera arabidopsidis* and *Albugo* spp. [25, 152, 157-161].

Two *P. capsici* RXLR effector genes, *Pc03192* and *Pc16737* showed a clear upregulation during the biotrophic phase at 8, 24 and 30 hrs post inoculation, but they were also expressed at lower levels in the necrotrophic phase. This might however be due to contamination during the harvest of later time points with fresh *P. capsici* mycelium. As an endogenous control gene, *PcTubulin* was tested, which showed expression throughout all infection stages in all three plant species. Although a quantitative RT-PCR with known concentrations of spiked in controls would be useful in addition to determine if *PcTubulin* is really being expressed at the same level in all infection samples.

Phenotypic observations throughout the course of infection suggested that the rate of pathogen growth is not affected by the host. However, on the molecular level *P. capsici* expresses genes specific to the host. A microarray experiment was conducted to compare the three host species and showed that 80 genes are specific to *N. benthamiana* or pepper during biotrophy and necrotrophy, respectively. To validate the host specific gene expression, a quantitative RT-PCR would be required. Also, to confirm the host specific expression of the four putative RXLR effector genes (Figure 2.11), quantitative RT-PCR analyses are required and more time points sampled would give a better chance of detecting host specific genes. There is the possibility that other host specific RXLRs were missed out due to slight differences in the timing of their expression in the hosts tested. In addition a third replicate for the microarray would give the possibility to execute statistical tests on the three host comparison assay. Based on the presented results of differential gene expression patterns between hosts on the microarray, it can be hypothesised that *P. capsici* features host specific genes, which could help the pathogen for an infection strategy that allows it to adopt a broad host range spectrum. However, the low number of host specific RXLR genes suggests that most effectors have similar functions in all tested Solanaceae hosts. The inclusion of cucumber as a more distant host for the

microarray study will in the future provide additional insight into differential expression of genes between more distantly related plant species.

It was interesting to note that RXLR_1 and RXLR_4 were not detected on the microarray or by PCR in the first generation of spores coming from V8-agar plates and used to infect the experimental plants, but could be detected host specifically after 78 hours. These genes might have been activated for the following generation by plant compounds. To fully confirm whether the three presented RXLR effectors are host-specific, a follow up experiment needs to be conducted that uses two or more generations of *P. capsici* harvested initially from V8-plates to infect tomato, *N. benthamiana* and pepper. Spores harvested from these three hosts are then used to independently inoculate tomato, *N. benthamiana* and pepper again. Genes that are host specific won't be transcribed when the spores are transferred between species, but will remain expressed when transferred within the same host species.

The development, described here, of a model infection system on the molecular level will add to a better understanding of the mechanisms of pathogenicity and infection processes and therefore forms a scaffold for future studies.

3 *Phytophthora capsici*-tomato interaction features dramatic shifts in gene expression associated with a hemi-biotrophic lifestyle

This chapter was published as article in Genome Biology 2013, and most parts of the text are taken from this publication. Work carried out by people other than me, is indicated in the text.

3.1 Introduction

In Chapter 2, microarray analysis gave an indication for the complex signal interplay between pathogens and their hosts. Despite the availability of genome sequences of tomato as a host and *P. capsici* as its pathogen, little is known about their signal interplay during infection. In particular, accurate descriptions of coordinated relationships between host and microbe transcriptional programs are lacking.

Here, the molecular interaction between the hemi-biotrophic broad host range pathogen *Phytophthora capsici* and tomato was explored. Infection assays and use of a composite microarray allowed unveiling of distinct changes in both *P. capsici* and tomato transcriptomes. These included two distinct transcriptional changes associated with early infection and the transition from biotrophy to necrotrophy that may contribute to infection and completion of the *P. capsici* lifecycle.

For the microarray analyses, a custom design was created that combined the full predicted transcriptomes of pathogen and tomato on one array. This special design helped to define transcriptional changes in *Phytophthora,* linked to (disease) development, as well as the identification of distinct transcriptional responses in tomato, linked to pathogen lifestyle. The requirement for *Phytophthora* enhanced protein production and metabolism in biotrophy was unveiled, as well as the catabolism during its transition to necrotrophy and the induction of signalling and developmental processes upon sporulation. The results provide a unique insight into coordinated transcriptional reprogramming in host and pathogen during infection and lay the foundation for future studies of transcriptional programmes that drive parasitic lifestyles. This work opens the door towards comparative transcriptomics that should help unravel pathogen infection strategies and exploit host basal defense responses.

3.2 Material and Methods

Plant material

Solanum lycopersicum 'Moneymaker' plants were grown in controlled growth chambers at 22 °C, a photoperiod of 16 h, and supplemented by artificial light. The third leaf from the top of six weeks old plant were detached and placed upside down in humid transparent plastic trays in a controlled incubator with the same settings as in the growth chamber. Leaf discs centred on infected lesions and mock-inoculated tissue were harvested by a cork borer (ϕ 7 mm) and frozen in liquid nitrogen before RNA extraction.

***Phytophthora capsici* inoculation and *in vitro* samples**

Phytophthora capsici wild type strain LT1534 was grown in Petri dishes on V8 agar medium [146] in a dark climate chamber at 25 °C for four days and for three days under standard light at 22 °C. To induce zoospore release, plates were flooded with ice-cold distilled water and spores were harvested from sporulating mycelia by dislodging the sporangia with a sterile glass spreader. Sporangial suspensions were collected and incubated at room temperature under bright light conditions. Release of zoospores was followed and numbers counted under the microscope in a haemocytometer and adjusted to $1x10^5$ ml. The detached leaves were inoculated with four droplets (each 20 µl) of the zoospore solution. In addition to the infectious stages, three *in vitro* samples were taken: sporangia/zoospores (Spor), germinating cysts (GC) and mycelia (Myc) grown *in vitro*. Spor (taken at 0 hpi) and GC (taken at 16 hpi) were sampled from the same inoculum/sporangial suspension, differing in harvesting times. They were collected from 10 ml of sporangial suspension after an incubation time of 1 h (Spor) and 16 h (GC) at 22 °C. The mycelia were grown in 1 ml pea broth, infected with 20 µl of inoculum at 22 °C and harvested 48 hpi by collecting the mycelial mat into 10ml-tubes. All samples were placed in the controlled environment with the same settings and conditions as the leaf samples and harvested by centrifugation for 2 min at 1500 rcf. After taking off the supernatant, the pellets were collected and frozen in liquid nitrogen.

RNA extractions and cDNA synthesis

RNA was isolated from frozen leaf tissue following the protocol of the RNeasy Plant Mini Kit (Qiagen) and treated afterwards with DNaseI (DNA-free™ DNA Removal Kit (DNaseI),

Ambion/Life Technologies) to remove genomic DNA contamination according to the manufacturer's instructions. To test for genomic DNA contamination, a PCR using GoTaq Flexi polymerase (Promega) and primers specific for *PcTubulin* (Forward: GACTCGGTGCTTGATGTTGTC; Reverse: CCATCTCATCCATACCCTCGCCAG), was performed on the extracted RNA in 50 µl reactions following manufacturers recommendations and as described previously in chapter 2. cDNA was synthesized using 500 ng of total RNA, using Oligo dT primer and the SuperScript (TM)II cDNA synthesis kit (Invitrogen) following the manufacturer's instructions.

Microarray design and analysis

A custom 60-mer oligonucleotide microarray was designed from predicted transcripts of the *P. capsici* (LT1534 v11.0 [7]), and *S. lycopersicum* (ITAG 2.3, [35]) genomes using eArray software (https://earray.chem.agilent.com/earray/) in cooperation with Pete Hedley (James Hutton Institute, Dundee, UK), Edgar Huitema and Remco Stam (University of Dundee, UK). The *P. capsici* predicted transcriptome (Phyca11_No.) was supplemented with separately predicted CRN effectors (Scaffold_No.), as described by Stam et al. [86], and RxLR effectors (PhycaSCAFFOLD_No.) as described below. The design is available at ArrayExpress (accession A-MEXP-2253; http://www.ebi.ac.uk/arrayexpress/) and represents 20,530 transcripts for *P. capsici* and 34,510 transcripts for *S. lycopersicum*. RNA labeling and microarray hybridisation procedures were performed together with Jenny Morris at Genome Technology, James Hutton Institute, as described in Chapter 2 and Appendix 1, with the difference that one-colour labeling has been used here. In short, fluorescent one-colour labelling of the RNA and hybridization was performed as recommended (Agilent One-Color Microarray-Based Gene Expression Analysis (Low Input Quick Amp Labeling) v. 6.5) using 8x60k format slides. The microarray experimental design, along with raw datasets is published and available at ArrayExpress (Accession A-MEXP-2253). The extracted dataset was separated for each array into *P. capsici* and *S. lycopersicum* data to allow independent processing. The data extraction was carried out by Pete Hedley. Datasets were each independently quality filtered using flag values (present or marginal in 2/3 replicates) and then quantile normalised in Genomics Suite software (Partek), prior to loading into Genespring (Agilent v. 7.3) software for analysis. The analysis was carried out in cooperation with Pete Hedley, Edgar Huitema and Remco Stam, whereupon the quantile normalization

was done by Runxuan Zhang and Pete Hedley (James Hutton Institute, Dundee, UK). Statistical tests were performed using 1-way ANOVA (Benjamini & Hochberg multiple testing correction, p-value ≤0.005) to identify significantly changing genes across the *in planta* timecourse. For grouping genes that are co-regulated with markers of *Phytophthora* infection stages, a Minimum Pearson Correlation of at least 85% was used to define clusters. Candidate secreted proteins were identified by using SignalP (version 3; http://www.cbs.dtu.dk/services/SignalP-3.0/) analyses on the predicted *P. capsici* proteome [162], applying an HMM cut off score of <0.5. Predicted membrane proteins were identified using TMHMM [163] (http://www.cbs.dtu.dk/services/TMHMM-2.0/) and removed from the secreted protein set as described previously [86].

Marker gene sequences

For all marker genes, the original *P. infestans* sequences were retrieved from NCBI (http://www.ncbi.nlm.nih.gov/guide/) using the published accession numbers (*PiHmp1:* EU680858.1 *; PiNPP1*: AF356840.1; *PiCDC14:* AY204881.1). The sequences were then applied in a tBLASTn and BLASTp [149] search (default settings) against the *P. capsici*-genome version 11 (http://genome.jgi-psf.org/Phyca11/) to get the corresponding *P. capsici* homologous sequences to which following primer pairs (as described previously in chapter 2) have been designed (*PcHmp1*-F: CATGATGGCAGTCATGGTCGGTGAAG, *PcHmp1*-R: TTAGCTAACATTGAGGCGGGCATGCAG; *PcNPP1*-F: CAGCTCCACATCACCAACGGct, *PcNPP1*-R: CTCTTCCCGTTCAAATAGTTC; *PcCDC14*-F: GGAAGCGATTGAGTTCTTGC, *PcCDC14*-R: TTCTCCACACGCTCAAAGTG). RT-PCRs were performed in 25-µl reaction volumes with 1 µl of cDNA (1:5 dilution) as template. The GoTaq® Flexi DNA Polymerase from Promega was used with all components according to the manufacturer's protocol. Thermocycling conditions of the PCR were: 94 °C for 2 min, followed by 30 cycles at 94 °C for 30 sec, 57 °C for 30 sec and 72 °C for 2:30 min. Extension was finalized at 72 °C for 10 min to allow filling of incomplete polymerizations. Amplicons from cDNA were Sanger sequenced and derived sequences were aligned to *P. infestans* reference sequences using the program ClustalW Multiple Sequence Alignment [150] to investigate the levels of sequence similarity. *P. capsici* marker genes were highly similar to those identified in *P. infestans* with a similarity of the protein sequences as follows: *Hmp1*: 77%, *NPP1*: 77% and *CDC14*: 88%.

Identification of PcRXLR complement

Analysis of previously published *Phytophthora capsici* RXLRs [43] indicated that the present database was incomplete. Therefore a new identification strategy was implemented whereby RXLRs were sought using previously published methods [26, 103, 151]. All output was collated and compared to the previously predicted *Phytophthora capsici* RXLR complement using BLASTN. Redundancies were removed and in case of difference in predicted ORF length, sequences were compared with known *P. infestans* RXLR sequences and manually curated. This yielded a set of 516 RXLR candidates, of which 471 were represented on the array (Digital file 10). The identification of RXLR coding genes was carried out by Remco Stam and Edgar Huitema.

Confocal imaging

Zoospores ($5x10^5$ ml generated as described above) of transformed *P. capsici* LT1534:tdTOMATO were inoculated in 20 µl droplets onto leaves of *Solanum lycopersicum* 'Moneymaker' or *Nicotiana benthamiana* (CB28) plants. Plants were incubated in a small controlled environment chamber to keep humidity and maintained at 20 °C for a maximum of 72 hours to allow *P. capsici* to infect leaves, form haustoria and colonise host tissues. Imaging was conducted on a Zeiss LSM 710 confocal microscope using a W Plan-Apochromat 40x/1.0 DIC M27 water dipping lens and using the following settings: tdTOMATO (561 nm excitation and 573-612 nm emission) and chlorophyll (488 nm excitation and 650-700 nm emission). Haustoria are indicated with white arrows. The scale bars shown are 20 uM. The confocal microscopy experiment was repeated by Andrew Howden (University of Dundee, UK) as a confirmation of my experiments, described in Chapter 2.

GO enrichment analysis

To look for enrichment of specific gene ontologies in either *P. capsici* stage specifc marker gene co-regulated genes or *S. lycopersicum* genes in our pairwise analysis, we used a Singular Enrichment Analysis (SEA) strategy. All genes with no GO annotations were filtered from the set and compared to a customized background set containing all genes on the array with known ontologies for *P. capsici* or tomato, respectively. SEA was done using AgriGO servers (http://bioinfo.cau.edu.cn/agriGO/analysis.php). Significance was tested using Fishers exact test, results were reported for $p < 0.05$ after correction for FDR [164]. *P.*

capsici results were reported using GO slim annotations and tomato results with GO plant slim.

3.3 Results

3.3.1 *P. capsici*-tomato interactions feature an early biotrophic and late necrotrophic phase

The interaction between *P. capsici* strain LT1534 and tomato (*S. lycopersicum* 'Moneymaker') was investigated in time course experiments (Figure 3.1), which have been conducted in collaboration with Andrew Howden. Inoculations, followed by phenotypic analyses across time points, suggested that in the early stages of infection (up to 24 hpi), *P. capsici* ingress features a biotrophic phase during which host tissues appear healthy and unaffected, followed by a necrotrophic phase (> 24 hpi), marked by tissue collapse (Figure 3.1 A). Multiple inoculation experiments showed distinct phenotypic changes in the later stages of infection that included host tissue water-soaking, cell death and tissue collapse (Figure 3.1 A).

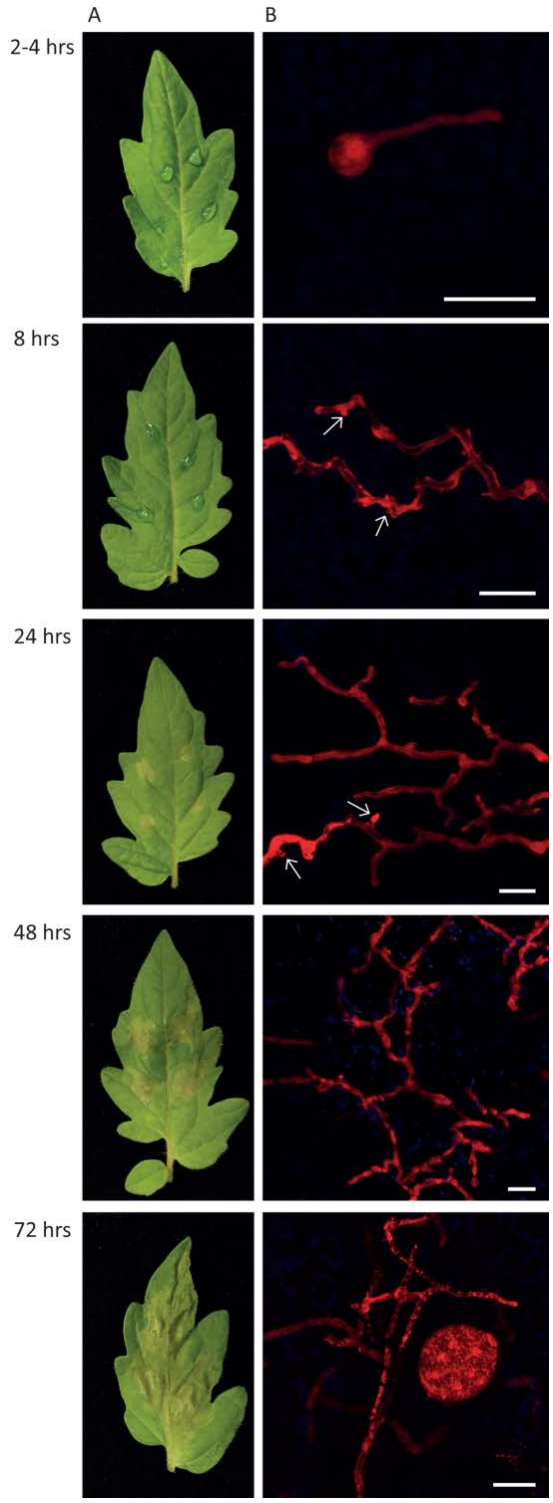

Figure 3.1: *Phytophthora capsici* infection of tomato features a hemi-biotrophic lifecycle
(A) Tomato leaves infected with zoospore suspensions of *P. capsici* at 0, 8, 24, 48 and 72 hours after infection. **(B)** Confocal microscopy images of tomato leaves infected with a transgenic *P. capsici* strain expressing the fluorescent protein TdTomato (in red). Infection features rapid germination of cysts and infection at 8 hrs, formation of biotrophy associated haustoria (arrowheads) visible up to 48 hrs after infection, rapid growth and sporulation at 48 and 72 hours after infection respectively. Bar = 20 µm. This experiment was conducted by Andrew Howden.

Considering the observations, it was investigated whether *P. capsici* forms haustoria *in planta*. Tomato plants were inoculated with zoospores derived from a transgenic *P. capsici* strain, expressing the red fluorescent protein-coding gene tdTomato and infection was monitored through confocal microscopy (Figure 3.1 B). The confocal microscopy experiment was repeated by Andrew Howden as a confirmation of my experiments, described in Chapter 2. Germinating cysts were observed as early as one hour after inoculation and cysts with hyphae penetrating into the plant cells at 8 hrs (Figure 3.1 B). Infection and subsequent colonization of leaf tissue was evidenced by growth of red fluorescent *P. capsici* hyphae in inoculated host tissues and the formation of distinct haustorial structures at the early time points (Figure 3.1 B). Confocal microscopy on leaf tissues in the late infection stages showed significant colonization of tissues with the formation of sporangia 72 hours after infection (Figure 3.1 B). To assess whether cells are viable, in addition transgenic *Nicotiana benthamiana* plants expressing mGFP (associated to the endoplasmatic reticulum) were inoculated and cell viability at relevant timepoints at drop inoculation sites assessed (Figure 3.2). These analyses showed haustoria in living cells and low levels of cell death in the early phase (0-16 hours) and increasing numbers of dead cells 24 and 48 hours after infection (Figure 3.2), which can be seen as the ER network disrupted by the unstructured distribution of GFP, suggesting dead or dying cells. After tissue collapse at inoculation sites, living cells containing haustoria were commonly observed at lesion edges, suggesting a dynamic infection cycle where phase transition is seperated spatially. These results are consistent with a hemi-biotrophic infection cycle and further confirm the presence of distinct developmental stages accompanying tomato infection.

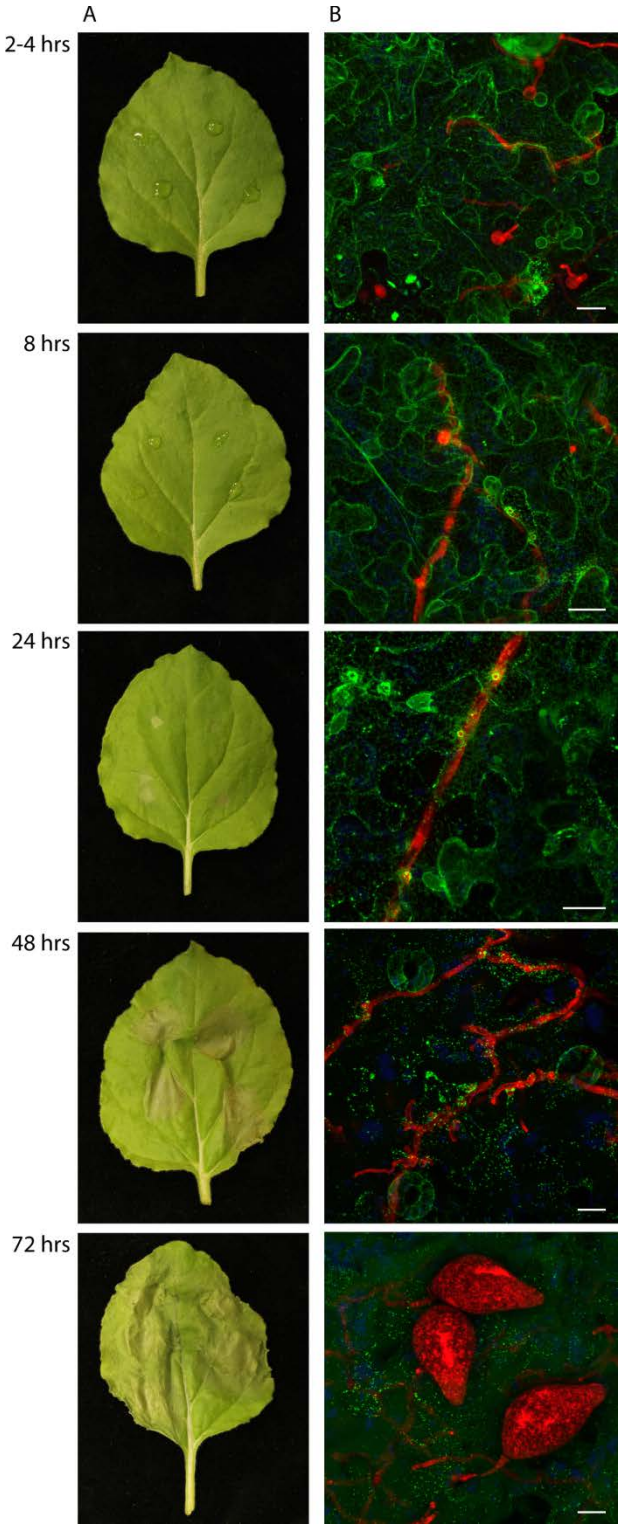

Figure 3.2: Assessment of cell viability during *P. capsici* infection
Transgenic *Nicotiana benthamiana* plants constitutivly expressing GFP localised to the endoplasmic reticulum (mGFP) were used to assess whether host cells were alive during the course of infection. (A) Photographs of *N. benthamiana* leaves infected with zoospore suspensions of *P. capsici* at 0, 8, 24, 48 and 72 hours after infection. (B) Confocal microscopy images of *N. benthamiana* leaves infected with a transgenic *P. capsici* strain expressing the fluorescent protein TdTomato. Within the first 24 hours the host ER is largely intact despite the presence of *P. capsici* and haustoria are often seen to invaginate living cells. After 24 hours the ER network is disrupted as shown by the unstructured distribution of GFP, suggesting dead or dying cells. Bar = 20 µm. This experiment was conducted by Andrew Howden.

3.3.2 A composite host-pathogen microarray approach to simultaneously profile transcriptional changes during the *P. capsici*-tomato interaction

Considering that PTI features a shift in gene expression and cellular activity towards defense and that pathogen effectors act to modulate defense gene induction, simultaneous profiling of both pathogen and host gene expression should help deduce coordinated relationships between transcriptional programmes in host and pathogen. To understand the processes underpinning both *P. capsici* infection and disease progression in tomato, an Agilent custom microarray with 60-mer oligonucleotide probes to all gene models of *P. capsici* and *S. lycopersicum* [86] was designed and gene expression changes of both organisms across the same time-course infection experiment were measured. Drop inoculated sites on detached tomato leaves were harvested at 0, 8, 16, 24, 48 and 72 hours post inoculation (hpi) with *P. capsici* strain LT1534 (Figure 3.3). In addition to the infectious stages, samples were taken from mock inoculated tomato as non-infected tissue (Ni) control sample at 0 hpi. Further sporangia and zoospores (taken at 0 hpi), germinating cysts (taken at 16 hpi), and mycelia grown *in vitro* (harvested at 48 hpi), were derived directly from the inoculum after the various incubation times. This experiment was repeated two times to generate three fully independent biological replicates for these analyses.

P. capsici gene expression analyses revealed that from 20,530 gene models represented on the array, 15,430 (75%) were expressed in at least one of the six infection and three *in vitro* stages sampled (Figure 3.3 A, B). In each of the stages, a significant fraction of expressed genes encode secreted proteins ranging from 10.4% to 12.6% during all stages of infection and up to 17.4 % in the *in vitro* stages (Figure 3.3, Digital file 2). Given the dynamic nature of pathogen infection and development, expression patterns were assessed and large suites of *P. capsici* genes that are specifically expressed in early stages of infection as well as throughout the infection process were found (Figure 3.3 B). Differences were not solely due to low levels of detection in the early stages as distinct sets of genes, expressed only in the early stages, were identified (Figure 3.3 B).

Subsequent statistical analyses identified 3,691 differentially expressed genes (1-way ANOVA, using Benjamini & Hochberg multiple testing correction, p-value ≤0.005), suggesting dramatic transcriptional changes throughout the infection and growth process of *P. capsici* (Figure 3.3 C).

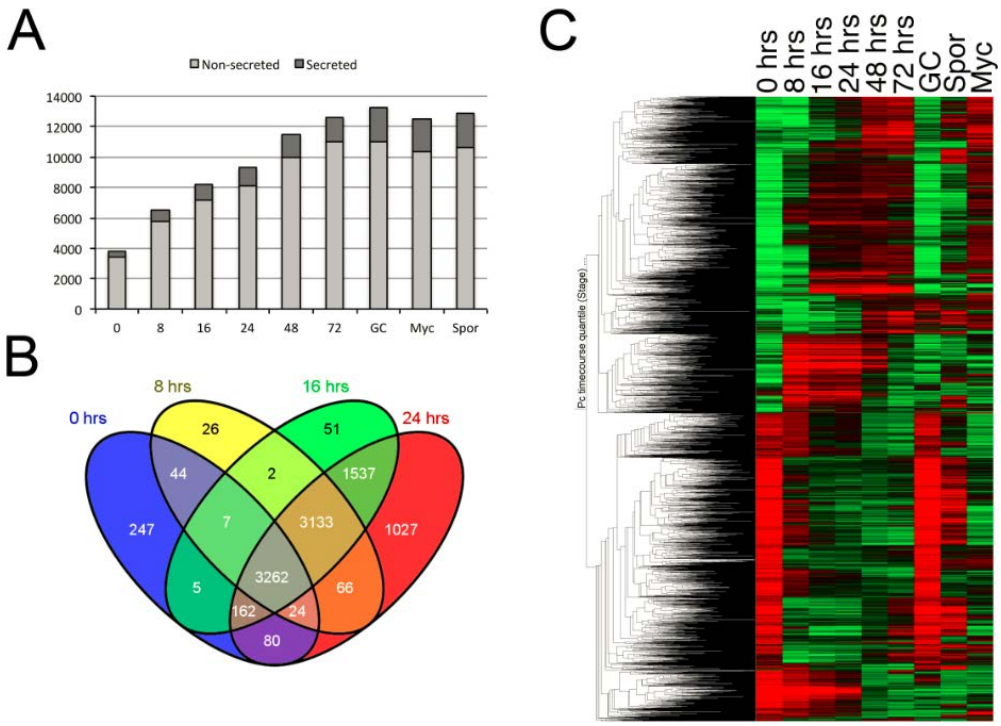

Figure 3.3. Expression of *P. capsici* gene complement during infection and disease progression
(A) Overview of genes that were expressed as detected on the *P. capsici*-tomato two genome microarray. The proportion of genes encoding putative secreted proteins (effectors) are indicated as dark grey. **(B)** Assessment of overlap of genes expressed in infectious stages and **(C)** overall assessment of differentially expressed *P. capsici* genes as determined by ANOVA as described. Red and green represents upregulated and downregulated genes respectively. Y-axis shows average linkage of Pearson correlations of gene expression profiles. Venn diagram was generated by using Venny [165].

3.3.3 *P. capsici* shows defined shifts in gene expression during specific life stages

To understand the infection process in more detail, the *P. capsici* gene model set was explored. Pre-existing information was used to identify genes that mark specific infection stages in *Phytophthora* and their gene expression profiles across the time course experiment were assessed. Expression of *PcHmp1* (*P. capsici* ortholog of the *P. infestans* Haustorial membrane protein 1, *Pi*Hmp1) [152], *PcNpp1* (Nep1-like Protein 1) [90, 92] and *PcCdc14* [154], markers for biotrophy, necrotrophy and sporulation respectively, showed distinct expression patterns in the microarray data (Figure 3.4 A) as well as sqRT-PCR (Figure 3.5) and are consistent with stage specific gene expression observed in other *Phytophthora* species [166]. The results also agreed with phenotypic changes and disease progression observed in the infection assays on tomato leaves (Figure 3.1 and 3.2).

To refine the view of transcriptional changes associated with infectious stages in *P. capsici*, the differentially expressed gene model set was further explored and the microarray

derived expression values were used to identify *P. capsici* genes that are co-regulated with *PcHmp1*, *PcNpp1* and *PcCdc14* (Figure 3.4 B). Based on expression patterns, it was possible to group 57 *PcHmp1* co-regulated genes, 209 genes co-expressed with *PcNpp1* and 533 genes with *PcCdc*14 (Figure 3.4 B, Appendix 2, Digital file 3). Then these co-regulated genes, based on available gene annotations and their corresponding proposed biological processes, were classified and enrichment for specific terms assessed (Figure 3.4 C, Table 3.1, Digital file 3). An overview of significantly enriched ontologies that are present in the marker co-regulated genes, is also given in Figure 3.4 C and separately in Table 3.1. as a quick summary. These analyses show that for the *PcHmp1* co-regulated genes, annotation terms are significantly enriched ($p<0.05$) for protein metabolism, (GO:0044267), gene expression (GO:0010467) and biosynthetic processes (GO:0034645) (Figure 3.4 C, Table 3.1, Digital file 3).

Table 3.1: Overview of significantly enriched ontologies that are present in the marker co-regulated genes and as demonstrated in a column-graph in Figure 3.4C

marker	GO	Description	p-value
Hmp1	GO:0006412	translation	1.50E-07
Hmp1	GO:0044267	cellular protein metabolic process	9.30E-05
Hmp1	GO:0010467	gene expression	9.40E-05
Hmp1	GO:0009059	macromolecule biosynthetic process	0.001
Hmp1	GO:0034645	cellular macromolecule biosynthetic process	0.00096
Hmp1	GO:0019538	protein metabolic process	0.002
Hmp1	GO:0044249	cellular biosynthetic process	0.0022
Hmp1	GO:0009058	biosynthetic process	0.0032
Npp1	GO:0009056	catabolic process	0.00036
Cdc14	GO:0050794	regulation of cellular process	2.50E-05
Cdc14	GO:0050789	regulation of biological process	5.40E-05
Cdc14	GO:0065007	biological regulation	0.00012
Cdc14	GO:0007165	signal transduction	0.00073
Cdc14	GO:0019222	regulation of metabolic process	0.0014

The results suggest an activation of cellular machineries required for gene expression and translation. Transcriptional reprogramming would allow an increase in the production and processing of protein factors required for initiation and maintenance of biotrophy. Consistent with association of *Hmp1* to biotrophy, candidate effector genes that are co-

regulated with *Hmp1* (Appendix 2, Digital file 4) were also found, suggesting effector mediated dampening of host immune responses in biotrophy.

A biotrophic phase was consistently observed in the first 24 hours observed, followed by host tissue collapse and necrosis in the inoculation experiments, suggesting a distinct transition to necrotrophy. Thus, expression of *PcNpp1*, a marker for this transition was determined and 209 genes that are co-regulated in *P. capsici* identified (Appendix 2, Digital file 3). Annotation term enrichment analyses of this gene set show specific enrichment for catabolic processes (GO:0009056) (Figure 3.4 C, Table 3.1, Digital file 4). Amongst this set, a large number of peptidases and proteasomal subunits are present, suggesting an active involvement of proteosomal degradation of pathogen proteins during the biotrophy to necrotrophy transition (Digital file 3).

Although the mechanisms of this proteasomal machinery and its targets need to be characterised, the results suggest dramatic shifts in protein modification and degradation processes which may represent a committed step in disease development. In the late infection stages, *Phytophthora spp.* form sporangia that emerge from necrotic tissues, a process which in *P. infestans* features upregulation of *Cdc14*. The identified *Cdc14* co-expressed genes are again enriched for signal transduction (GO:0007165) and metabolic processes (GO:0019222) (Figure 3.4 C, Table 3.1, Digital file 4), processes that could be required for extensive cellular reprogramming underpinning spore formation. Altogether, these results are consistent with the view that *Phytophthora* infection features stage-specific transcriptional programs [166].

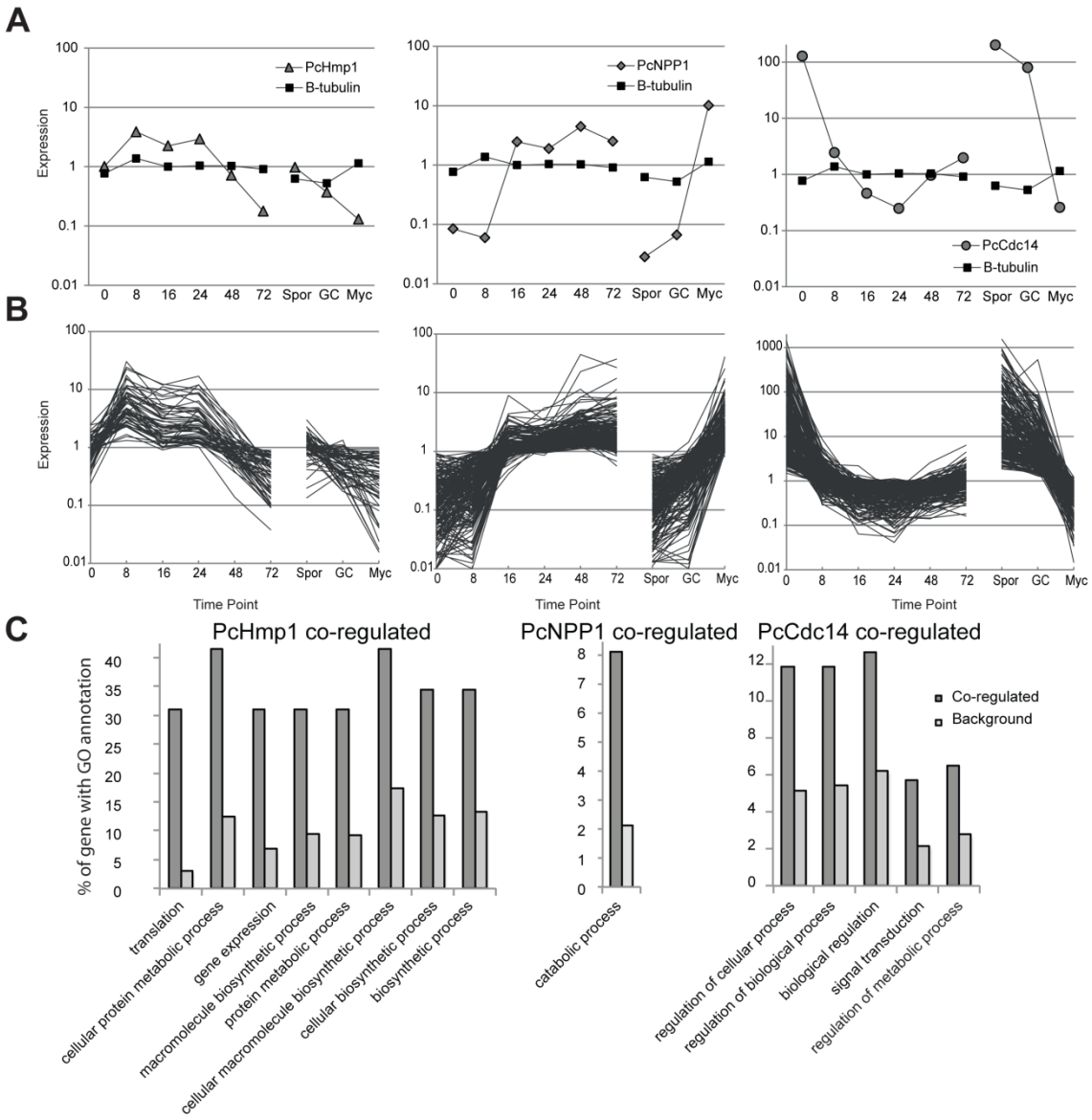

Figure 3.4: Marker gene assisted identification of stage specific processes in *P. capsici*
(A) Expression of *PcHmp1* (left panel), *PcNpp1* (middle panel) and *PcCdc14* (right panel) as determined by whole transcriptome microarray analyses and compared to the constitutive control β-tubulin. Marker genes were used in cluster analyses to identify genes that are co-regulated shown in **(B)**. Y-axis represents fold change expression values, determined by calculating fold changes over mean expression values across all treatments. **(C)** Overview of significantly enriched ontologies present in marker co-regulated genes. Dark bar shows the percentage of genes in the co-regulated fraction compared to the fraction in background set in light grey. All ontologies shown are significantly enriched ($p<0.05$, FDR<0.05).

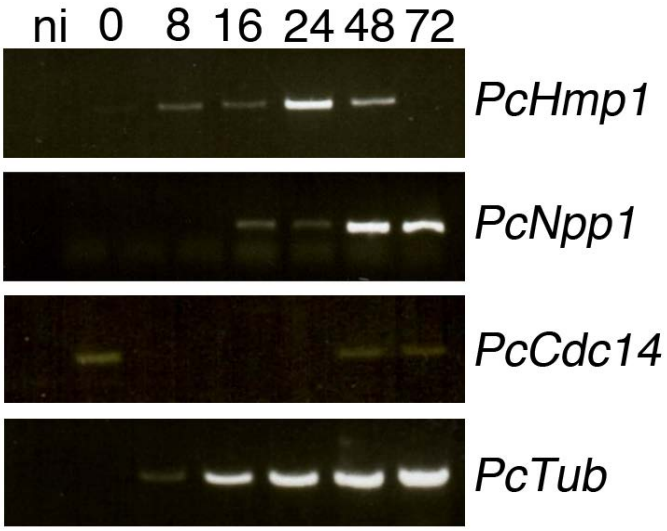

Figure 3.5: sqRT-PCR verification of marker gene expression during infection
Expression of marker genes *PcHmp1*, *PcNpp1*, *PcCdc14* and *PcTub* (constitutive control) was tested by semiquantitative PCR on cDNA derived from a time course infection series used for the microarrays. Amplification of genes from cDNA derived from water inoculated control (n.i.) and tomato harvested 0, 8, 16, 24, 48 and 72 hours after inoculation with *P. capsici*.

3.3.4 *P. capsici* infection features dynamic transcriptional regulation of effector-coding genes

To learn about expression of known effector genes in *P. capsici*, expression profiles were extracted for RXLR genes identified in the *P. capsici* genome ([43]; Digital file 5). Expression of 346 RXLR encoding genes (73%) were detected in all tested stages and treatments, amongst which 73 were differentially expressed (Figure 3.6 A, Digital file 5) during infection. Based on differential expression patterns, the RXLR genes were grouped and four classes were defined using cluster analyses (Figure 3.6 B, C, D, E).

These analyses identified 26 genes upregulated during biotrophy (8-24 hpi), and 13 RXLRs that were expressed in the early infection stages (0-16 hpi), but showed lower expression in only one biotrophic time point (24 hpi) and necrotrophy. Nine RXLR genes that were only expressed in sporulation stages were found and 13 genes that are specifically expressed in the late infection stages. 273 RXLR protein genes are expressed without any significant changes in transcript levels (Digital file 5). This shows that regulation of the expression of *P. capsici* genes takes place before and during infection. These results suggest an active involvement of pathogen effector proteins in the initiation and progression of disease, facilitated by modification of host cellular processes.

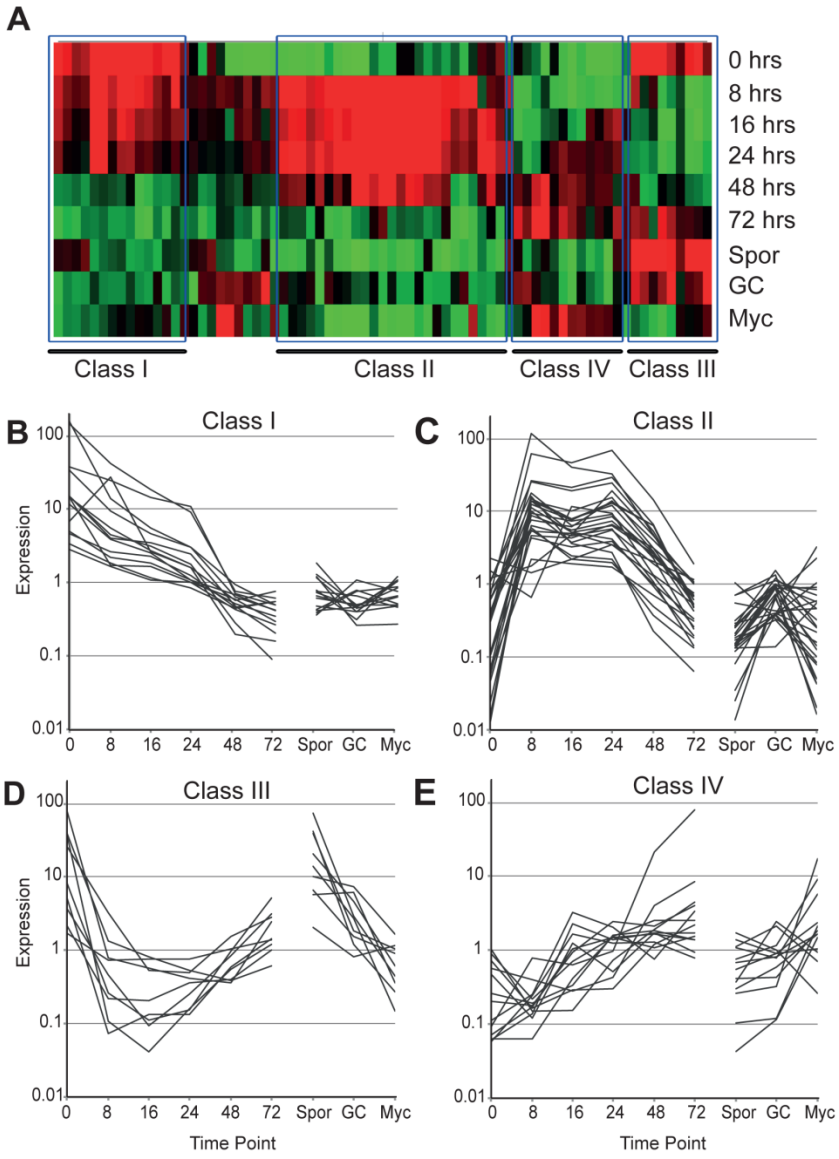

Figure 3.6: Identification of classes of differentially expressed RXLR genes in *P. capsici*
(A) Cluster analyses of putative RXLR genes that were found to be differentially expressed across infectious and developmental stages, identifies four different groups of genes. **(B-E)** overview of expression patterns corresponding to the groups shown in A. Values on the Y-axis represents fold change over mean expression as determined across all treatments.

3.3.5 Host transcriptional changes associated with *P. capsici* infection

To learn more about *P. capsici* mediated changes in host gene regulation, the host gene expression during infection with *P. capsici* was simultaneously measured. The measurements of transcript levels for 34,727 gene models (ITAG 2.3 [133]) revealed detectable expression of 24,390 genes in at least one timepoint, representing 65% of the predicted tomato transcriptome. It was aimed to identify genes that were differentially expressed in the time course experiment and 12,883 genes for which significant changes in

gene expression were measured have been identified (1-way ANOVA, using Benjamini & Hochberg multiple testing correction, p-value ≤0.005). Given that a significant change may occur between two unrelated treatments or timepoints (for example 8 vs 72 hpi), pairwise comparisons were also used (Student's t-tests) to identify genes that were differentially regulated between adjacent timepoints (Figure 3.7). These analyses identified a set of 7,314 non-redundant tomato genes suggesting dynamic transcriptional changes in tomato gene expression over the course of infection (Digital file 6). The number of differentially expressed genes per comparison was determined and large differences in the number of genes that are either up or down regulated between timepoints have been noted (Figure 3.7 A). Analyses of host transcriptional changes in *P. capsici* were carried out by Edgar Huitema (University of Dundee, UK) and Pete Hedley (James Hutton Institute, UK).

These analyses suggest a major shift in gene expression between the 0 and 8 hour time points (3,720 genes, Figure 3.8 A, Digital file 7) and a drastic transcriptional reprogramming, associated with *P. capsici* ingress and disease establishment. A water inoculated control was used as the non-infected tissue (Ni) sample that shows no significant upregulation of genes. Comparisons between the later infection stages revealed a further major shift in gene expression between the 24 and 48 hour time points (Figure 3.8 A, Digital file 7), coinciding with the biotrophy to necrotrophy transition observed during infection (Figure 3.1, Figure 3.4). Given the dramatic changes in gene expression, the level of overlap of differentially expressed genes between sampled time points were determined (Figure 3.8 B,C). These analyses revealed only a limited number of genes that were up or down regulated in multiple timepoints and large suites of genes uniquely regulated between 0 vs 8 (2,087), 8 vs 16 (1,117) and 24 vs 48 (1,757) hours post infection (Figure 3.8 B, C). Crucially, little overlap was found between differentially expressed gene sets from the 0 vs 8 h and 24 vs 48 h (Figure 3.8 B, C). These results suggest two major but distinct transcriptome changes in the host occur during the initial infection (0-8 h) and during the transition from biotrophy to necrotrophy (24-48 h). These analyses were carried out by Edgar Huitema (University of Dundee, UK) and Pete Hedley (James Hutton Institute, UK).

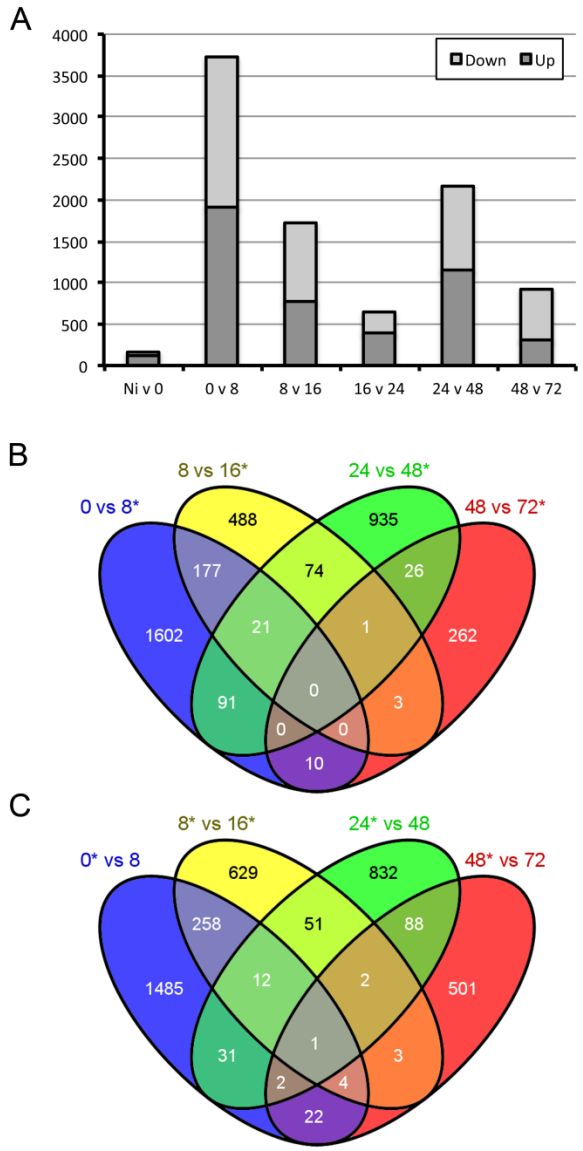

Figure 3.7: *P. capsici* infection of tomato results in two distinct transcriptional responses
(A) Overview on the number of significantly upregulated (dark grey) or downregulated (light grey) between adjacent timepoints. Differences in the number of differentially expressed genes can be seen between specific early (0 vs 8 hrs) and late (24 vs 48 hrs) timepoint comparisons. Ni (Non infected tissue) was used as a water inoculated control sample. Comparisons between gene lists generated in pairwise comparisons revealed limited overlap in both upregulated **(B)** and down regulated **(C)** gene sets. Diagrams were generated using Venny [165]. The analysis and preparation of this figure were performed by Edgar Huitema.

3.3.6 *P. capsici* infection leads to two distinct transcriptional responses in tomato

Analyses of transcriptional changes in tomato were carried out by Edgar Huitema (University of Dundee, UK) and Pete Hedley (James Hutton Institute, UK). To identify the biological processes affected by those two distinct responses, relative enrichment of annotation categories from genes that were present in both the ANOVA and pairwise comparisons sets

were assessed. As expected, no enrichment of processes in the non-infected vs 0 hour infection timepoints was found, partly due to a relatively small number (171) of differentially expressed genes identified between these treatments. Further assessment of sets emerging from other comparisons however, revealed significant enrichment for specific processes in the 0 vs 8 hours and 24 vs 48 hours time points (Figure 3.8, Digital file 8). Processes associated with (primary) metabolism (GO:0008152, GO:0044238) were significantly enriched in the fraction upregulated at 0 hours, suggesting a drop in expression of core metabolic genes after infection (Figure 3.8, Digital file 8). Catabolic processes (GO:0009056), but also specific metabolic processes, are enriched in the fraction upregulated at 8 hours post infection, suggesting major metabolic reprogramming in early infection (Figure 3.8, Digital file 8).

The switch from 24 to 48 hours post inoculation shows drastic re-regulation of metabolic and biosynthetic processes. Interestingly, the genes specifically upregulated at 48 hours show enrichment for a relatively large number of ontologies, including response to stimulus (GO:0006950) and response to stress (GO:0050896) and a number of gene regulation related ontologies (Figure 3.8, Digital file 8). These results suggest an active response of the host that accompanies the initiation of necrotrophy by *P. capsici*, suggesting a pathogen derived cue that causes host cell death. If true, perturbation of this process may limit initiation of pathogen necrotrophy which in turn, could lead to reduced pathogen growth and sporulation.

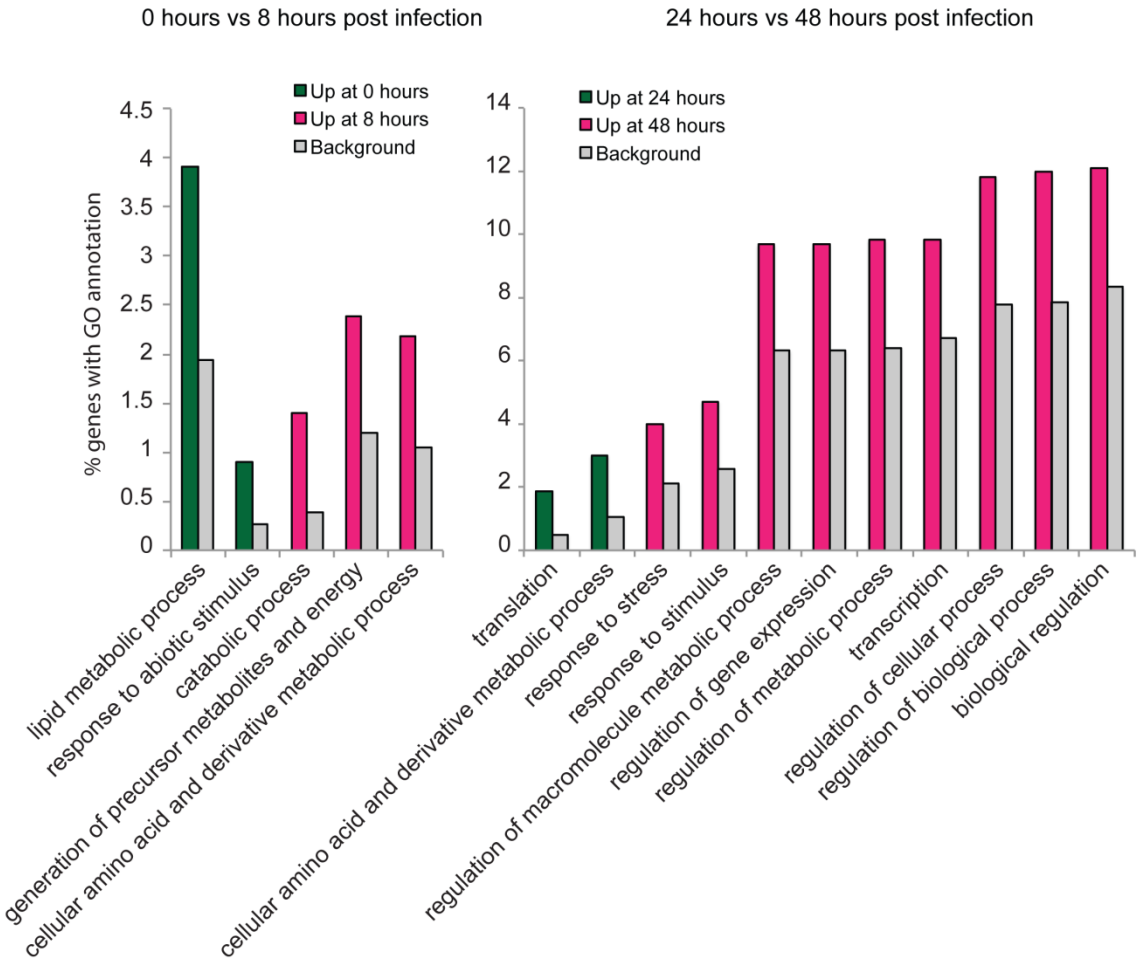

Figure 3.8: Gene ontology enrichment analyses of tomato genes identified in the early (0 vs 8) and late (24 vs 48) transcriptional response
Percentage of genes with significantly enriched GO terms that are specifically expressed in either of the time points (magenta/green) in our pairwise comparisons, compared to the background (grey). Y-Axis: percentage of genes that fall within each given GO annotation class. The analysis and preparation of this figure were performed by Edgar Huitema.

3.3.7 *P. capsici* infection features differential expression of candidate PAMP perception and signalling genes in tomato

These analyses of transcriptional changes in tomato were carried out by Edgar Huitema (University of Dundee, UK), Pete Hedley (James Hutton Institute, UK) and Remco Stam (University of Dundee, UK). A vast transcriptional shift in tomato was noted between the 0 and 8 hours timepoint and hypothesized that these changes are either due to an initial PAMP or effector induced-response upon pathogen ingress. It was also hypothesized that upon infection, the PTI response is dampened by effectors that are expressed and delivered during infection and biotrophy (Figure 3.6). If true, immune signalling gene candidates that

help determine interaction outcomes could be identified. Thus, transcriptional changes in gene classes involved in pathogen perception and signalling were investigated. Available annotations for tomato gene models were exploited in MAPMAN and 202 signalling genes in the differentially regulated dataset identified (Figure 3.9, Digital file 9). Subsequent cluster analyses and classification revealed a set of 84 genes that are induced between 0 and 8 hrs but decrease in expression in the later stages (Group A, Figure 3.9, Digital file 9) and 61 genes that appear specifically suppressed in biotrophy (Group B, Figure 3.9, Digital file 9). Another group of 57 genes (Group C, Figure 3.9, Digital file 9) were found to be transcriptionally activated throughout the timecourse after pathogen ingress, possibly reflecting activation of signalling networks that allow pathogen growth. Notably, amongst the differentially regulated set, 61 genes of receptor like kinases that are downregulated in biotrophy (Group B) were identified, suggesting that they may be targeted by *P. capsici* effectors and their downregulation enhances pathogenicity. It was noted that some differentially regulated receptor-like genes are annotated as receptors involved in nodulation, suggesting overlap between symbiotic and pathogenic associations with host plants. Importantly, amongst the set of RLKs, a homolog of AtPepR1 [168] was identified, which is suppressed during disease progression (Group B), suggesting that immune suppression is important in biotrophy. Approaches that aim to maintain or enhance their expression during biotrophy may limit disease progression.

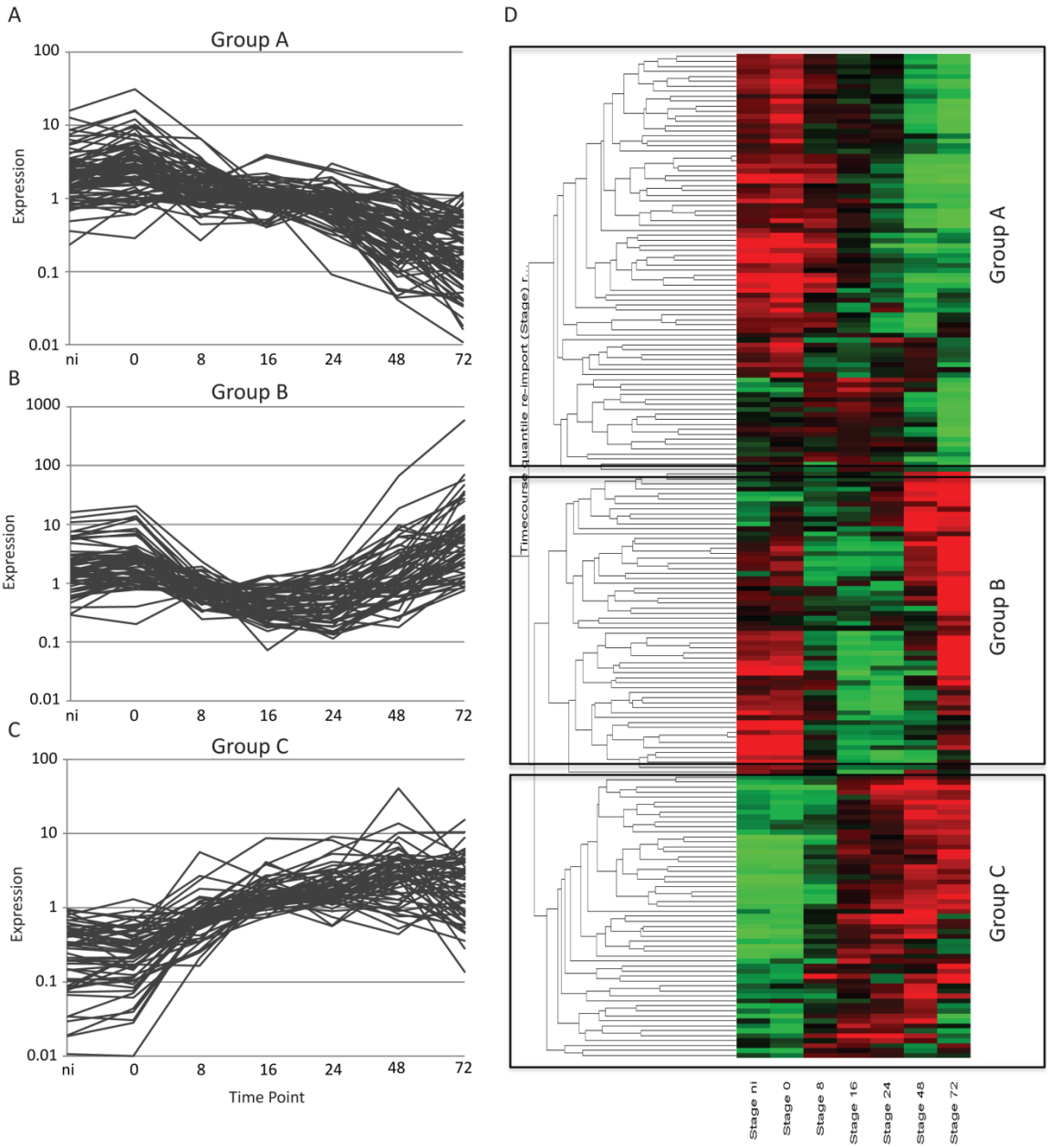

Figure 3.9: Microarray analyses identifies differentially expressed immune signalling candidate genes
Overview of differentially expressed immune signalling candidate genes identified in pairwise comparisons between timepoints (Student's t-test) and ANOVA (p=0.005) analyses. Expression profiles (Panel A-C) are presented for Class A, B and C genes, identified by cluster analyses in Genespring (Panel D). Red and green represents upregulated and downregulated genes respectively, Y-axis shows average linkage of Pearson correlations of gene expression profiles. Ni (Non infected tissue) was used as a water inoculated control sample. The analysis and preparation of this figure were performed by Edgar Huitema.

3.3.8 Differential regulation of host transcription factors underpins transcriptional responses to *P. capsici* infection in tomato

These analyses of host transcription factors in tomato were carried out by Edgar Huitema (University of Dundee, UK) and Remco Stam (University of Dundee, UK).

The observed dramatic changes in gene expression early in infection and during the biotrophy to necrotrophy transition, gave the reason to extract expression profiles for 323 known and differentially regulated transcription factors (Figure 3.10). Clustering and subsequent grouping of these transcription factors based on expression pattern, revealed the presence of distinct transcriptional profiles, consistent with wholesale transcriptional changes in tomato during infection. 119 transcription factors were found to be induced upon infection (Class A, Figure 3.10, Digital file 9), whereas 106 were either repressed during biotrophy (Class B, Figure 3.10, Digital file 9) or 98 expressed throughout infection but specifically downregulated during necrotrophy (Class C, Figure 3.10, Digital file 9). The transcription factor family membership amongst each of these expression classes was addressed and found that Class A contains a large fraction of the WRKY- type transcription factor families (Digital file 9). These results are consistent with the activation of genes involved in (biotic) stress responses and suggest execution of specific transcriptional programmes possibly leading to tissue necrosis. The results also suggest involvement of the phytohormone ethylene and its responsive transcription factors in disease development was found to fall in the A and B Classes (Figure 3.10, Digital file 9). These results suggest repression of specific transcriptional regulators by *P. capsici* during early and biotrophic infection stages.

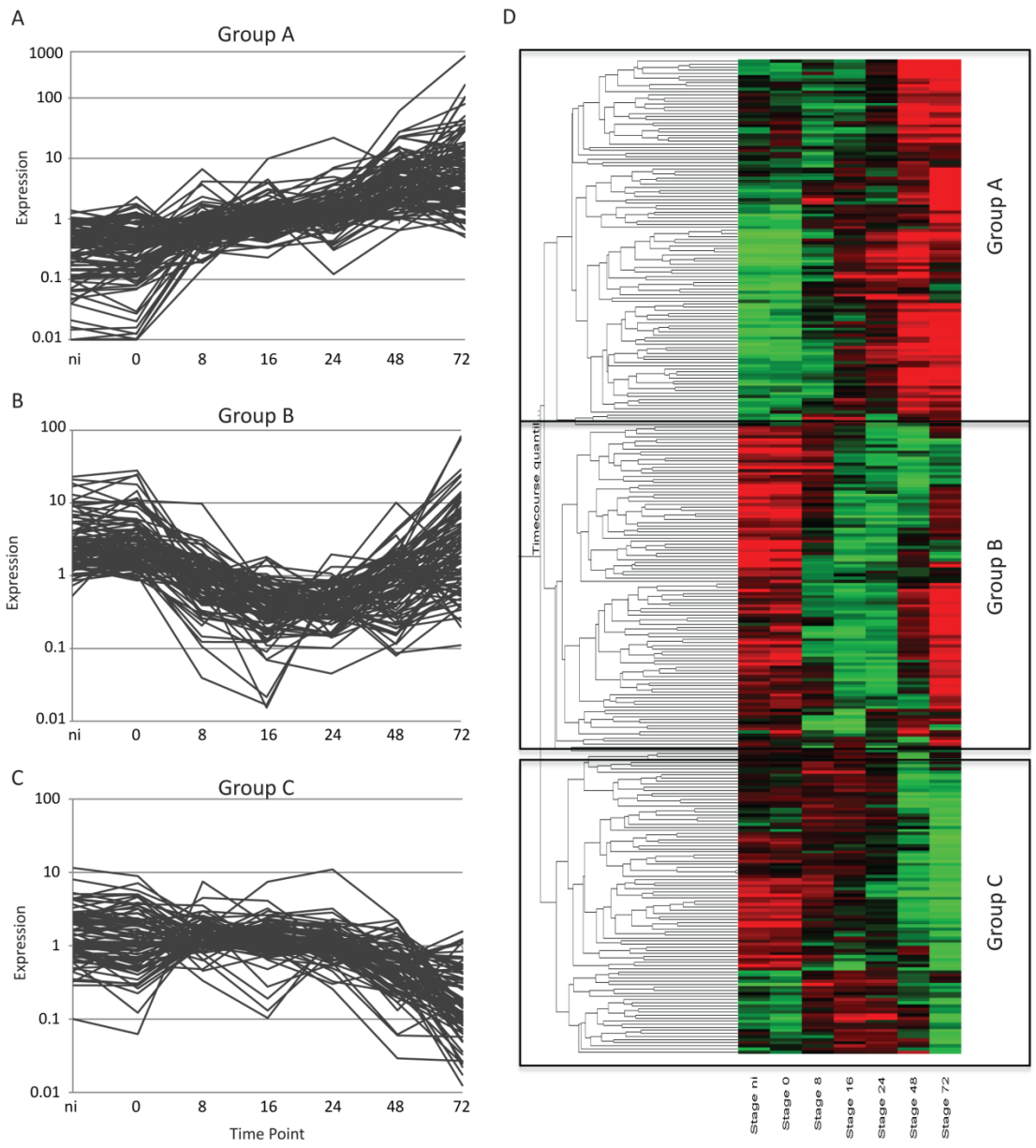

Figure 3.10: *P. capsici* infection leads to dynamic changes in expression of host transcription factor genes
Overview of differentially expressed candidate transcription factor genes, identified in pairwise comparisons between timepoints (Student's t-test) and ANOVA (p=0.005) analyses. Expression profiles (Panel A-C) are presented for Class A, B and C genes, identified by cluster analyses in Genespring (Panel D), showing distinct expression changes during infection. Red and green represents upregulated and downregulated genes respectively. Y-axis shows average linkage of Pearson correlations of gene expression profiles. Ni (Non infected tissue) was used as a water inoculated control sample. The analysis and preparation of this figure were performed by Edgar Huitema and Remco Stam.

3.4 Discussion

Here we report on a genome wide analysis of transcriptional changes that take place in tomato and its pathogen *Phytophthora capsici*. The work provides the first detailed simultaneous overview of gene expression changes during the course of infection in both a pathogen and its plant host by utilising their full genomes. This approach allows an unprecedented view on the processes that underpin infection, disease progression and lifestyle transitions in great detail. Given the immense damage *Phytophthora* species continue to cause in important crops, these analyses will thus provide new means and exciting opportunities to investigate complex yet important plant-microbe interactions, where extensive signal interplay is known to occur. The approach sets the stage for standardized experiments suited to compare the impact of pathogen infection strategies on a given host, or the importance of host factors on pathogen transcriptional programmes.
Using confocal microscopy and microarray analyses, evidence of a distinct biotrophic phase followed by transition to necrotrophy after 24 hours and sporulation at 72 hours on susceptible tomato was found (Figure 3.1). Biotrophy is marked by the formation of distinct haustorial structures that penetrate living cells, an important feature we were able to demonstrate on *N. benthamiana* plants expressing ER-EGFP (Figure S 3.1). These results are similar to observations made in other *Phytophthora* species [152, 169, 170], although it was noted that *P. capsici* has a relatively short infection cycle when compared to *P. infestans* for example [41]. Advantage was taken of the availability of genome sequences for both *P. capsici* and tomato, and the information was used to design a custom two-genome array and to measure gene expression in both organisms in a detailed timecourse experiment. Using this approach, it was possible to demonstrate the expression of 20,530 *P. capsici* and 24,390 tomato genes in a replicated timecourse experiment and transcriptional programmes which are associated with distinct stages of pathogen infection could be determined.
Using existing literature, three selected *Phytophthora* marker genes that could inform on disease progression and development after infection were identified. Assessment of expression for *PcHmp1*, *PcNpp1* and *PcCdc14* during *P. capsici* infection confirmed the presence of a hemibiotrophic lifecycle that features biotrophy in the first 24 hours, a switch to necrotrophy between 24 and 48 hours, and sporulation at 72 hrs after infection (Figure

3.2). Identification of co-regulated genes followed by GOterm enrichment analyses revealed that genes associated with expression and translation of genes and protein metabolism were overrepresented in biotrophy (Figure 3.3). These analyses suggest that the *de novo* expression and production of proteins form a critical requirement for initiation and maintenance of biotrophy. This is consistent with previous work from *P. infestans* that shows germinating cysts with appressoria that have a relatively high expression of amino acid biosynthesis genes [171].

Given that the plant-haustorial membrane interface is a crucial site where effector proteins are secreted and delivered into host tissues and cells, it is plausible that *Hmp1* coregulated genes are required for haustorial development and enhancement of effector protein production and delivery. The identification of stage-specific genes, encoding secreted proteins of unknown function or cellular destination, may help identify novel effector (classes) and help determine their roles in virulence.

The NEP1-like protein superfamily forms an important class of necrosis inducing peptides with proposed roles in pathogen virulence. Here it was shown that together with *PcNPP1*, a significant group of genes is induced during the transition from biotrophy to necrotrophy, suggesting a committed transcriptional shift between stages. Enrichment analyses revealed a significant gene complement associated with catabolism and degradation, suggesting that transcriptional shifts may result in cellular reprogramming of *Phytophthora* hyphae or accommodate the breakdown of compounds released during host cell death. These results illustrate a dynamic transcriptional programme employed by *P. capsici* to drive differentiation and adaptation.

Successful *Phytophthora* infection must lead to the formation of sporangia, an essential developmental process required for propagation of the *Phytophthora* disease cycle. Given the devastation caused by often explosive *Phytophthora* epidemics, there is considerable interest in the mechanisms governing sporulation and dissemination. Here, genes co-regulated with the sporulation marker *Cdc14* have been reported and genes required for signalling, regulation and expression have been identified. These results are consistent with the idea of extensive signalling cascades that drive the formation and differentiation of sporangia from a hyphal stage. Although the exact cascades driving sporulation still require elucidation, this work together with gene expression studies on other *Phytophthora* spp,

should allow identification of common genes associated with spore formation, which in turn could inform strategies that stop pathogen dissemination and limit epidemics on crops. More detailed cluster analyses and investigation of candidate gene function may give rise to additional sets of marker genes suited to study *Phytophthora* infection.

With assessing gene expression patterns for the RXLR-class of effectors, expression for a relatively high proportion of RXLR coding genes (73%) was detected. These results could be due to the high level of sensitivity provided by the Agilent platform (evidenced by the large number of *P. capsici* genes detected at 0 hrs), the number of timepoints and stages assayed in the microarray experiments (9), or reflect the biology of a broad host range pathogen. It was found that based on expression changes, RXLR genes can be grouped into four distinct classes. Class I and III RXLRs were highly expressed in the early phase of infection and showed either low levels of expression in germinating cysts (Class I) or high expression levels in germinating cysts (Class III). These results suggest the presence of both a developmental programme as well as specific plant signals that drive RXLR gene induction. Given their expression early in infection, these genes are likely to play roles in prevention or suppression of initial immune responses. Besides genes expressed in the early infection stages, RXLR coding genes were also found to be upregulated in biotrophy (Class II and IV), of which most of them were downregulated in necrotrophy (Class II) and some that remained highly expressed in the late stages (Class III). Given the observation that biotrophy features suppression of defense responses, it was suggested that secretion and delivery of effectors are required for the maintenance of biotrophy. The results also suggest continuous reprogramming of host cells in favour of pathogen growth. Effector genes expressed in the late stages could stimulate cell death in the necrotrophic phase or modulate host metabolism.

By characterizing host gene expression during *P. capsici* infection, processes associated with pathogen infection and lifestyle were identified. Pairwise comparisons between timepoints identified two distinct transcriptional changes in tomato, coinciding with initial infection (0 vs 8 hrs) and the biotrophy to necrotrophy transition (24 vs 48 hrs). Characterization of the early response revealed downregulation of genes required for (primary) metabolism whereas genes falling into secondary metabolism categories were induced as part of early responses to infection. These results are in line with observations made previously and could reflect production of antimicrobial compounds upon initial *Phytophthora* ingress.

Whereas some *Phytophthora*-host interactions feature suppression of initial defense responses by the host [172], evidence was found suggesting activation of defense responses early in infection. These included differential regulation of genes encoding receptor-like kinases, including the PEPR1 receptor and classes with similarity to Nod factor receptors. These results suggest activation of PAMP or effector triggered immune responses that may overlap with pathways that are regulated by Nod receptor-like genes in plants. The results may indicate co-opting of signalling pathways normally activated in symbiosis and would give weight to recent observations made in *Lotus japonicus* [173]. Crucially, amongst a set of differentially expressed RLK coding genes, a subset of candidate receptors was identified for which expression was specifically repressed in biotrophy. These results, together with the identification of effectors induced in the early stages of infection, suggest that consistent with current models describing plant-microbe interactions, *P. capsici* secretes and delivers effectors into host tissues to limit PAMP perception, inhibit immune signalling and promote virulence. With both effector and immune signalling genes now characterized in *P. capsici* and tomato respectively, the mechanisms driving *P. capsici* virulence and host immune signalling can now be investigated. Over-expression of host RLKs normally downregulated in biotrophy may lead to enhanced PTI responses that limit pathogen growth and disease development.

4 Characterisation of the RXLR effector *Pc03192* and its putative host targets NAC-Transcription Factor 1 and 2

4.1 Introduction

Only few oomycete effector targets have been identified to date. Mechanistic information relating to effector-target interactions are however missing. Effectors are important players in host-microbe interactions and the identification of the T3S-system and its effector substrates in pathogenic bacteria, has led to a change in our understanding of host-microbe interactions and the role of effectors in modulating host signalling [174, 175]. Soon after the first RXLR effector proteins were identified [25, 26, 176], the interest in the effector repertoire of oomycetes and their virulence function increased significantly. The observation that those effector molecules are capable of suppressing host immunity led to the question as to whether eukaryotic pathogens deploy effectors to aid infection. Several studies suggested possible roles for RXLR effectors in the suppression of PTI and ETI [128, 177]. For example, *P. sojae* RXLRs were found to suppress ETI triggered cell death and RXLRs of *Hyaloperonospora arabidopsidis* were found to supress PTI in various ecotypes of *Arabidopsis thaliana* [177]. Large-scale protein interaction screens of *A. thaliana* proteins with *Pseudomonas syringae* and *H. arabidopsidis* proteins yielded several effector target candidates [178], and indicated large interaction networks amongst these. These screens further identified 165 putative host targets, however most interactions have not yet been confirmed *in planta*. Only little is known about plant targets of oomycete effectors, how they are manipulated, and how perturbation events lead to effector triggered susceptibility. One of the most recent examples of a plant-pathogen interaction is the RXLR effector *Avr2* from *P. infestans* that is recognised by the resistance protein *R2* and interacts with the plant phosphatase BSL1 [125]. Another example is the RXLR effector *Avrblb2* from *P. infestans*, which hampers the secretion of the plant defence-related protease C14 into the plant apoplast [78]. A third example is the *P. infestans* effector *Avrblb1 (IPIO1)* that enhances the pathogenicity by disrupting the plasma membrane through an interaction with the lectin receptor kinase LecRK1.9 [179]. Live-cell imaging studies of RXLR effectors from *H. arabidopsidis* have revealed diverse subcellular localisations including the nucleus, the ER and the membrane trafficking network, suggesting diverse host targets and functions [129].

However, recent experiments with evolutionary conserved effectors from the two different oomycete species *H. arabidopsidis* and *P. sojae* have demonstrated that in some cases, effectors can share conserved host targets [180]. The two computationally predicted RXLR effectors *HaRxL96* and *PsAvh163* share 43% amino acid identity, are both induced during the early stages of infection and suppress or induce plant immunity in diverse plant species [180]. If true, these results suggest that conserved effector-target interactions are important for oomycete pathogenesis or virulence on host plants.

Phylogenetic studies have shown that *P. infestans* and *P. capsici* are related, as both species are in nearby clades, suggesting a common ancestor not too long ago [49, 181]. It can be hypothesized that several virulence factors, especially those linked to reproduction in the host, are highly conserved between species [178]. These conserved genes could thus be of high importance for the life style of *Phytophthora*, and might play important roles in oomycete pathogenicity. Therefore it is crucial to study these genes more closely to better understand their function. A critical step in understanding effector function is to identify (conserved) host targets and study the mechanisms of action.

I have used knowledge of the effector repertoire in the two related *Phytophthora* species, *P. infestans* and *P. capsici*, as well as the availability of functional data, to undertake a comparative study and to investigate whether candidate effectors share functional roles in virulence. For this study the gene *Pc03192* was chosen, because it is expressed during biotrophy (see Chapter 2) and has a putative orthologue in *P. infestans*, *Pi03192,* for which plant targets have been identified in potato by collaborators [126]. These plant targets belong to the important NAC transcription factor (TF) family, which is one of the largest in plants, consisting of 110 members in potato (*StNAC*) [182]. NAC (NAM/ ATAF/ CUC) proteins play essential roles in many diverse biological processes, such as in plant defence, developmental programmes or stress responses [183].

The effector gene *Pi03192* interacts with *StNAC1* and *StNAC2* at the ER inside the plant cells. Upon infection, these two TFs are released from the ER to enter the nucleus to limit disease. With different studies it was shown that *Pi03192* prevents the plant TFs from accumulating in the host nucleus, suggesting a novel strategy of manipulating host susceptibility [126].

In this chapter I investigated whether the RXLR effector protein Pc03192 interacts with the same pair of the potato NAC-transcription factors *StNAC1* and *StNAC2* at the ER inside plant cells. The effector *Pc03192* was transiently expressed *in planta* using *Agrobacterium*, and

phenotypic analyses as well as localisation studies have been compared to profiles available for the corresponding protein of *P. infestans Pi03192*. Protein-protein interactions with the two plasma membrane associated potato *StNAC1* and *StNAC2* as well as NAC orthologs identified in *Solanum lycopersicum*, *N. benthamiana* and *A. thaliana* have been tested in Y2H assays. A colocalization study of *Pc03192* and the tomato *SlNAC1* and *SlNAC2* verified an interaction at the ER-membrane. This is similar to results for *Pi03192*, which prevents relocalisation of the two potato *StNAC1* and *StNAC2* from the ER to the nucleus, and therefore it was hypothesized that this effector gene may share a conserved role in virulence.

4.2 Material and Methods

Identification of *Pc03192*

The most similar *P. capsici* sequence to the *P. infestans* RXLR effector *Pi03192* (McLellan *et al.* 2013) [126] was identified through reciprocal tBLASTn and BLASTp [149] searches (default settings) against the *P. capsici*-genome version 11 (http://genome.jgipsf.org/Phyca11/Phyca11.home.html;2011). This identified PHYCAscaffold_2_f_854137_854433_1 (named *Pc03192*) was used further. A primer pair (F:5'-AAAAAGGATCCCCAAGACTTCCGTTACGGTGAACAC; R:5'-AAAAAGAATTCCTATCTTCTCCCCCAGACC) was designed to amplify the effector domain, using the same design and PCR conditions as described previously in Chapter 2, and amplicons from cDNA were Sanger sequenced. Derived sequences were aligned to *P. infestans* reference sequence *Pi03192* using the program ClustalW Multiple Sequence Alignment [150] and Jalview [184] to investigate the levels of sequence similarity in *P. capsici*.

Identification of tomato orthologs *SlNAC1* and *SlNAC2*

To identify the tomato sequences with the highest sequence similarity to the potato *StNAC1* and *StNAC2*, BLASTn and BLASTp analyses were carried out against the SGN tomato database (solgenomics.net/tools/blast). This identified *SlNAC1* (Solyc03g080090.2.1) and *SlNAC2* (Solyc04g072220.2.1). Derived sequences were aligned to the potato *StNAC1* and

StNAC2 as reference sequences, using the program ClustalW Multiple Sequence Alignment [150] and Jalview [184] to investigate the levels of sequence similarity in tomato. Normalized microarray probes of these genes were extracted (Chapter 3) and plotted in Excel to compare expression values with the effector gene *Pc03192* (PHYCAscaffold_2_f_854137_854433_1).

Yeast-2-hybrid (Y2H) protein-protein interaction assay

The yeast assays for protein-protein interactions were performed using the ProQuest system of Invitrogen. The effector Pc03192 and interactors SlNACs were cloned and recombined into the prey vector pDEST22 using the Gateway® recombination cloning technology (Invitrogen) as described in the following section. Afterwards the constructs were transformed into the yeast strain MaV203, according to the manufacturer's protocol from Invitrogen (ProQuest-Two-Hybrid System Manual). In addition, the truncated sequences of the two membrane associated transcription factors *StNAC1* and *StNAC2* as well as the full length sequences of the orthologs to *Solanum tuberosum* (St) [126] identified in *N. benthamiana* (Nb), *A. thaliana* (At) and *S. lycopersicum* (Sl) were transformed into the bait vector pDEST32 (cloning method described in following section). The NAC orthologs to the potato *StNAC1* and *StNAC2* from *N. benthamiana* and *A. thaliana* have been previously identified and cloned in the group of Prof. Paul Birch (University of Dundee, UK), and were also included in my Y2H assays. The bait and prey vector-constructs were co-transformed into the yeast strain MaV203 (see protocol for Two-Hybrid System, Invitrogen, as mentioned above). Transformants were recovered and grown on various selective drop out medium plates, lacking the amino acids: -leucine, and –leucine plus tryptophan. The activation assay was carried out on the triple drop out medium plates, lacking leucine, tryptophan and histidine (LTH) and the more stringent quadruple drop out also lacking uracil. The media lacking LTH was supplemented with the inhibitor of the *HIS3*-gene, 3AT (3-Amino-1,2,4-triazole) at a concentration of 25 mM. A β-galactosidase activity reporter assay was conducted to test the activation of lacZ gene expression, specifically due to effector-target interactions. Three or four independent colonies were tested from each construct. The *P. infestans* constructs from McLellan *et al.* (2013) [126] as well as the *StNAC1* and *StNAC2* orthologs from Nb and At were kindly provided by Miles Armstrong (University of Dundee, UK) and included in my assays. As controls, the empty bait vector together with the *Pi03192*

and *StNAC1* and *StNAC2* and the prey vector with *Pc03192* were transformed. Three replicates were made for each construct combination in the yeast assays.

Cloning of the effector *Pc03192* and the tomato orthologs *SlNAC1* and *SlNAC2*

For the cell death by overexpression assays *in planta*, the *P. capsici* genes *Pc03192,* along with *Pc16737* as control, were first cloned via restriction enzymes (BamH1 and EcoR1) and the Phusion® High-Fidelity DNA Polymerase (New England BioLabs) into the vector pENTR1A. The PCR conditions (with an annealing temperature of 55 °C) and the primers have been used as mentioned in Chapter 2 (Table 2.2). After the amplification of the required gene, the final PCR product was run on a 1% agarose, 1x TBE gel, the band of the expected size was cut and gel purified using the QIAquick Gel Extraction Kit (Qiagen) according to the manufacturer's instructions. Afterwards the genes were recombined into the vector pB7WGF2.0 [185] (containing the 35S promoter) using the Gateway® recombination cloning technology (Invitrogen) with the Gateway LR clonase-kit (Invitrogen). The latter plasmid adds a GFP-tag to the cloned gene, allowing for subsequent microscopic localization studies.

Each construct was sent for sequencing to confirm that the cloned insert was correct and in frame with the GFP-protein. All constructs were transformed into the *Agrobacterium tumefaciens* strain AGL1 [186], which was routinely cultured at 28 °C in yeast extract broth medium using appropriate antibiotics. The DNA transformations of AGL1 were conducted by electroporation according to a standard protocol [186].

For the confocal microscopy assays, full length *SlNAC* genes were cloned from tomato cDNA with the gene specific primers: (*NAC1*: F:5'-CACCATGGCCGTACTTCCTGG, R:5'-CTATACACAGAGTCTAAAGCAACTCC; *NAC2*: F:5'- CACCATGAAGGTTTTGATGGATT, R:5'-CTATGTCCCCGCGATTTTAGC). The PCR conditions (with an annealing temperature of 55 °C) are used as described above. The genes were cloned into the vector pENTR/D-TOPO (Invitrogen), recombined into the vector pB7WGF2.0 using the Gateway LR clonase-kit (Invitrogen) and transformed into AGL1, as mentioned above.

Overexpression assays *in planta*

All transformed constructs in AGL1 were infiltrated into the following *Nicotiana* species: *N. benthamiana* 'Sainsbury', *N. tabacum* 'Samsun' and *N. glutinosa*. All plant species were

grown in a greenhouse at 22 °C and 16 h light. Agroinfiltrations were carried out as described in Huitema *et al.* (2004) [187]. Briefly, the *Agrobacterium*-cultures were grown for 48h at 28 °C in Luria broth (LB) medium supplemented with the antibiotic spectinomycin (50 µg/ml) , diluted to an OD600=0.3 or 0.5, pelleted and resuspended in infiltration medium (10 mM $MgCl_2$ and 150 µM acetosyringone). The infiltrations were carried out with a 1-ml syringe without needle. The elicitin *INF1* induces a hypersensitive response when expressed in *Nicotiana* species as described by Kamoun *et al*. (1998) [17]; the described protein expression construct 35S:INF1 was used as positive control as well as the constructs of the *P. infestans* homologs pB7WGFP2:Pi03192 and pB7WGFP2:Pi16737 (provided by Tanya Bukharova, University of Dundee, UK) for comparison. Each lesion or cell death symptom was recorded from four to seven days post infiltration and pictures from detached leaves were taken under white and UV-light.

Confocal microscopy

All constructs plus empty vector control were infiltrated into leaves of 4-week old *N. benthamiana* as described above. The cells expressing fluorescent protein fusions were observed two days post infiltration on a Leica TCS-SP2 AOBS confocal microscope using HC PL FLUOTAR 63×0.9 or HCX APO LUVI 40×0.8 water dipping lenses. GFP was imaged using 488nm excitation from an argon laser, with emissions collected between 500 and 530nm and mRFP was imaged using an excitation wavelength of 568nm from a 'lime' diode laser with emissions collected between 600 and 630nm.

Western blot and Coomassie stain

N. benthamiana 'Sainsbury' plants were infiltrated as described above with constructs expressing GFP-SlNAC1, GFP-SlNAC2, GFP-Pc03192 and GFP(-) empty vector control. Leaf disks (Ø8mm) were harvested at 3 dpi. Per sample, four disks were ground in liquid nitrogen and resuspended in 200 µl extraction buffer (4x SDS PAGE, 50x Protein inhibitor and 1M DTT). Samples were boiled at 95 °C for 10 min and cooled down on ice. After a centrifugation step at 13.000 rpm for 5 min, the supernatant was collected and 10 µl each sample loaded onto Mini-PROTEAN® TGX™ Precast Gels (BIO-RAD) with 1X SDS running buffer for 1.5h at 95V (Invitrogen). Gels were blotted onto a nitrocellulose membrane (Immobilon IPVH, Filter type PVDF, 0.45 um pore size) for 1.5h at 50V. Membranes were blocked in 5% milk in 1X TBS before addition of the primary antibody specific to GFP

(GFP(FL)HRP rabbit polyclonal lgG, Santa Cruz) at a 1:5000 dilution. Afterwards the membranes were washed with 1X TBS-Tween and SuperSignal® West Femto (Thermo Scientific) ECL detection was used according to the manufaturer's instructions.
After the gel electrophoresis, one gel was used to stain o/n with Coomassie Brilliant Blue (BIO-RAD) to demonstrate the extracted protein amounts of all tested constructs.

4.3 Results

4.3.1 Inter-species conservation of the RXLR effector *Pi03192*

To retrieve the *P. capsici* gene with the highest sequence similarity to the *P. infestans* RXLR effector *Pi03192* [126], reciprocal tBLASTn and BLASTp analyses were conducted against the *P. capsici* genome sequence. The reciprocal best hit sequence is PHYCAscaffold_2_f_854137_854433_1 (named as *Pc03192*) and has 43.5% pairwise identity on the amino acid level which is shown in an alignment with *Pi03192* in Figure 4.1. Pairwise alignment of the nucleotide sequences shows 63.4% identity.

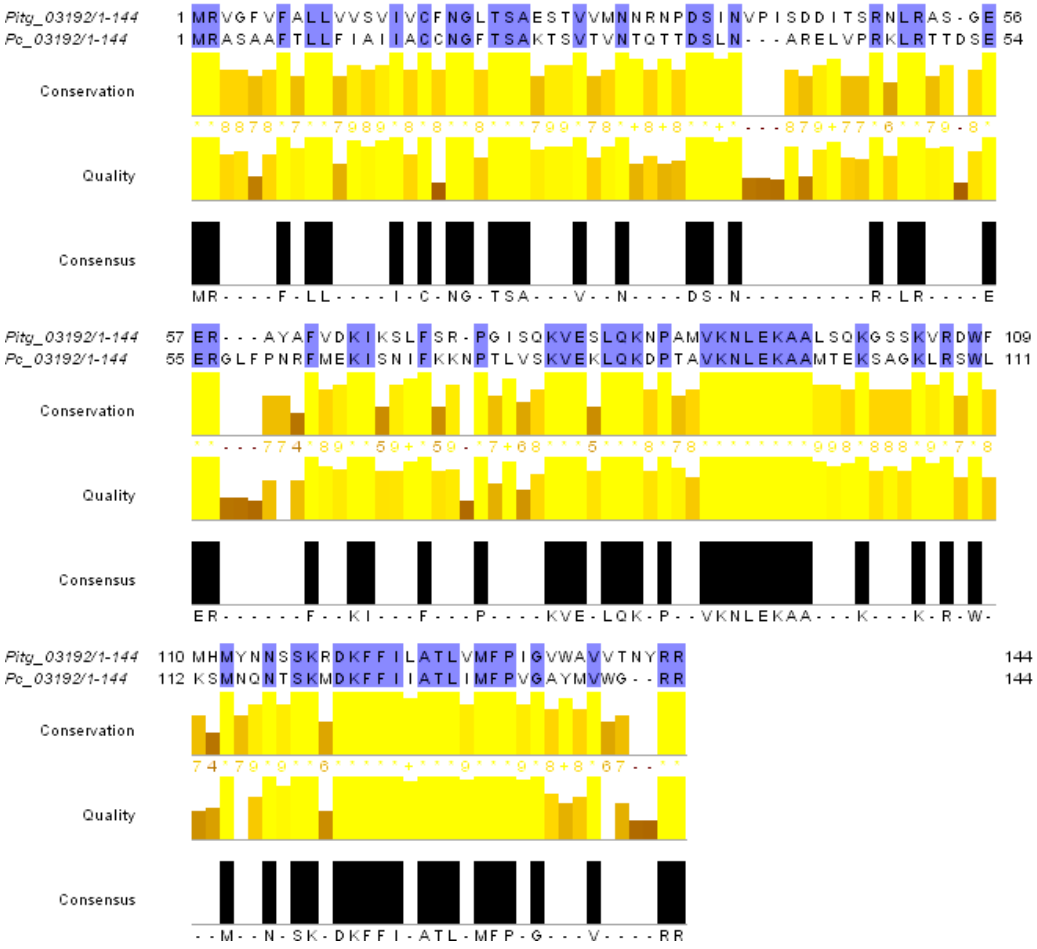

Figure 4.1: Alignment of the *P. infestans* effector gene *Pi03192* and the orthologous sequence from *P. capsici*
Protein sequences revealed conserved regions (marked in blue) with a percentage of 43.54% pairwise identity. The alignment was conducted with ClustalW and is visualized with the program Jalview.

4.3.2 *Pc03192* interacts with two potato and tomato NACs in yeast

To identify whether the potato and tomato homologs *NAC1* and *NAC2* are host targets for the RXLR effector *Pc03192* from *P. capsici,* a yeast-2-hybrid (Y2H) assay was carried out to test for direct interaction. The truncated version of the potato *StNAC1* and *StNAC2* [126] were tested first for interaction with the effector *Pc03192* and *Pi03192* as positive control. Indeed, the fragments of both NACs interacted equally with *Pc03192* and *Pi03192*, shown in Figure 4.2. Interaction is shown as yeast colonies grown on selective media (- histidine, LTH) and positive β-galactosidase (Xgal) activity on plates as indicated by blue colouration.

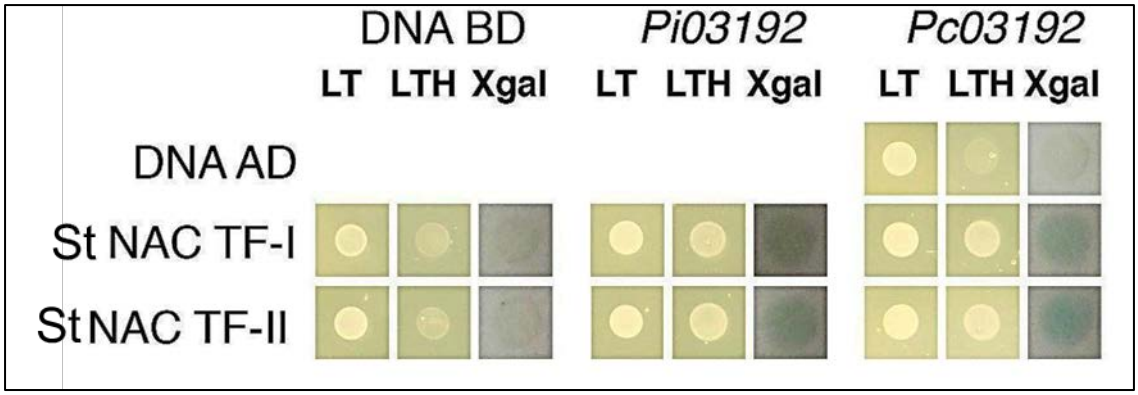

Figure 4.2: Testing the effector gene *03192* and the potato NAC-TFs for direct interaction in Y2H assays
Potato NACI and II are grown on selective media –histidine (LTH)(yellow colonies) and shown β-galactosidase (Xgal) activity (blue colonies) when co-transformed with the effector gene *Pc03192*, but not with the empty vector control (DNA Binding domain (BD)).

Since the StNAC1 and StNAC2 were found to interact with both *Pi03192* (as previously reported [126]) and *Pc03192*, I tested whether this interaction occurs also with potential orthologs from *N. benthamiana*, *A. thaliana* and tomato respectively. BLAST analyses were carried out against the SGN tomato database to identify the tomato *SlNAC1* (Solyc03g080090.2.1) and *SlNAC2* (Solyc04g072220.2.1) as most similar sequences to the potato *StNAC1* and *StNAC2.* Sequences were then aligned and showed more than 80% pairwise identity on the amino acid level.

Full length *NAC1* and *NAC2* sequences from the four plant species (*St, Sl, Nb, At*) were tested against *Pc03192* and *Pi03192* and resulted in growth of yeast colonies on – histidine (-HIS) plates, with one exception, the *A. thaliana AtNAC2* ortholog, which did not interact with either *Pi03192* or *Pc03192,* as it is shown in Figure 4.3 A and B. The co-transformations with the empty vector as negative control did not show any yeast growth (Figure 4.3). The interaction could, however, neither be confirmed on the more stringent quadruple drop out (– uracil) plates nor with β-galactosidase activity, with one exception: A direct interaction could be detected on the stringent drop out (– uracil) plates as well as β-galactosidase activity for *Pi03192* and also *Pc03192* with the *AtNAC1* ortholog from *A. thaliana* (Figure 4.3 B). Apart from this exception, an interaction of the effector *Pc03192* as well as *Pi03192* with the plant NAC-TFs can therefore only be detected on –HIS media (Figure 4.3 A) in several replicates.

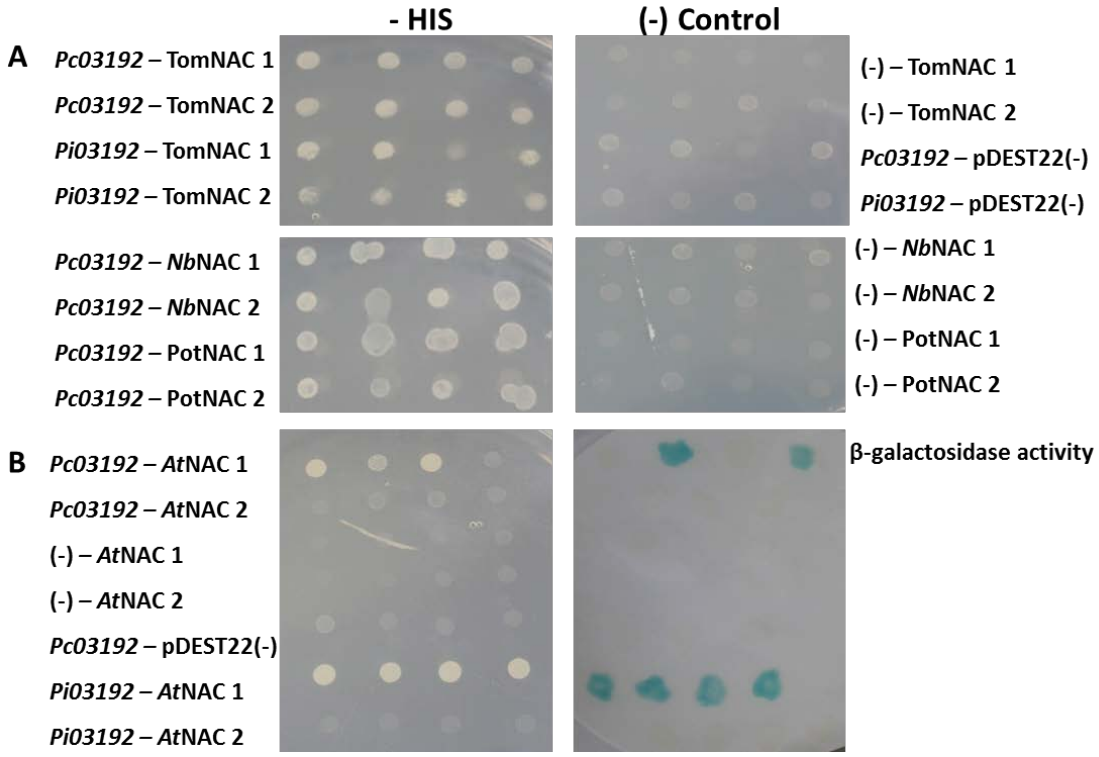

Figure 4.3: Testing the *P. capsici* effector *Pc03192* and orthologs of *NAC1* and *NAC2* from various plant species for direct interaction in Y2H assays
Tomato (Tom), *N. benthamiana* (Nb) and Potato (Pot) (A) and *A. thaliana* (At) (B) *NAC1* and *NAC*2 orthologs are grown on selective LTH media –histidine (-HIS) when co-transformed with the effector gene *03192* of *P. capsici* (Pc) and *P. infestans* (Pi). The co-transformations with the empty vector as negative control (right side as well as in B) did not show any colony growth. Detection of β-galactosidase activity for 03192 with the *AtNAC1* ortholog from *A. thaliana* is shown as blue colonies in B. To distinguish the *SlNAC* and *StNAC* from each other in a more simple way, the terms Tom for Tomato and Pot for Potato have been used in this figure.

4.3.3 Expression level of the effector *Pc03192* and *SlNACs* during infection

To analyse the expression level of the *P. capsici* effector *Pc03192* and its potential interactors *SlNAC1* and *SlNAC*2 from tomato (Figure 4.4), data from the microarray experiment in Chapter 3 was used. Normalized expression values, reported on probes designed against each gene, were plotted together into a graph and the expression values were compared. As it is shown in Figure 4.4, expression levels of the RXLR effector gene increased rapidly with the onset of infection at 0 hpi and peaked at 8 hpi.

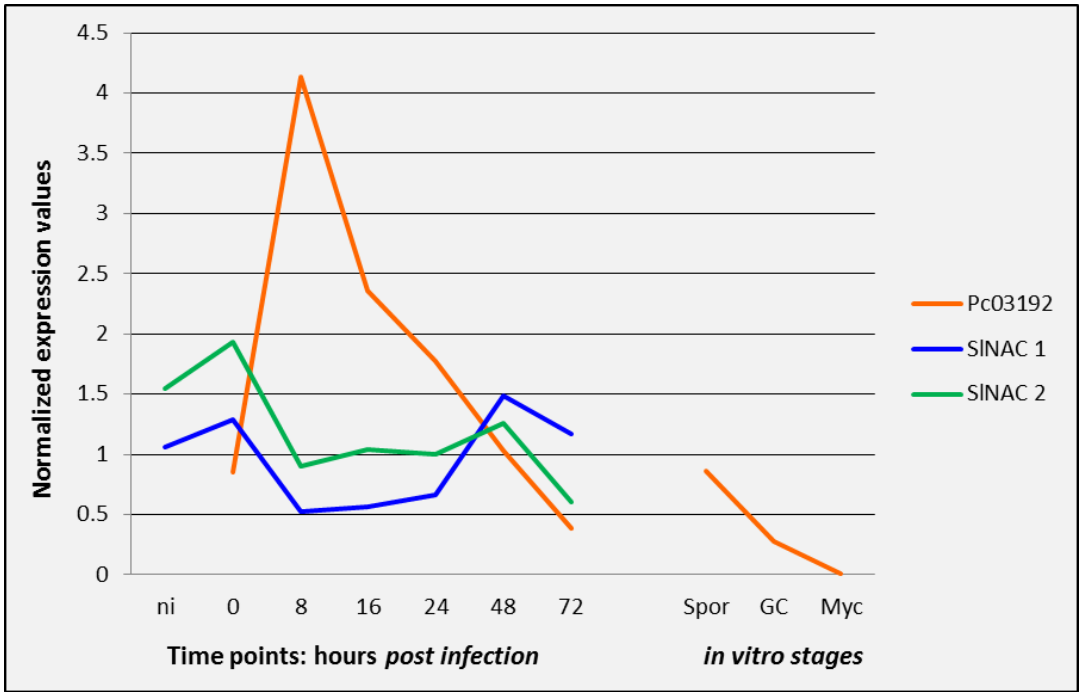

Figure 4.4: Expression analysis of the *P. capsici* effector gene *Pc03192* and its two host interactors from tomato *SlNAC1* and *SlNAC2*
Normalized probes for a pathogen-host interaction are compared: *Pc03192* expression level increased rapidly with the infection timepoint at 0 hpi and peaked at 8 hpi, whereas expression levels of the *SlNACs* decreased contrarily from 0 to 8 hpi and were upregulated again at 48 hpi.

On the contrary, expression levels of the *SlNACs* decreased from 0 to 8 hpi and are both downregulated during the early stages of *P. capsici* infection, but are upregulated again at 48 hpi, coinciding with the down regulation of *Pc03192*. These shifts at the beginning of the biotrophic phase suggest an effector-mediated reduction of a host immune response. The two *SlNACs* might have a role in defence and might thus be targeted by the effector *Pc03192* to repress transcriptional regulation.

To test whether overexpression of the effector orthologs *Pi03192* and *Pc03192* might have a phenotype *in planta*, a cell death assay was conducted in the three previously described *Nicotiana* species (Figure 4.5). The effector gene *Pi03192* was used as positive control together with an empty vector and *InfI*. In addition, the orthologous effector genes *Pi16737* and *Pc16737* (see chapter 2) were tested for cell death. As shown in Figure 4.5 (A), cell death phenotypes could be determined by overexpressing both effectors *Pc03192* and *Pi03192* six days post infiltration in *N. glutinosa* and *N. tabacum* 'Samsun'.

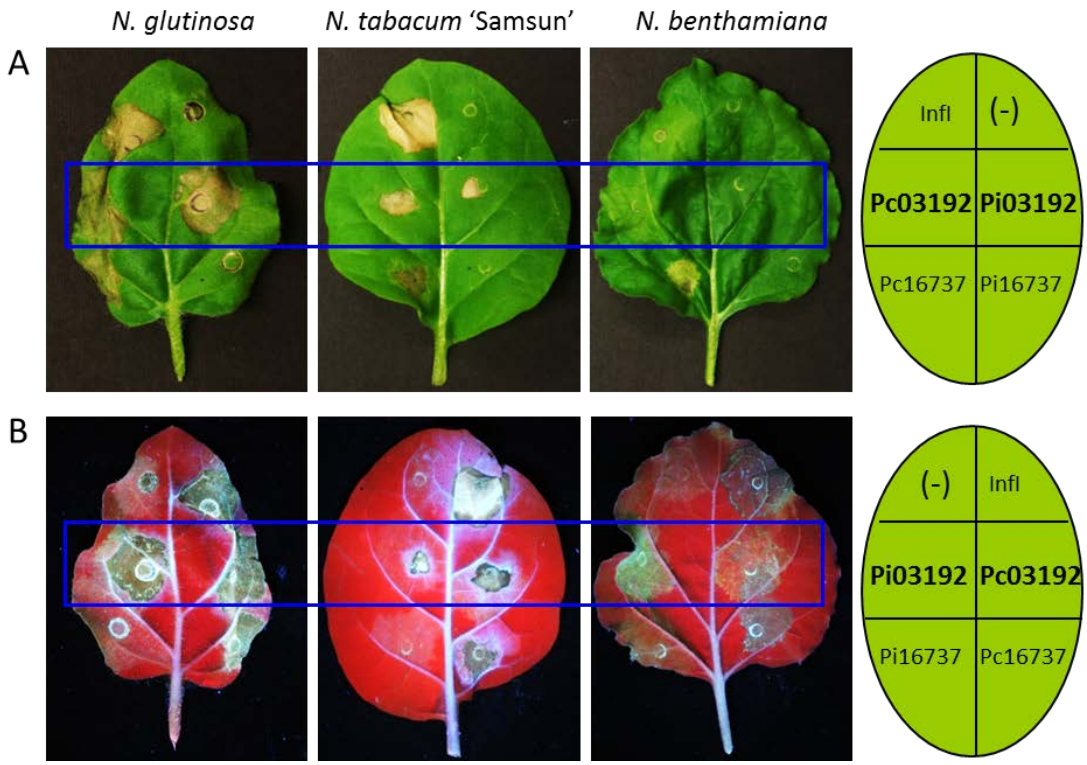

Figure 4.5: Phenotypic characterization of the *P. capsici* effector gene *Pc03192* on *N. glutinosa*, *N. tabacum* 'Samsun' and *N. benthamiana*
Images are taken at 6 days *post* infiltration. **(A)** Detached leaves were placed under normal light and **(B)** under UV-light. The transient expression of *Pc03192*, leads to cell death. Additionally cell death is visible for the control effector *Pi03192* and *Infl.* Expression of the effector gene *16737* from *P. capsici* and *P. infestans* shows the same phenotype in all *Nicotiana* species. The assay determined that overexpression causes a cell death phenotype for both effector genes of *P. capsici* and *P. infestans.*

In *N. benthamiana*, the phenotype of *Pc03192* could hardly be detected by eye. Therefore the leaves have been scored and evaluated under UV-light, as it is demonstrated in Figure 4.5 (B). The expression in *N. benthamiana* showed some cell death but this was substantially less compared to the other plant species (Figure 4.5 B).

4.3.4 *Pc03192* and *SlNAC1* and *SlNAC2* localise to the ER membrane *in planta*

I hypothesised that *Pc03192* and *Pi03192* are orthologs with conserved functions towards conserved targets. If true, both effectors should co-localise with *SlNAC1* and *SlNAC2* in plant cells. To test this hypothesis, I determined the subcellular localisations of *Pc03192* as well as the tomato *SlNACs* by confocal microscopy. The GFP-tagged *Pc03192* as well as *SlNACs* were transiently expressed in *N. benthamiana* plants together with an empty vector control and an RFP-tagged ER-marker using *A. tumefaciens* infiltration and were imaged two days post

infiltration. The images of cells expressing either the effector or plant target revealed a localisation to the ER membrane *in planta* (Figure 4.6), similar to the previously reported *Pi*03192 and the potato *StNAC1* and *StNAC2* [126]. Both were observed to co-localise to the ER network as it is shown by the merge of the green and red channels. A significant co-localisation of the effectors, the NAC targets and the ER marker was detected in these experiments (Figure 4.6 A,B). As an additional experiment, to see whether *Pc03192* and *Pi03192* localize to the ER on the same level, both effectors (GFP- *Pc03192* and RFP-*Pi03192*) were co-infiltrated and imaged three days post infiltration. The co-localization is shown as an overlay of channels in Figure 4.6 C.

To test the stability of the fusion proteins, Western blots that hybridised with an antibody specific to GFP of the tagged *P. capsici* effector Pc03192 and SlNAC1 and SlNAC2, were conducted. Stability of the GFP- Pc03192 fusion protein was shown by a band of the predicted size (41 kDa; Figure 4.7A). The SlNAC proteins could, however, not be detected in any of the three replicated Western blot assays. To confirm the protein extractions, a Coomassie stained gel was used to show equal loading of the extracted protein (Figure 4.7B).

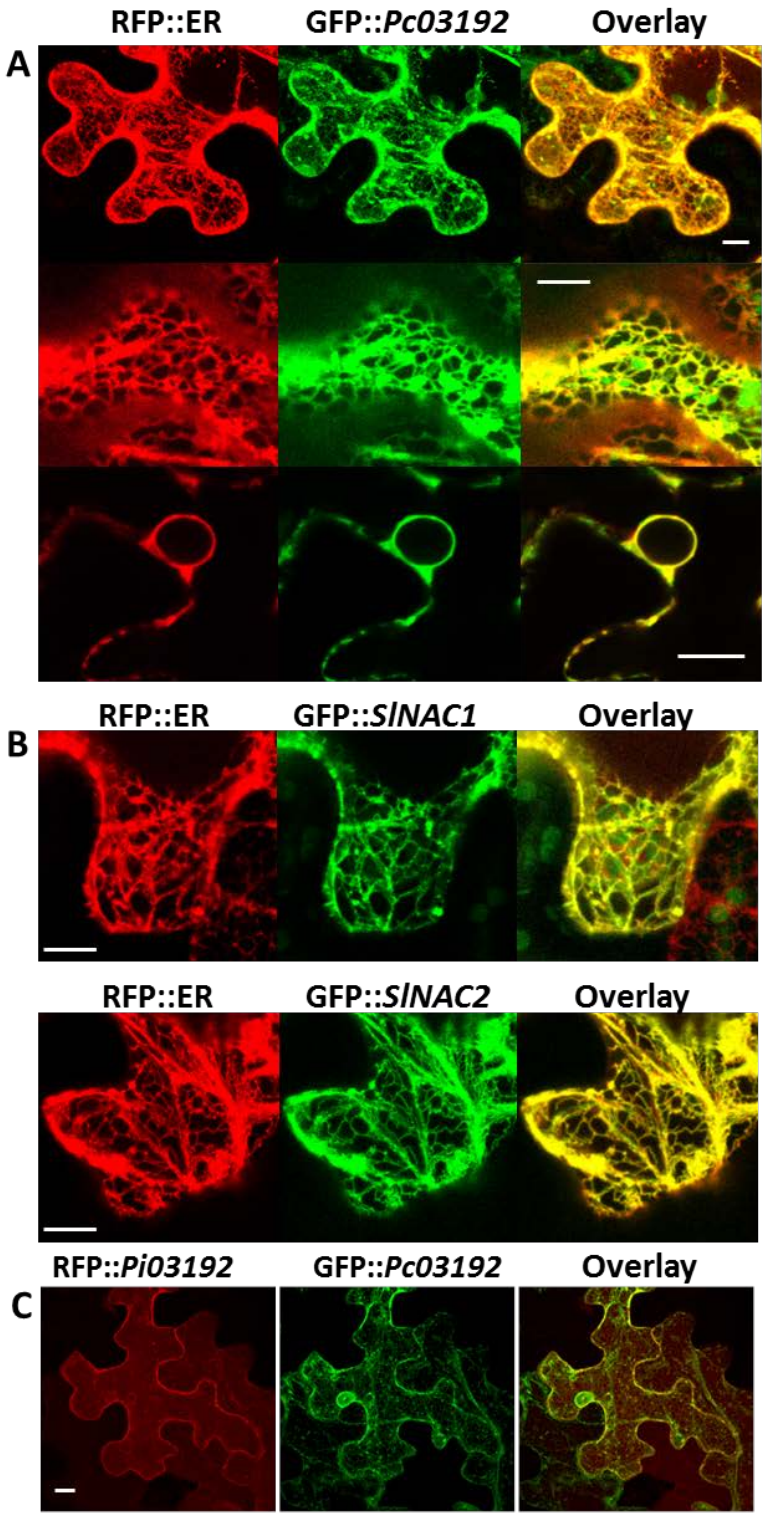

Figure 4.6: Subcellular localisations of *Pc03192* and tomato *SlNAC1* and *SlNAC2* by confocal microscopy
(A) GFP-*Pc03192* co-localises to the ER membrane with an RFP tagged ER marker. Three images showing the ER membrane and the ER around the nucleus. **(B)** GFP-*SlNAC1* and *SlNAC2* from tomato co-localise to the ER membrane with an RFP tagged ER marker **(C)** Both effector genes from *P. capsici* and *P. infestans* co-localise to the ER membrane. The merge of the red and green channels are demonstrated in yellow. Scale bars indicate 10 µm.

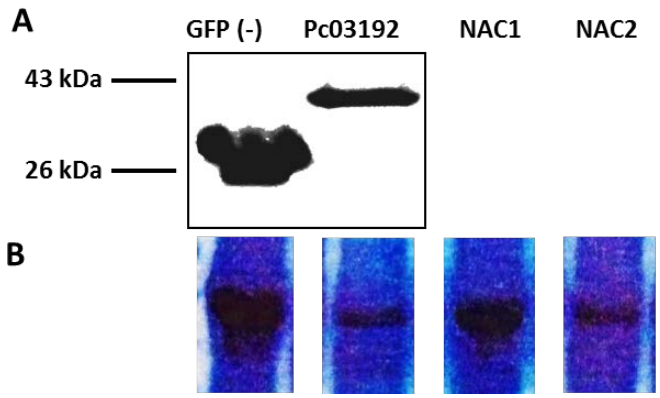

Figure 4.7: Western blot and Coomassie stain images of the protein Pc03192 and tomato SlNAC1 and SlNAC2 **(A)** Western blot of GFP-Pc03192 and GFP(-) empty vector control showing the stability of the full length constructs when probed with an antibody specific to GFP. The band of GFP-Pc03192 equals the predicted size of 41 kDa. **(B)** Coomassie stained gel (in blue) demonstrating the extracted protein amounts of the GFP-fluorescent tagged Pc03192 and SlNACs.

4.4 Discussion

Very little is known about plant host proteins that are targeted by effectors of filamentous pathogens and about the role of such targets in disease progression or plant immunity. Given the enormous size of the effector repertoire in all oomycete pathogens it is possible that closely evolved species have effectors that share common targets. Identification of plant targets deepen the understanding of the pathogen- and interaction-biology, but also allow the prediction of evolutionary conservation amongst closely related pathogen species. With the availability of the annotated genomes of *P. capsici* and *P. infestans*, a first glance was taken at both effector repertoires and first comparisons to find effectors with conserved sequences were conducted. The literature describes that a preserved gene with high sequence similarity in all species and only a few duplications along its evolutionary history, may be an ortholog with the same function in different species [188]. To test whether effector sequences that are conserved among *Phytophthora* species equal conserved functions in the respective hosts, there was a collaboration started with the group of Prof. Paul Birch (University of Dundee, UK), who only recently identified the *P. infestans* effector *Pi03192*, and two members of the potato NAC transcription factor family as targets [126]. Anderson *et al.* (2012) [180] suggested that conserved effectors manipulate the same or similar targets in the pathogens' hosts. They could show that the two conserved

RxLR effectors *HaRxL96* from *H. arabidopsidis* and *PsAvh163* from *P. sojae* share amino acids with 43% similarity and both suppress immune responses in soybean [180].

With the identification of a sequence relatively similar to the well-studied *P. infestans* effector gene *Pi03192,* it was aimed to test the hypothesis whether the *P. capsici* 03192 counterpart has a similar function in virulence. Although the most similar sequence showed only less than 50% pairwise identity over the full amino acid sequence, both sequences have the rare feature of a transmembrane domain in the C-terminus, and this sequence was continued to use as the putative ortholog to Pi03192. Orthology was defined by Walter Fitch in 1970 as "*Where the homology is the result of speciation so that the history of the gene reflects the history of the species(…), the genes should be called orthologous (ortho = exact).*" [189]. Orthology is a phylogenetic term which is used for functional equivalence in distantly related species that might have diverse functions from their common ancestor [190]. Although the sequence identity is not very high, *Pc03192* from *P. capsici* was assumed to be an ortholog also due to the relationship in the taxa with *P. infestans*. Similar to *Pi03192* it was shown that *Pc03192* is expressed mainly during biotrophy. The *P. capsici* effector *Pc03192* also co-localised with the NACs, which suggest that both proteins are active within the same part of the cell. Due to their function as transcription factors, NACs are expected to localise to the nucleus following release from the ER and are tightly regulated and rapidly turned over by the 26S proteasome [191-193]. NACs and their localisation in the cell are generally conserved across plant species, and it is thought that the mechanistic need for a rapid regulatory response by release from the subcellular membranes is under tight control [126].

However, the Y2H assays could not detect a strong interaction of *Pc03192* with the full length NAC1 and NAC2 orthologs of potato, tomato or *N. benthamiana* in several replicates. These results do not yet answer the question, whether the two effector orthologs 03192 evolved independently, supported by the low sequence similarity, or are derived from the same ancestor, supported by the high conservation of the plant target. Sequence analysis in more closely related species might help answer this question at least partially.

Taken together, the results suggest that Pc03192 interacts with SlNAC1 and SlNAC2 in the *P. capsici*-tomato system and provide an interesting insight into effectors that are shared between two related *Phytophthora* species, and that share the same plant targets.

4.5 Future experiments

The presented results lack partial depth in statistical and analytical support. To gain deeper insight into whether *Pc03192* shares conserved roles in virulence with *Pi03192*, further experiments based on the study of McLellan *et al.* (2013) [126] are necessary. These were partially initiated and preliminary data was achieved, but due to time constraints at the end of my PhD these could not be finished. The following experiments will be described as future follow up of this project.

Bimolecular fluorescence complementation (BiFC) assays to determine *in planta* interaction

To investigate further the potential protein interaction between *Pc03192* and the tomato NACs *in planta,* bimolecular fluorescence complementation (BiFC, also referred to as split YFP assays) was conducted as described in McLellan *et al.* (2013) [126]. Due to variable outcomes and non-repeatable results after more than four replicates, the experiment would need to be repeated with a different design. Although BiFC is a frequently used method in plant sciences to conduct in-depth analyses of protein-protein interactions in living cells, the method has weaknesses. For example, overexpression is known to produce artificial and simulated results [194]. High amounts of vector DNA, containing N- and C-terminal YFP sensor peptides, can trigger non-specific fluorescence emission, as was shown in a transfection study with COS cells [195]. This necessitates a tight control of the level of protein expression in BiFC assays to avoid false positive interactions. In addition one should be aware that the commonly used BiFC vectors for *in planta* expression assays contain the strong constitutive CaMV 35S-promoter [196, 197] which can cause a certain degree of fluorescence and may result in ectopic expression and/or overexpression and may result in artefactual protein-protein interactions. With this knowledge and several attempts using this method, I would suggest to employ the more sensitive and reliable fluorescence resonance energy transfer (FRET) [198, 199] method, which also permits the detection and quantification of fusion protein levels independently of their interaction [194]. This would be an essential follow up experiment to test the interaction between *Pc03192* and the tomato NAC *in planta*. An additional confirmation experiment to show the pathogen-host

interaction and to analyse the protein-protein interaction would be co-immunoprecipitation (pull down) assays.

Transient and stable silencing of effector and *NbNACs*

To further assess the role of the selected effector gene, several attempts have been undertaken to silence *Pc03192* in *P. capsici,* with the aim to generate stable transgenic lines. Unfortunately transformations were not stable and no transgenic line was recovered for experiments. Using an updated protocol, e.g. switching to another vector, this experiment must be repeated to fully understand the role of *Pc03192* in the biology or pathogenicity of *P. capsici*.

To test the role of NAC1 and NAC2 in defence, Virus Induced Gene Silencing (VIGS) constructs that transiently silenced the corresponding NbNACs [126] were infiltrated into *N. benthamiana*, and plants expressing the VIGS constructs have been infected with a fluorescent *P. capsici* strain expressing tdTomato (kindly provided by Ariane Kemen, Jonathan Jones-Lab at TSL). No differences in *P. capsici* colonisation were observed between silenced or control plants. However, this experiment was only conducted once, using high levels of zoospores and therefore needs to be repeated. Although the use of VIGS constructs have been shown previously, assessing whether NbNAC genes are indeed silenced in these experiments will be important before definite conclusions can be drawn on the impact of NbNAC proteins on immunity to *P. capsici*.

Inoculation with *P. capsici* culture filtrate

In McLellan *et al.* (2013) [126] it was suggested that an application of culture filtrate from *P. infestans* triggers the release of the potato StNAC1 and StNAC2 from the ER membrane and lead to nuclear accumulation. This experiment should be repeated using *Pc03192* and SlNAC1 and SlNAC2. As shown in McLellan *et al.* (2013) [126], *Pi03192* prevents the re-localisation of the target genes from the ER to the nucleus *in planta*. Interestingly, the effector *Pi03192* (also known as RD28) is recognized in *S. stoloniferum* resulting in HR [102, 200]. As another confirmation of conserved function, it would be of high interest to test *Pc03192* in Agroinfiltration assays or *P. capsici* inoculations for a hypersensitive response in the resistant *Solanum* genotype.

Screening of a Y2H-library

The assumption in this chapter was that the effector *Pc03192* works in the same way as *Pi03192*, but a definitive experiment would be to verify, if *Pc03192* interacts with anything else other than the two NAC-Tfs tested in this study. Therefore, to screen a Y2H library from *N. benthamiana* or *S. lycopersicum* would be critical to conduct and test the hypothesis further.

4.6 Concluding remarks

In this chapter I have chosen the closest ortholog to the *P. infestans* effector 03192 within the *P. capsici* genome, and I was able to show a co-localisation with the NAC and weak interaction in yeast. While the co-localisation and expression pattern during biotrophy do not allow any conclusions to whether the effector and NACs definitely interact, they suggest at least that both proteins are active within the same part of the cell and their expression patterns during virulence are tightly linked. However, given the low sequence similarity, this effector might not have been the best choice to test the hypothesis that conserved sequences equal conserved functions between different *Phytophthora* species. An effector with a higher sequence conservation (>80% for example) might have been the better choice to test this hypothesis. Follow up experiments on *Pc03192* in line with the study from McLellan *et al.*(2013) [126] will in the future however show how much conservation is necessary.

5. General Discussion

Research into the mechanisms behind plant-microbe interactions has generated a good understanding over the last decades; however, nothing has revolutionized research in this field more than the availability of high-quality full genome sequences of crop and model plants, but also their pathogens. This thesis gives a first insight into how the genome assemblies of *Phytophthora capsici* and tomato provided novel opportunities to deepen our understanding of the mechanisms behind the interaction of this pathogen with this economically important host.

The first step towards elucidation of the molecular interaction between *P. capsici* and several host species was the creation of a novel model infection system, described in the first part of this thesis (chapter 2). Phenotypical observations were linked to molecular and developmental events through the identification of a valuable set of biological marker genes that discriminate the three distinct phases of infection: biotrophy, necrotrophy and sporulation. Parts of this work have been published in *Molecular Plant Pathology* (Lamour,K.H., Stam,R., Jupe,J. and Huitema,E. 2011) [42].

This model infection system was subsequently used to study the specific interaction between *P. capsici* and tomato on the gene expression level, utilizing a novel approach in which probes reporting on expression for the complete gene model sets of both organisms were synthesized onto one microarray chip. This work allowed unprecedented insight into the molecular reprogramming during attack and defence in both organisms, and was published in *Genome Biology* (Jupe,J. *et al.* 2013) [67] (Chapter 3) and *PLOS One* (Stam,R., Jupe,J. *et al.* 2013) [86].

In the last Chapter 4, information gained from these microarray expression analyses was used in a case study of a putative *P. capsici* RXLR effector protein for which a potential orthologous sequence has earlier been described from *P. infestans* to interact with two potato NAC transcription factors [126].

The complexity of a hemibiotrophic lifestyle

Hemibiotrophy is a very complex lifestyle that requires the pathogen to have full control over its host especially during the initial biotrophic phase. An adapted plant might respond with, for example, local cell death to counter the pathogen's requirement for living host

tissue. However, in the non-adapted plant the pathogen will initially be a non-killer (biotroph). Once the pathogen's needs are fulfilled, it will switch the mode of action from non-killer to killer (necrotroph) in order to continue with the life cycle. In Chapter 3 evidence was found that the host organism runs through a transcriptional reprogramming to try and defend against the invading pathogen. Gene expression analysis during the interaction of *P. capsici* and tomato in the microarray assay identified 81 plant genes that were specifically regulated during the active penetration and growth of *P. capsici*, and that are either engaged to defend or that were specifically triggered to produce or supply nutrients (Chapter 3 and Jupe *et al.* 2013) [67]. An interesting experiment to conduct would be to identify the transcriptional changes during a semi-compatible infection event where, unlike a single dominant resistance gene that is sufficient to fend off *P. capsici*, a QTL like the one found in the pepper accession 'Criollo de Morelos 334' [5, 6] is used. However, to conduct a similar study a pepper genome annotation needs to be available, which might happen in the near future.

Analyses presented in Chapter 3 have shown the downregulation of 61 tomato genes during biotrophy, whereas 57 specific *P. capsici* genes were upregulated only during this phase. More detailed research in the future might show which host genes are involved in defence against the pathogen, or which were specifically triggered by *Phytophthora* to create a food source.

Large microarray data-set provides scaffold for further studies

This thesis presents a study of the widespread oomycete *P. capsici*, a pathogen of high interest due to its severe damage to diverse crops and its relatedness to other important oomycete pathogens. These days, genome-wide expression studies are carried out either using microarrays or by RNA-seq. Both technologies are efficient ways to generate enormous data that represent expressed genes on quantitative levels [201]. RNA-seq allows flexibility where no reference genome is available to design probes from. However, in studies as these presented in this thesis, where infected plant material is harvested at several stages post-inoculation, suitable protocols are missing to normalize the minute amounts of pathogen present during the early stages of infection to the much larger quantity of plant material. A microarray containing both organisms is much more suitable for this approach as no separate normalization of the DNA is necessary.

From the large amount of data that was derived from the unique microarray experiment, first insights were gained into transcriptional changes during the *P. capsici*-tomato interaction. In addition, the generated data-sets of this microarray will enable further analysis of both the pathogen as well as the tomato transcripts from a variety of aspects. As presented in this thesis, *P. capsici* is an attractive model oomycete with broad host range and the transcriptional data could for example be used to analyse all genes and pathways involved in the molecular switch from biotrophy to necrotrophy [42, 67]. Interesting further subjects of study could be the reprogramming of developmental processes or signalling pathways in both organisms. Focus should not only be towards those responsible for the infection process, but also the supply of nutrients to the pathogen. These might reveal a further set of potential plant targets, specifically sugar cycle hubs for example, but also targets for resistance breeding against this pathogen.

***Phytophthora*-wide conservation of effectors**

Effectors that are conserved among several *Phytophthora* species are potentially ancient in their origin, and might thus reveal infection pathways that are of greatest importance to the pathogen. With the identification of the potential plant targets of these, a different way of resistance breeding could be followed. In this study, the most similar *P. capsici* sequence was determined for a well characterised *P. infestans* effector [126] using reciprocal BLAST. However, a large-scale phylogenetic analysis based on an alignment of the C-terminal region of all RXLR encoding genes of *P. capsici, P. infestans* and, for example, *P. sojae* would provide a better scaffold to identify those genes that sit in a common clade and thus have evolved from a common ancestor. Candidates for the study of the hypothesis that conserved sequence equals conserved functions in virulence should then be chosen from these clades.

6. Concluding Remarks

Overall, with this study and the identification of biological marker genes for the distinct infection phases of *P. capsici*, molecular and phenological aspects could be linked for the first time. An important next step is to identify conserved effector proteins within *Phytophthora* species and determine how they manipulate host processes on a wide host range. This will help, respectively, to explain the mechanisms of pathogenicity and further to design novel control strategies for the diseases caused by not only *P. capsici*, but also other *Phytophthora* species.

7. References

1. Dangl JL, Jones JD: **Plant pathogens and integrated defence responses to infection.** *Nature* 2001, **411:**826-833.
2. Chisholm ST, Coaker G, Day B, Staskawicz BJ: **Host-microbe interactions: shaping the evolution of the plant immune response.** *Cell* 2006, **124:**803-814.
3. Abramovitch RB, Anderson JC, Martin GB: **Bacterial elicitation and evasion of plant innate immunity.** *Nature Reviews. Molecular Cell Biology* 2006, **7:**601-611.
4. Jones JD, Dangl JL: **The plant immune system.** *Nature* 2006, **444:**323-329.
5. Maekawa T, Kufer TA, Schulze-Lefert P: **NLR functions in plant and animal immune systems: so far and yet so close.** *Nature Immunology* 2011, **12:**817-826.
6. Dangl JL HD, Staskawicz BJ: **Pivoting the plant immune system from dissection to deployment.** *Science* 2013, **341(6147):**746-751.
7. Boller T HS: **Innate immunity in plants: an arms race between pattern recognition receptors in plants and effectors in microbial pathogens.** *Science* 2009, **8;324(5928):**742-744.
8. Cui H, Xiang T, Zhou J-M: **Plant immunity: a lesson from pathogenic bacterial effector proteins.** *Cellular Microbiology* 2009, **11:**1453-1461.
9. Hein I, Gilroy EM, Armstrong MR, Birch PR: **The zig-zag-zig in oomycete-plant interactions.** *Molecular Plant Pathology* 2009, **10:**547-562.
10. Boller T, Felix G: **A renaissance of elicitors: perception of microbe-associated molecular patterns and danger signals by pattern-recognition receptors.** *Annual Review of Plant Biology* 2009, **60:**379-406.
11. Nürnberger T, Brunner F, Kemmerling B, Piater L: **Innate immunity in plants and animals: striking similarities and obvious differences.** *Immunological Reviews* 2004, **198:**249-266.
12. Ingle RA, Carstens M, Denby KJ: **PAMP recognition and the plant–pathogen arms race.** *BioEssays* 2006, **28:**880-889.
13. Felix G, Duran JD, Volko S, Boller T: **Plants have a sensitive perception system for the most conserved domain of bacterial flagellin.** *The Plant Journal* 1999, **18:**265-276.
14. Salomon S, Robatzek S: **Induced endocytosis of the receptor kinase FLS2.** *Plant Signaling & Behavior* 2006, **1:**293-295.
15. Zipfel C, Robatzek S, Navarro L, Oakeley EJ, Jones JDG, Felix G, Boller T: **Bacterial disease resistance in Arabidopsis through flagellin perception.** *Nature* 2004, **428:**764-767.
16. Chinchilla D, Bauer,Z., Regenass,M., Boller,T. and Felix,G.: **The Arabidopsis receptor kinase FLS2 binds flg22 and determines the specificity of flagellin perception.** *Plant Cell* 2006, **18:**465-476.

17. Kamoun S, van West P, Vleeshouwers VG, de Groot KE, Govers F: **Resistance of *Nicotiana benthamiana* to *Phytophthora infestans* is mediated by the recognition of the elicitor protein INF1.** *Plant Cell* 1998, **10:**1413-1426.
18. Kamoun S: **A catalogue of the effector secretome of plant pathogenic oomycetes.** *Annual Review of Phytopathology* 2006, **44:**41-60.
19. Bos JIB, Armstrong MR, Gilroy EM, Boevink PC, Hein I, Taylor RM, Zhendong T, Engelhardt S, Vetukuri RR, Harrower B, et al: ***Phytophthora infestans* effector AVR3a is essential for virulence and manipulates plant immunity by stabilizing host E3 ligase CMPG1.** *Proceedings of the National Academy of Sciences* 2010, **107:**9909-9914.
20. Birch PRJ, Rehmany AP, Pritchard L, Kamoun S, Beynon JL: **Trafficking arms: oomycete effectors enter host plant cells.** *Trends in Microbiology* 2006, **14:**8-11.
22. Grant SR, Fisher EJ, Chang JH, Mole BM, Dangl JL: **Subterfuge and manipulation: type III effector proteins of phytopathogenic bacteria.** *Annual Review of Microbiology* 2006, **60:**425-449.
23. Bos JIB, Prince D, Pitino M, Maffei ME, Win J, Hogenhout SA: **A functional genomics approach identifies candidate effectors from the aphid species *Myzus persicae* (Green Peach Aphid).** *PLoS Genetics* 2010, **6:**e1001216.
24. Hewezi T, Baum TJ: **Manipulation of plant cells by cyst and root-knot nematode effectors.** *Molecular Plant-Microbe Interactions* 2012, **26:**9-16.
25. Rehmany AP, Gordon A, Rose LE, Allen RL, Armstrong MR, Whisson SC, Kamoun S, Tyler BM, Birch PR, Beynon JL: **Differential recognition of highly divergent downy mildew avirulence gene alleles by *RPP1* resistance genes from two *Arabidopsis* lines.** *Plant Cell* 2005, **17:**1839-1850.
26. Whisson SC, Boevink PC, Moleleki L, Avrova AO, Morales JG, Gilroy EM, Armstrong MR, Grouffaud S, van West P, Chapman S, et al: **A translocation signal for delivery of oomycete effector proteins into host plant cells.** *Nature* 2007, **450:**115-118.
27. Schornack S, Huitema E, Cano L, Bozkurt T, Oliva R, Van Damme M, Schwizer S, Raffaele S, Chaparro-Garcia A, Farrer R: **Ten things to know about oomycete effectors.** *Molecular Plant Pathology* 2009, **10:**795 - 803.
28. van den Burg HA, Harrison SJ, Joosten MH, Vervoort J, de Wit PJ: ***Cladosporium fulvum* Avr4 protects fungal cell walls against hydrolysis by plant chitinases accumulating during infection.** *Molecular Plant-Microbe Interactions* 2006, **19:**1420-1430.
29. Jupe F, Pritchard L, Etherington G, MacKenzie K, Cock P, Wright F, Sharma SK, Bolser D, Bryan G, Jones J, Hein I: **Identification and localisation of the NB-LRR gene family within the potato genome.** *BMC Genomics* 2012, **13:**75.
30. van der Hoorn RAL, Kamoun S: **From guard to decoy: a new model for perception of plant pathogen effectors.** *Plant Cell* 2008, **20(8):**2009-17
31. Armstrong MR, Whisson SC, Pritchard L, Bos JIB, Venter E, Avrova AO, Rehmany AP, Bohme U, Brooks K, Cherevach I, et al: **An ancestral oomycete locus contains late**

blight avirulence gene *Avr3a*, encoding a protein that is recognized in the host cytoplasm. *Proceedings of the National Academy of Sciences of the USA* 2005, **102:**7766-7771.

32. Engelhardt S, Boevink PC, Armstrong MR, Ramos MB, Hein I, Birch PRJ: **Relocalization of late blight resistance protein R3a to endosomal compartments is associated with effector recognition and required for the immune response.** *Plant Cell* 2012, **24(12):**5142-58
33. Mackey D, Holt BF, Wiig A, Dangl JL: **RIN4 interacts with *Pseudomonas syringae* type III effector molecules and is required for *RPM1*-mediated resistance in Arabidopsis.** *Cell* 2002, **108:**743-754.
34. Tang X FR, Zhou J, Halterman DA, Jia Y, Martin GB: **Initiation of plant disease resistance by physical interaction of AvrPto and Pto kinase.** *Science* 1996, **274:**2060-2063.
35. Salmeron JM, Oldroyd GED, Rommens CMT, Scofield SR, Kim H-S, Lavelle DT, Dahlbeck D, Staskawicz BJ: **Tomato Prf is a member of the leucine-rich repeat class of plant disease resistance genes and lies embedded within the Pto kinase gene cluster.** *Cell* 1996, **86:**123-133.
36. Rossman AYaP, M.E.: **Why are *Phytophthora* and other Oomycota not true Fungi?** *APSnet, adapted from Research Information Ltd Outlooks on Pest Management* 2006, **17:**217-219.
37. Baldauf SL: **The deep roots of eukaryotes.** *Science* 2003, **300:**1703-1706.
38. Govers F: *Oomycete Genetics and Genomics, Diversity, Interactions and Research Tools.* Wiley-Blackwell; 2009.
39. Fisher MC, Henk DA, Briggs CJ, Brownstein JS, Madoff LC, McCraw SL, Gurr SJ: **Emerging fungal threats to animal, plant and ecosystem health.** *Nature* 2012, **484:**186-194.
40. de Bary A: **Researches into the nature of the potato-fungus (*Phytophthora Infestans*)**. William Clowes; 1876.
41. Fry WE: ***Phytophthora infestans*: the plant (and *R* gene) destroyer.** *Molecular Plant Pathology* 2008, **9:**385–402.
42. Lamour KH, Stam R, Jupe J, Huitema E: **The oomycete broad-host-range pathogen *Phytophthora capsici*.** *Molecular Plant Pathology* 2011, **13:**329-337.
43. Lamour KH, Mudge J, Gobena D, Hurtado-Gonzales OP, Schmutz J, Kuo A, Miller NA, Rice BJ, Raffaele S, Cano L, et al: **Genome sequencing and mapping reveal loss of heterozygosity as a mechanism for rapid adaptation in the vegetable pathogen *Phytophthora capsici*.** *Molecular Plant-Microbe Interactions* 2012.
44. Erwin DC, Ribeiro OK: ***Phytophthora* diseases worldwide**. St. Paul, Minnesota: APS Press; 1996.
45. Davidson CR, Carroll RB, Evans TA, Mulrooney RP, Kim SH: **First report of *Phytophthora capsici* infecting Lima bean (*Phaseolus lunatus*) in the mid-atlantic region.** *Plant Disease* 2002, **86:**1049-1049.

46. Hausbeck M, Lamour H: ***Phytophthora capsici* on vegetable crops: research progress and management challenges.** *Plant Disease* 2004, **88:**1292-1303.
47. Leonian LH: **Stem and fruit blight of peppers caused by *Phytophthora capsici* sp.nov.** *Phytopathology* 1922, **12:**401-408.
48. Blair JE, Coffey MD, Park S-Y, Geiser DM, Kang S: **A multi-locus phylogeny for *Phytophthora* utilizing markers derived from complete genome sequences.** *Fungal Genetics and Biology* 2008, **45:**266-277.
49. Kroon LPNM, Brouwer H, de Cock AWAM, Govers F: **The genus *Phytophthora* anno 2012.** *Phytopathology* 2011, **102:**348-364.
50. Waterhouse GM: **Key to the species of *Phytophthora* de Bary**. Commonwealth Mycological Institute; 1963.
51. Aragaki MaU, J.: **Morphological distinctions between *Phytophthora capsici* and *P. tropicalis* sp. nov.** *Mycologia* 2001, **93:**137-145.
52. Zhang ZG, Zhang JY, Zheng XB, Yang YW, Ko WH: **Molecular distinctions between *Phytophthora capsici* and *Ph. tropicalis* based on ITS sequences of ribosomal DNA.** *Journal of Phytopathology* 2004, **152:**358-364.
53. Lamour KH, Hausbeck MK: **Investigating the spatiotemporal genetic structure of *Phytophthora capsici* in Michigan.** *Phytopathology* 2001, **91:**973-980.
54. Lamour KH, Hausbeck MK: **The spatiotemporal genetic structure of *Phytophthora capsici* in Michigan and implications for disease management.** *Phytopathology* 2002, **92:**681-684.
55. Quesada-Ocampo LM, Granke LL, Mercier MR, Olsen J, Hausbeck MK: **Investigating the genetic structure of *Phytophthora capsici* populations.** *Phytopathology* 2011, **101:**1061-1073.
56. Tian D, Babadoost M: **Host range of *Phytophthora capsici* from pumpkin and pathogenicity of isolates.** *Plant Disease* 2004, **88:**485-489.
57. Hurtado-Gonzáles O, Aragon-Caballero L, Apaza-Tapia W, Donahoo R, Lamour K: **Survival and spread of *Phytophthora capsici* in coastal Peru.** *Phytopathology* 2008, **98:**688-694.
58. Gobena D, Roig J, Galmarini C, Hulvey J, Lamour K: **Genetic diversity of *Phytophthora capsici* isolates from pepper and pumpkin in Argentina.** *Mycologia* 2012, **104:**102-107.
59. Ko W: **Hormonal heterothallism and homothallism in *Phytophthora*.** *Annual Review of Phytopathology* 1988, **26:**57-73.
60. Bowers JHP, G. C.; Johnston, S. A. : **Effect of soil temperature and soil-water matric potential on the survival of *Phytophthora capsici* in natural soil.** *Plant Disease* 1990, **74:**771-777.
61. van West P, Shepherd SJ, Walker CA, Li S, Appiah AA, Grenville-Briggs LJ, Govers F, Gow NAR: **Internuclear gene silencing in *Phytophthora infestans* is established through chromatin remodelling.** *Microbiology* 2008, **154:**1482-1490.

62. Schornack S, van Damme M, Bozkurt TO, Cano LM, Smoker M, Thines M, Gaulin E, Kamoun S, Huitema E: **Ancient class of translocated oomycete effectors targets the host nucleus.** *Proceedings of the National Academy of Sciences* 2010, **107:**17421-17426.
63. Judelson HS, Blanco FA: **The spores of *Phytophthora*: Weapons of the plant destroyer.** *Nature Reviews Microbiology* 2005, **3:**47-58.
64. Horbach R, Navarro-Quesada AR, Knogge W, Deising HB: **When and how to kill a plant cell: Infection strategies of plant pathogenic fungi.** *Journal of Plant Physiology* 2011, **168:**51-62.
65. Koeck M, Hardham AR, Dodds PN: **The role of effectors of biotrophic and hemibiotrophic fungi in infection.** *Cellular Microbiology* 2011, **13:**1849-1857.
66. Perfect SE, Green JR: **Infection structures of biotrophic and hemibiotrophic fungal plant pathogens.** *Molecular Plant Pathology* 2001, **2:**101-108.
67. Jupe J, Stam R, Howden A, Morris J, Zhang R, Hedley P, Huitema E: ***Phytophthora capsici*-tomato interaction features dramatic shifts in gene expression associated with a hemi-biotrophic lifestyle.** *Genome Biology* 2013, **14:**R63.
68. Tan MYA, Hutten RB, Visser RF, Eck H: **The effect of pyramiding *Phytophthora infestans* resistance genes *R Pi-mcd1* and *R Pi-ber* in potato.** *Theoretical and Applied Genetics* 2010, **121:**117-125.
69. Zhu S, Li Y, Vossen J, Visser RF, Jacobsen E: **Functional stacking of three resistance genes against *Phytophthora infestans* in potato.** *Transgenic Research* 2012, **21:**89-99.
70. Ballvora A, Ercolano MR, Weiß J, Meksem K, Bormann CA, Oberhagemann P, Salamini F, Gebhardt C: **The *R1* gene for potato resistance to late blight (*Phytophthora infestans*) belongs to the leucine zipper/NBS/LRR class of plant resistance genes.** *The Plant Journal* 2002, **30:**361-371.
71. Champouret N, Bouwmeester K, Rietman H, van der Lee T, Maliepaard C, Heupink A, van de Vondervoort PJI, Jacobsen E, Visser RGF, van der Vossen EAG, et al: ***Phytophthora infestans* isolates lacking class I ipiO variants are virulent on *Rpi-blb1* potato.** *Molecular Plant-Microbe Interactions* 2009, **22:**1535-1545.
72. Walker SJ, Bosland PW: **Inheritance of *Phytophthora* root rot and foliar blight resistance in pepper.** *Journal of the American Society for Horticultural Science* 1999, **124:**14-18.
73. Quesada-Ocampo LM, Hausbeck MK: **Resistance in tomato and wild relatives to crown and root rot caused by *Phytophthora capsici*.** *Phytopathology* 2010, **100:**619-627.
74. Wang Y, Bouwmeester K, van de Mortel JE, Shan W, Govers F: **Induced expression of defense-related genes in *Arabidopsis* upon infection with *Phytophthora capsici*.** *Plant Signaling & Behavior* 2013, **8:**e24618.

75. Tyler B, Tripathy S, Zhang X, Dehal P, Jiang R, Aerts A, Arredondo F, Baxter L, Bensasson D, Beynon J: ***Phytophthora*** **genome sequences uncover evolutionary origins and mechanisms of pathogenesis.** *Science* 2006, **313:**1261 - 1266.
76. Haas BJ, Kamoun S, Zody MC, Jiang RHY, Handsaker RE, Cano LM, Grabherr M, Kodira CD, Raffaele S, Torto-Alalibo T, et al: **Genome sequence and analysis of the Irish potato famine pathogen *Phytophthora infestans*.** *Nature* 2009, **461:**393-398.
77. Morgan W, Kamoun S: **RXLR effectors of plant pathogenic oomycetes.** *Current Opinion in Microbiology* 2007, **10:**332-338.
78. Bozkurt TO, Schornack S, Win J, Shindo T, Ilyas M, Oliva R, Cano LM, Jones AME, Huitema E, van der Hoorn RAL, Kamoun S: ***Phytophthora infestans*** **effector AVRblb2 prevents secretion of a plant immune protease at the haustorial interface.** *Proceedings of the National Academy of Sciences* 2011, **108:**20832-20837.
79. Bozkurt TO, Schornack S, Banfield MJ, Kamoun S: **Oomycetes, effectors, and all that jazz.** *Current Opinion in Plant Biology* 2012, **15:**9.
80. Saunders DGO, Win J, Cano LM, Szabo LJ, Kamoun S, Raffaele S: **Using hierarchical clustering of secreted protein families to classify and rank candidate effectors of rust fungi.** *PLoS ONE* 2012, **7:**e29847.
81. Oliva R, Win J, Raffaele S, Boutemy L, Bozkurt TO, Chaparro-Garcia A, Segretin ME, Stam R, Schornack S, Cano LM, et al: **Recent developments in effector biology of filamentous plant pathogens.** *Cellular Microbiology* 2010, **12:**1015-1015.
82. Rose JK, Ham KS, Darvill AG, Albersheim P: **Molecular cloning and characterization of glucanase inhibitor proteins: coevolution of a counterdefense mechanism by plant pathogens.** *Plant Cell* 2002, **14:**1329-1345.
83. Tian M, Benedetti B, Kamoun S: **A second kazal-like protease inhibitor from *Phytophthora infestans*** **inhibits and interacts with the apoplastic pathogenesis-related protease P69B of tomato.** *Plant Physiology* 2005, **138:**1785-1793.
84. Birch PR, Boevink PC, Gilroy EM, Hein I, Pritchard L, Whisson SC: **Oomycete RXLR effectors: delivery, functional redundancy and durable disease resistance.** *Current Opinion in Plant Biology* 2008, **11:**373-379.
85. Torto T, Li S, Styer A, Huitema E, Testa A, Gow NAR, van West P, Kamoun S: **EST mining and functional expression assays identify extracellular effector proteins from *Phytophthora*.** *Genome Research* 2003, **13:**1675-1685.
86. Stam R, Jupe J, Howden AJM, Morris JA, Boevink PC, Hedley PE, Huitema E: **Identification and characterisation CRN Effectors in *Phytophthora capsici*** **shows modularity and functional diversity.** *PLoS ONE* 2013, **8:**e59517.
87. Bailey BA: **Purification of a protein from culture filtrates of *Fusarium oxysporum*** **that induces ethylene and necrosis in leaves of *Erythroxylum coca*.** *Phytopathology* 1995, **85:**1250-1255.
88. Feng BZ, Li, P.Q., Fu,L., Sun,B.B. and Zhang,X.G.: **Identification of 18 genes encoding necrosis-inducing proteins from the plant pathogen *Phytophthora capsici*** **(Pythiaceae: Oomycetes).** *Genetics and Molecular Research* 2011, **10 (2):**910-922.

89. Li P, Feng B, Wang H, Tooley PW, Zhang X: **Isolation of nine *Phytophthora capsici* pectin methylesterase genes which are differentially expressed in various plant species.** *Journal of Basic Microbiology* 2011, **51:**61-70.
90. Kanneganti TD, Huitema E, Cakir C, Kamoun S: **Synergistic interactions of the plant cell death pathways induced by *Phytophthora infestans* Nep1-like protein PiNPP1.1 and INF1 elicitin.** *Molecular Plant-Microbe Interactions* 2006, **19:**854-863.
91. Fellbrich G, Romanski A, Varet A, Blume B, Brunner F, Engelhardt S, Felix G, Kemmerling B, Krzymowska M, Nürnberger T: **NPP1, a *Phytophthora*-associated trigger of plant defense in parsley and *Arabidopsis*.** *Plant Journal* 2002, **32:**375-390.
92. Qutob D, Kamoun S, Gijzen M: **Expression of a *Phytophthora sojae* necrosis-inducing protein occurs during transition from biotrophy to necrotrophy.** *Plant Journal* 2002, **32:**361-373.
93. Dou D, Kale SD, Wang X, Chen Y, Wang Q, Jiang RH, Arredondo FD, Anderson RG, Thakur PB, McDowell JM, et al: **Conserved C-terminal motifs required for avirulence and suppression of cell death by *Phytophthora sojae* effector Avr1b.** *Plant Cell* 2008, **20:**1118-1133.
94. Jiang RH, Tripathy S, Govers F, Tyler BM: **RXLR effector reservoir in two *Phytophthora* species is dominated by a single rapidly evolving superfamily with more than 700 members.** *Proceedings of the National Academy of Sciences of the USA* 2008, **105:**4874-4879.
95. Baxter L, Tripathy S, Ishaque N, Boot N, Cabral A, Kemen E, Thines M, Ah-Fong A, Anderson R, Badejoko W, et al: **Signatures of adaptation to obligate biotrophy in the *Hyaloperonospora arabidopsidis* genome.** *Science* 2010, **330:**1549-1551.
96. van West P, De Bruijn I, Minor KL, Phillips AJ, Robertson EJ, Wawra S, Bain J, Anderson VL, Secombes CJ: **The putative RxLR effector protein SpHtp1 from the fish pathogenic oomycete *Saprolegnia parasitica* is translocated into fish cells.** *FEMS Microbiology Letters* 2010, **310:**127-137.
97. Links M, Holub E, Jiang R, Sharpe A, Hegedus D, Beynon E, Sillito D, Clarke W, Uzuhashi S, Borhan M: **De novo sequence assembly of *Albugo candida* reveals a small genome relative to other biotrophic oomycetes.** *BMC Genomics* 2011, **12:**503.
98. Levesque CA, Brouwer H, Cano L, Hamilton JP, Holt C, Huitema E, Raffaele S, Robideau GP, Thines M, Win J, et al: **Genome sequence of the necrotrophic plant pathogen *Pythium ultimum* reveals original pathogenicity mechanisms and effector repertoire.** *Genome Biology* 2010, **11:**22.
99. Allen RL, Bittner-Eddy PD, Grenville-Briggs LJ, Meitz JC, Rehmany AP, Rose LE, Beynon JL: **Host-parasite coevolutionary conflict between *Arabidopsis* and downy mildew.** *Science* 2004, **306:**1957-1960.
100. van Poppel PM, Guo J, van de Vondervoort PJ, Jung MW, Birch PR, Whisson SC, Govers F: **The *Phytophthora infestans* avirulence gene *Avr4* encodes an RXLR-dEER effector.** *Molecular Plant-Microbe Interactions* 2008, **21:**1460-1470.

101. Shan W, Cao M, Leung D, Tyler BM: **The *Avr1b* locus of *Phytophthora sojae* encodes an elicitor and a regulator required for avirulence on soybean plants carrying resistance gene *Rps1b*.** *Molecular Plant-Microbe Interactions* 2004, **17:**394-403.
102. Vleeshouwers VG, Rietman H, Krenek P, Champouret N, Young C, Oh SK, Wang M, Bouwmeester K, Vosman B, Visser RG, et al: **Effector genomics accelerates discovery and functional profiling of potato disease resistance and *Phytophthora infestans* avirulence genes.** *PLoS ONE* 2008, **3:**e2875.
103. Win J, Morgan W, Bos J, Krasileva KV, Cano LM, Chaparro-Garcia A, Ammar R, Staskawicz BJ, Kamoun S: **Adaptive evolution has targeted the C-terminal domain of the RXLR effectors of plant pathogenic oomycetes.** *Plant Cell* 2007, **19:**2349-2369.
104. Rietman H, Bijsterbosch G, Cano LM, Lee H-R, Vossen JH, Jacobsen E, Visser RGF, Kamoun S, Vleeshouwers VGAA: **Qualitative and quantitative late blight resistance in the potato cultivar Sarpo Mira is determined by the perception of five distinct RXLR effectors.** *Molecular Plant-Microbe Interactions* 2012, **25:**910-919.
105. Whisson SC, Basnayake S, Maclean DJ, Irwin JAG, Drenth A: ***Phytophthora sojae* avirulence genes *Avr4* and *Avr6* are located in a 24kb, recombination-rich region of genomic DNA.** *Fungal Genetics and Biology* 2004, **41:**62-74.
106. May KJ, Whisson SC, Zwart RS, Searle IR, Irwin JAG, Maclean DJ, Carroll BJ, Drenth A: **Inheritance and mapping of 11 avirulence genes in *Phytophthora sojae*.** *Fungal Genetics and Biology* 2002, **37:**1-12.
107. Van Poppel PMJA, Jiang RHY, ŚLiwka J, Govers F: **Recognition of *Phytophthora infestans* Avr4 by potato R4 is triggered by C-terminal domains comprising W motifs.** *Molecular Plant Pathology* 2009, **10:**611-620.
108. Dou D, Kale SD, Liu T, Tang Q, Wang X, Arredondo FD, Basnayake S, Whisson S, Drenth A, Maclean D, Tyler BM: **Different domains of *Phytophthora sojae* effector *Avr4/6* are recognized by soybean resistance genes *Rps4* and *Rps6*.** *Molecular Plant-Microbe Interactions* 2010, **23:**425-435.
109. Dong S, Qutob D, Tedman-Jones J, Kuflu K, Wang Y, Tyler BM, Gijzen M: **The *Phytophthora sojae* avirulence locus *Avr3c* encodes a multi-copy RXLR effector with sequence polymorphisms among pathogen strains.** *PLoS ONE* 2009, **4:**e5556.
110. Hiller NL, Bhattacharjee S, van Ooij C, Liolios K, Harrison T, Lopez-Estrano C, Haldar K: **A host-targeting signal in virulence proteins reveals a secretome in malarial infection.** *Science* 2004, **306:**1934-1937.
111. Marti M, Good RT, Rug M, Knuepfer E, Cowman AF: **Targeting malaria virulence and remodeling proteins to the host erythrocyte.** *Science* 2004, **306:**1930-1933.
112. Bhattacharjee S, Hiller NL, Liolios K, Win J, Kanneganti T-D, Young C, Kamoun S, Haldar K: **The malarial host-targeting signal is conserved in the Irish potato famine pathogen.** *PLoS Pathogens* 2006, **2:**e50.
113. Grouffaud S, van West P, Avrova AO, Birch PR, Whisson SC: ***Plasmodium falciparum* and *Hyaloperonospora parasitica* effector translocation motifs are functional in *Phytophthora infestans*.** *Microbiology* 2008, **154:**3743-3751.

114. Kale SD, Gu B, Capelluto DGS, Dou D, Feldman E, Rumore A, Arredondo FD, Hanlon R, Fudal I, Rouxel T, et al: **External lipid PI3P mediates entry of eukaryotic pathogen effectors into plant and animal host cells.** *Cell* 2010, **142:**284-295.
115. Wawra S, Bain J, Durward E, de Bruijn I, Minor KL, Matena A, Löbach L, Whisson SC, Bayer P, Porter AJ, et al: **Host-targeting protein 1 (SpHtp1) from the oomycete *Saprolegnia parasitica* translocates specifically into fish cells in a tyrosine-O-sulphate–dependent manner.** *Proceedings of the National Academy of Sciences* 2012, **109:**2096-2101.
116. Tyler BM, Kale SD, Wang Q, Tao K, Clark HR, Drews K, Antignani V, Rumore A, Hayes T, Plett JM, et al: **Microbe-independent entry of oomycete RxLR effectors and fungal RxLR-Like effectors into plant and animal cells is specific and reproducible.** *Molecular Plant-Microbe Interactions* 2013, **26:**611-616.
117. Kale SD, Tyler BM: **Entry of oomycete and fungal effectors into plant and animal host cells.** *Cellular Microbiology* 2011, **13:**1839-1848.
118. Wawra S, Djamei A, Albert I, Nürnberger T, Kahmann R, van West P: **In vitro translocation experiments with RxLR-reporter fusion proteins of Avr1b from *Phytophthora sojae* and AVR3a from *Phytophthora infestans* fail to demonstrate specific autonomous uptake in plant and animal cells.** *Molecular Plant-Microbe Interactions* 2013, **26:**528-536.
119. Petre B, Kamoun S: **How do filamentous pathogens deliver effector proteins into plant cells?** *PLoS Biology* 2014, **12:**e1001801.
120. Hann DR, Gimenez-Ibanez S, Rathjen JP: **Bacterial virulence effectors and their activities.** *Current Opinion in Plant Biology* 2010, **13:**388-393.
121. de Jonge R, Bolton MD, Thomma BPHJ: **How filamentous pathogens co-opt plants: the ins and outs of fungal effectors.** *Current Opinion in Plant Biology* 2011, **14:**400-406.
122. González-Lamothe R, Tsitsigiannis DI, Ludwig AA, Panicot M, Shirasu K, Jones JDG: **The U-Box protein CMPG1 is required for efficient activation of defense mechanisms triggered by multiple resistance genes in tobacco and tomato.** *Plant Cell* 2006, **18:**1067-1083.
123. Gilroy EM, Taylor RM, Hein I, Boevink P, Sadanandom A, Birch PRJ: **CMPG1-dependent cell death follows perception of diverse pathogen elicitors at the host plasma membrane and is suppressed by *Phytophthora infestans* RXLR effector AVR3a.** *New Phytologist* 2011, **190:**653-666.
124. Gilroy EM, Breen S, Whisson SC, Squires J, Hein I, Kaczmarek M, Turnbull D, Boevink PC, Lokossou A, Cano LM, et al: **Presence/absence, differential expression and sequence polymorphisms between PiAVR2 and PiAVR2-like in *Phytophthora infestans* determine virulence on R2 plants.** *New Phytologist* 2011, **191:**763-776.
125. Saunders DGO, Breen S, Win J, Schornack S, Hein I, Bozkurt TO, Champouret N, Vleeshouwers VGAA, Birch PRJ, Gilroy EM, Kamoun S: **Host protein BSL1 associates**

with *Phytophthora infestans* RXLR effector AVR2 and the *Solanum demissum* immune receptor R2 to mediate disease resistance. *Plant Cell* 2012, **24:**3420-3434.

126. McLellan H, Boevink PC, Armstrong MR, Pritchard L, Gomez S, Morales J, Whisson SC, Beynon JL, Birch PRJ: **An RxLR Effector from *Phytophthora infestans* prevents re-localisation of two plant NAC transcription factors from the endoplasmic reticulum to the nucleus.** *PLoS Pathogens* 2013, **9:**e1003670.
127. Dong S, Yin W, Kong G, Yang X, Qutob D, Chen Q, Kale SD, Sui Y, Zhang Z, Dou D, et al: ***Phytophthora sojae* avirulence effector Avr3b is a secreted NADH and ADP-ribose pyrophosphorylase that modulates plant immunity.** *PLoS Pathogens* 2011, **7:**e1002353.
128. Wang Q, Han C, Ferreira AO, Yu X, Ye W, Tripathy S, Kale SD, Gu B, Sheng Y, Sui Y, et al: **Transcriptional programming and functional interactions within the *Phytophthora sojae* RXLR effector repertoire.** *Plant Cell* 2011, **23:**2064-2086.
129. Caillaud M-C, Piquerez SJM, Fabro G, Steinbrenner J, Ishaque N, Beynon J, Jones JDG: **Subcellular localization of the Hpa RxLR effector repertoire identifies a tonoplast-associated protein HaRxL17 that confers enhanced plant susceptibility.** *The Plant Journal* 2012, **69:**252-265.
130. Malone J, Oliver B: **Microarrays, deep sequencing and the true measure of the transcriptome.** *BMC Biology* 2011, **9:**34.
131. Marioni J, Mason C, Mane S, Stephens M, Gilad Y: **RNA-seq: an assessment of technical reproducibility and comparison with gene expression arrays.** *Genome Research* 2008, **18:**1509 - 1517.
132. Birch PRJ, Avrova AO, Armstrong M, Venter E, Taleb N, Gilroy EM, Phillips MS, Whisson SC: **The potato – *Phytophthora infestans* interaction transcriptome.** *Canadian Journal of Plant Pathology* 2003, **25:**226-231.
133. Consortium TTG: **The tomato genome sequence provides insights into fleshy fruit evolution.** *Nature* 2012, **485:**635-641.
134. Consortium TPGS: **Genome sequence and analysis of the tuber crop potato.** *Nature* 2011, **475:**189-195.
135. Bengtsson T, Weighill D, Proux-Wera E, Levander F, Resjo S, Burra D, Moushib L, Hedley P, Liljeroth E, Jacobson D, et al: **Proteomics and transcriptomics of the BABA-induced resistance response in potato using a novel functional annotation approach.** *BMC Genomics* 2014, **15:**315.
136. Zhou L, Mideros S, Bao L, Hanlon R, Arredondo F, Tripathy S, Krampis K, Jerauld A, Evans C, St Martin S, et al: **Infection and genotype remodel the entire soybean transcriptome.** *BMC Genomics* 2009, **10:**49.
137. Moy P, Qutob D, Chapman BP, Atkinson I, Gijzen M: **Patterns of gene expression upon infection of soybean plants by *Phytophthora sojae*.** *Molecular Plant-Microbe Interactions* 2004, **17:**1051-1062.

138. Kim KH, Kang YJ, Kim DH, Yoon MY, Moon J-K, Kim MY, Van K, Lee S-H: **RNA-Seq analysis of a soybean near-isogenic line carrying bacterial leaf pustule-resistant and -susceptible alleles.** *DNA Research* 2011, **18:**483-497.
139. Lin F, Zhao M, Baumann D, Ping J, Sun L, Liu Y, Zhang B, Tang Z, Hughes E, Doerge R, et al: **Molecular response to the pathogen *Phytophthora sojae* among ten soybean near isogenic lines revealed by comparative transcriptomics.** *BMC Genomics* 2014, **15:**18.
140. Coppola V, Coppola M, Rocco M, Digilio M, D'Ambrosio C, Renzone G, Martinelli R, Scaloni A, Pennacchio F, Rao R, Corrado G: **Transcriptomic and proteomic analysis of a compatible tomato-aphid interaction reveals a predominant salicylic acid-dependent plant response.** *BMC Genomics* 2013, **14:**515.
141. Gusberti M, Gessler C, Broggini GAL: **RNA-Seq analysis reveals candidate genes for ontogenic resistance in *Malus*-*Venturia* pathosystem.** *PLoS ONE* 2013, **8:**e78457.
142. Grünwald NJ, Goss EM, Press CM: ***Phytophthora ramorum*: a pathogen with a remarkably wide host range causing sudden oak death on oaks and ramorum blight on woody ornamentals.** *Molecular Plant Pathology* 2008, **9:**729-740.
143. Birch PRJ, Whisson SC: ***Phytophthora infestans* enters the genomics era.** *Molecular Plant Pathology* 2001, **2:**257-263.
144. Tyler BM: ***Phytophthora sojae*: root rot pathogen of soybean and model oomycete.** *Molecular Plant Pathology* 2007, **8:**1-8.
146. Huitema E, Smoker M, Kamoun S: **A straightforward protocol for electro-transformation of *Phytophthora capsici* zoospores.** In *Plant Immunity. Volume* 712. Edited by McDowell JM: Humana Press; 2011: 129-135: *Methods in Molecular Biology*.
147. Avrova AO, Venter E, Birch PR, Whisson SC: **Profiling and quantifying differential gene transcription in *Phytophthora infestans* prior to and during the early stages of potato infection.** *Fungal Genetics and Biology* 2003, **40:**4-14.
148. Grenville-Briggs LJ, Anderson VL, Fugelstad J, Avrova AO, Bouzenzana J, Williams A, Wawra S, Whisson SC, Birch PR, Bulone V, van West P: **Cellulose synthesis in *Phytophthora infestans* is required for normal appressorium formation and successful infection of potato.** *Plant Cell* 2008, **20:**720-738.
149. Altschul SF, Gish W, W. M, E.W. M, D.J. L: **Basic local alignment search tool.** *Journal of Molecular Biology* 1990, **215:**403-410.
150. Thompson JD, Higgins DG, Gibson TJ: **Improved sensitivity of profile searches through the use of sequence weights and gap excision.** *Computer applications in the biosciences : CABIOS* 1994, **10:**19-29.
151. Bhattacharjee S, Hiller NL, Liolios K, Win J, Kanneganti TD, Young C, Kamoun S, Haldar K: **The malarial host-targeting signal is conserved in the Irish potato famine pathogen.** *PLoS Pathogens* 2006, **2:**e50.

152. Avrova AO, Boevink PC, Young V, Grenville-Briggs LJ, van West P, Birch PR, Whisson SC: **A novel *Phytophthora infestans* haustorium-specific membrane protein is required for infection of potato.** *Cellular Microbiology* 2008, **10:**2271-2284.
153. Ah-Fong AMV, Xiang Q, Judelson HS: **Architecture of the sporulation-specific Cdc14 promoter from the oomycete *Phytophthora infestans*.** *Eukaryotic Cell* 2007, **6:**2222-2230.
154. Ah Fong AM, Judelson HS: **Cell cycle regulator Cdc14 is expressed during sporulation but not hyphal growth in the fungus-like oomycete *Phytophthora infestans*.** *Molecular Microbiology* 2003, **50:**487-494.
155. Kelley BS, Lee S-J, Damasceno CMB, Chakravarthy S, Kim B-D, Martin GB, Rose JKC: **A secreted effector protein (SNE1) from *Phytophthora infestans* is a broadly acting suppressor of programmed cell death.** *The Plant Journal* 2010, **62:**357-366.
156. Sharon A, Shlezinger N: **Fungi infecting plants and animals: Killers, non-killers, and cell death.** *PLoS Pathogens* 2013, **9:**e1003517.
157. Heath MC: **Signalling between pathogenic rust fungi and resistant or susceptible host plants.** *Annals of Botany* 1997, **80:**713-720.
158. Voegele RT, Mendgen K: **Rust haustoria: nutrient uptake and beyond.** *New Phytologist* 2003, **159:**93-100.
159. Allen R, Bittner-Eddy P, Grenville-Briggs L, Meitz J, Rehmany A, Rose L, Beynon J: **Host-parasite coevolutionary conflict between Arabidopsis and downy mildew.** *Science* 2004, **306:**1957 - 1960.
160. Lu Y-J, Schornack S, Spallek T, Geldner N, Chory J, Schellmann S, Schumacher K, Kamoun S, Robatzek S: **Patterns of plant subcellular responses to successful oomycete infections reveal differences in host cell reprogramming and endocytic trafficking.** *Cellular Microbiology* 2012, **14:**682-697.
161. Baka ZAM: **Occurrence and ultrastructure of *Albugo candida* on a new host, *Arabis alpina* in Saudi Arabia.** *Micron* 2008, **39:**1138-1144.
162. Dyrløv Bendtsen J, Nielsen H, von Heijne G, Brunak S: **Improved prediction of signal peptides: SignalP 3.0.** *Journal of Molecular Biology* 2004, **340:**783-795.
163. Krogh A, Larsson Br, von Heijne G, Sonnhammer ELL: **Predicting transmembrane protein topology with a hidden markov model: application to complete genomes.** *Journal of Molecular Biology* 2001, **305:**567-580.
164. Du Z, Zhou X, Ling Y, Zhang Z, Su Z: **agriGO: a GO analysis toolkit for the agricultural community.** *Nucleic Acids Research* 2010, **38:**W64-W70.
165. **VENNY. An interactive tool for comparing lists with Venn Diagrams:** [http://bioinfogp.cnb.csic.es/tools/venny/index.html]
166. Randall TA, Dwyer RA, Huitema E, Beyer K, Cvitanich C, Kelkar H, Ah Fong AMV, Gates K, Roberts S, Yatzkan E, et al: **Large-scale gene discovery in the oomycete *Phytophthora infestans* reveals likely components of phytopathogenicity shared with true fungi.** *Molecular Plant-Microbe Interactions* 2005, **18:**229-243.

168. Yamaguchi Y, Pearce G, Ryan CA: **The cell surface leucine-rich repeat receptor for AtPep1, an endogenous peptide elicitor in Arabidopsis, is functional in transgenic tobacco cells.** *Proceedings of the National Academy of Sciences* 2006, **103:**10104-10109.

169. Moy P, Qutob D, Chapman BP, Atkinson I, Gijzen M: **Patterns of gene expression upon infection of soybean plants by *Phytophthora sojae*.** *Molecular Plant-Microbe Interactions* 2004, **17:**1051-1062.

170. Qutob D, Kemmerling B, Brunner F, Kufner I, Engelhardt S, Gust AA, Luberacki B, Seitz HU, Stahl D, Rauhut T, et al: **Phytotoxicity and innate immune responses induced by NEP1-like proteins.** *Plant Cell* 2006, **18:**3721-3744.

171. Grenville-Briggs LJ, Avrova AO, Bruce CR, Williams A, Whisson SC, Birch PR, van West P: **Elevated amino acid biosynthesis in *Phytophthora infestans* during appressorium formation and potato infection.** *Fungal Genetics and Biology* 2005, **42:**244-256.

172. Schlink K: **Down-regulation of defense genes and resource allocation into infected roots as factors for compatibility between *Fagus sylvatica* and *Phytophthora citricola*.** *Functional and Integrative Genomics* 2010, **10**(2):253-64.

173. Lopez-Gomez M, Sandal N, Stougaard J, Boller T: **Interplay of flg22-induced defence responses and nodulation in *Lotus japonicus*.** *Journal of Experimental Botany* 2012, **63:**393-401.

174. Mattoo S, Lee YM, Dixon JE: **Interactions of bacterial effector proteins with host proteins.** *Current Opinion in Immunology* 2007, **19:**392-401.

175. Salmond GPC, Reeves PJ: **Membrance traffic wardens and protein secretion in Gram-negative bacteria.** *Trends in Biochemical Sciences* 1993, **18:**7-12.

176. Dou D, Kale SD, Wang X, Jiang RH, Bruce NA, Arredondo FD, Zhang X, Tyler BM: **RXLR-mediated entry of *Phytophthora sojae* effector Avr1b into soybean cells does not require pathogen-encoded machinery.** *Plant Cell* 2008.

177. Fabro G, Steinbrenner J, Coates M, Ishaque N, Baxter L, Studholme DJ, Kvðrner E, Allen RL, Piquerez SJM, Rougon-Cardoso A, et al: **Multiple candidate effectors from the oomycete pathogen *Hyaloperonospora arabidopsidis* suppress host plant immunity.** *PLoS Pathogens* 2011, **7**.

178. Mukhtar MS, Carvunis A-R, Dreze M, Epple P, Steinbrenner J, Moore J, Tasan M, Galli M, Hao T, Nishimura MT, et al: **Independently evolved virulence effectors converge onto hubs in a plant immune system network.** *Science* 2011, **333:**596-601.

179. Bouwmeester K, de Sain M, Weide R, Gouget A, Klamer S, Canut H, Govers F: **The lectin receptor kinase LecRK-I.9 is a novel *Phytophthora* resistance component and a potential host target for a RXLR effector.** *PLoS Pathogens* 2011, **7:**e1001327.

180. Anderson RG, Casady MS, Fee RA, Vaughan MM, Deb D, Fedkenheuer K, Huffaker A, Schmelz EA, Tyler BM, McDowell JM: **Homologous RXLR effectors from *Hyaloperonospora arabidopsidis* and *Phytophthora sojae* suppress immunity in distantly related plants.** *The Plant Journal* 2012, **72:**882-893.

181. Cooke DE, Drenth A, Duncan JM, Wagels G, Brasier CM: **A molecular phylogeny of *Phytophthora* and related oomycetes.** *Fungal Genetics and Biology* 2000, **30:**17-32.
182. Singh AK, Sharma V, Pal AK, Acharya V, Ahuja PS: **Genome-wide organization and expression profiling of the NAC transcription factor family in potato (*Solanum tuberosum* L.).** *DNA Research* 2013, **20:**403-423.
183. Olsen AN, Ernst HA, Leggio LL, Skriver K: **NAC transcription factors: structurally distinct, functionally diverse.** *Trends in Plant Science* 2005, **10:**79-87.
184. Clamp M, Cuff J, Searle S, Barton G: **The Jalview Java alignment editor.** *Bioinformatics* 2004, **20:**426 - 427.
185. Karimi M, InzÈ D, Depicker A: **GATEWAY(TM) vectors for *Agrobacterium*-mediated plant transformation.** *Trends in Plant Science* 2002, **7:**193-195.
186. Sambrook J, and Russell, D.W: **Molecular Cloning: A Laboratory Manual.** *Cold spring harbor laboratory press New York* 2001.
187. Huitema E, Bos JIB, Tian M, Win J, Waugh ME, Kamoun S: **Linking sequence to phenotype in *Phytophthora* -plant interactions.** *Trends in Microbiology* 2004, **12:**193-200.
188. Fang G, Bhardwaj N, Robilotto R, Gerstein MB: **Getting started in gene orthology and functional analysis.** *PLoS Computational Biology* 2010, **6:**e1000703.
189. Fitch WM: **Distinguishing homologous from analogous proteins.** *Systematic Zoology* 1970, **19:**99-113.
190. Sjölander K, Datta RS, Shen Y, Shoffner GM: **Ortholog identification in the presence of domain architecture rearrangement.** *Briefings in Bioinformatics* 2011, **12:**413-422.
191. Hoppe T, Matuschewski K, Rape M, Schlenker S, Ulrich HD, Jentsch S: **Activation of a membrane-bound transcription factor by regulated ubiquitin/proteasome-dependent processing.** *Cell* 2000, **102:**577-586.
192. Kim Y-S, Kim S-G, Park J-E, Park H-Y, Lim M-H, Chua N-H, Park C-M: **A membrane-bound NAC transcription factor regulates cell division in Arabidopsis.** *Plant Cell* 2006, **18:**3132-3144.
193. Seo PJ, Kim S-G, Park C-M: **Membrane-bound transcription factors in plants.** *Trends in Plant Science* 2008, **13:**550-556.
194. Bhat R, Lahaye T, Panstruga R: **The visible touch: *in planta* visualization of protein-protein interactions by fluorophore-based methods.** *Plant Methods* 2006, **2:**12.
195. Shyu Y, Liu H, Deng X, Hu C: **Identification of new fluorescent protein fragments for bimolecular fluorescence complementation analysis under physiological conditions.** *Biotechniques* 2006, **40:**61 - 66.
196. Walter M, Chaban C, Schutze K, Batistic O, Weckermann K, Nake C, Blazevic D, Grefen C, Schumacher K, Oecking C, et al: **Visualization of protein interactions in living plant cells using bimolecular fluorescence complementation.** *Plant Journal* 2004, **40:**428 - 438.

197. Bracha-Drori K, Shichrur K, Katz A, Oliva M, Angelovici R, Yalovsky S, Ohad N: **Detection of protein-protein interactions in plants using bimolecular fluorescence complementation.** *Plant Journal* 2004, **40:**419 - 427.
198. Jares-Erijman E, Jovin T: **FRET imaging.** *Nat Biotechnol* 2003, **21:**1387 - 1795.
199. Chapman S, Oparka K, Roberts A: **New tools for in vivo fluorescence tagging.** *Current Opinion in Plant Biology* 2005, **8:**565 - 573.
200. Oh SK, Young C, Lee M, Oliva R, Bozkurt TO, Cano LM, Win J, Bos JI, Liu HY, van Damme M, et al: ***In planta* expression screens of *Phytophthora infestans* RXLR effectors reveal diverse phenotypes, including activation of the *Solanum bulbocastanum* disease resistance protein Rpi-blb2.** *Plant Cell* 2009, **21:**2928-2947.
201. Chen X-R, Xing Y-P, Li Y-P, Tong Y-H, Xu J-Y: **RNA-Seq reveals infection-related gene expression changes in *Phytophthora capsici*.** *PLoS ONE* 2013, **8:**e74588.

8. Appendix

Appendix 1

This is the protocol used at Genome Technology (The James Hutton Institute, UK,) for RNA labeling and microarray hybridisation; changed and shortened by Jenny Morris and Pete Hedley from the original Agilent Technologies Protocol 'Two-Color Microarray-Based Gene Expression Analysis'

Two Colour Low Input Quick Amp Labelling Kit

Step 1: Prepare Spike A Mix and Spike B Mix

1. Equilibrate water bath to 37°C.
2. Mix the stock solution vigorously on a vortex mixer.
3. Heat at 37°C for 5 minutes, and mix on a vortex mixer again.
4. Briefly centrifuge to drive contents to the bottom of the tube prior to opening.

Table 1: Dilutions of One Colour Spike Mix for Cy3 labelling

Starting amount of total RNA (ng)	Serial dilution using Agilent dilution Buffer				Spike Mix volume to use (µL)
	First	Second	Third	Fourth	
25	1:20	1:40	1:16	1:8	2
50	1:20	1:40	1:16	1:4	2
100	1:20	1:40	1:16	1:2	2
200	1:20	1:40	1:16	-	2

Storage of Spike-Mix dilutions
Store the Agilent RNA Spike-In Kit, One-Color at –70°C to –80°C in a non-defrosting freezer for up to 1 year from the date of receipt. The first dilution of the Agilent Spike Mix positive controls can be stored up to 2 months in a non-defrosting freezer at –70°C to –80°C and freeze/thawed up to eight times. After use, discard the second, third and fourth dilution tubes.

Step 2: Prepare labelling reaction

Equilibrate water baths to 65°C, 80^{o}C and 40^{o}C.

1. Add 25 to 200ng RNA to a 1.5-mL microcentrifuge tube; in a volume of 1.5 µL. Samples can be diluted to a concentration of 67ng/µl, therefore 1.5µL of sample contains 100ng RNA sample.
2. Prepare Spike-In/water/ T7 Promoter Primer mix as listed in Table 2:

Table 2: Spike-In/Water/T7 Promoter Primer mix

Component	Volume (µl) per rxn **1x**	Volume for 4 rxn **5x**	Volume for 8 rxns **10x**	Volume for 12 rxns **14x**	Volume for 16 rxns **18x**
Spike-In dilution	2	10	20	28	36
T7 Promoter Primer (green cap)	0.8	4	8	11.2	14.4
Nuclease-free water (white cap)	1	5	10	14	18
Total Volume	3.8	19	38	53.2	68.4

3. Add 3.8µL of T7 Promoter Primer/water mix to each tube, each tube now contains a volume of 5.3µl.

4. Denature the primer and the template by incubating the reaction at 65°C in a circulating water bath for 10 minutes.

5. Place the reactions on ice and incubate for 5 minutes.

6. Immediately prior to use, gently mix the components listed in Table 3 for the cDNA Master Mix by adding in the order indicated, and put on ice.
Pre-warm the 5X first strand buffer at 80°C for 3 to 4 minutes to ensure adequate resuspension of the components, vortex and spin the tube briefly. Keep at room temperature until needed.
AffinityScript RNase block mix is a blend of enzymes, which needs to be kept on ice and added to the cDNA Master Mix just before starting the reactions.
Be sure to use the 10 mM dNTP mix tube from the kit.

Table 3: cDNA Master Mix

Component	Volume per rxn (µl)	Volume for 4 rxn **5x**	Volume for 8 rxns **10x**	Volume for 12 rxns **14x**	Volume for 16 rxns **18x**
5x First Strand Buffer	2	10	20	28	36
0.1M DTT	1	5	10	14	18
10mM dNTP mix	0.5	2.5	5	7	9
AffinityScript RNase block	1.2	6.0	12	16.8	21.6

7. Briefly spin each sample tube. Return the tubes to ice.
8. Add 4.7µL of cDNA Master Mix to each sample tube and mix by pipetting up and down, each tube now contains a volume of 10µl.
9. Incubate samples at 40°C in a circulating water bath for 2 hours.
10. Move samples to a 70°C circulating water bath and incubate for 15 minutes.
11. Move samples to ice and incubate for 5 minutes.
12. Spin samples briefly to drive down tube contents from the tube walls and lid.
13. Immediately prior to use, gently mix the components listed in Table 4 in the order indicated for the two Transcription Master Mixes by pipetting at room temperature. N.B. make up 2 mixes, one for Cy3 and one for Cy5.
    The T7 RNA polymerase blend is a blend of enzymes, which needs to be kept on ice and should be added to the Transcription Master Mix just before use.

Table 4: Transcription Master Mix

Component	Volume per rxn (µL)	Volume for 4 rxn **5x**	Volume for 8 rxns **9x**	Volume for 12 rxns **13x**	Volume for 16 rxns **18x**
Nuclease-free water	0.75	8.75	6.75	9.75	13.5
5x Transcription Buffer	3.2	16	28.8	41.6	57.6
0.1M DTT	0.6	3	5.4	7.8	10.8
NTP mix	1	5	9	13	18
T7 RNA Polymerase	0.21	1.05	1.89	2.73	3.78
Cy-dye 3 or 5	0.24	1.2	2.16	3.12	4.32

14. Add 6µL of Transcription Master Mix to each sample tube. Gently mix by pipetting.
15. Incubate samples in a circulating water bath at 40°C for 2 hours.

Step 3: Purify the labeled/amplified RNA

Qiagen's RNeasy mini spin columns are recommended for purification of the amplified cRNA samples.

16. Add 84µL of nuclease-free water to your cRNA sample, for a total volume of 100µL.
17. Add 350µL of Buffer RLT and mix well by pipetting.
18. Add 250µL of ethanol (96% to 100% purity) and mix thoroughly by pipetting. Do *not* centrifuge.
19. Transfer the 700µL of the cRNA sample to an RNeasy mini column in a 2mL collection tube. Centrifuge the sample at 4°C for 30 seconds at 13,000rpm. Discard the flow-through and collection tube.

20. Transfer the RNeasy column to a new collection tube and add 500µL of buffer RPE (containing ethanol) to the column. Centrifuge the sample at 4°C for 30 seconds at 13,000rpm. Discard the flow-through. Re-use the collection tube.

21. Add another 500µL of buffer RPE to the column. Centrifuge the sample at 4°C for 60 seconds at 13,000rpm. Discard the flow-through and the collection tube.

22. If any buffer RPE remains on or near the frit of the column, transfer the RNeasy column to a new 1.5mL collection tube and centrifuge the sample at 4°C for 30 seconds at 13,000rpm to remove any remaining traces of buffer RPE. Discard this collection tube and use a fresh tube to elute the cleaned cRNA sample.

23. Elute the cleaned cRNA sample by transferring the RNeasy column to a new 1.5mL collection tube. Add 30µL RNase-free water directly onto the RNeasy filter membrane. Wait 60 seconds, then centrifuge at 4°C for 30 seconds at 13,000rpm.

24. Maintain the cRNA sample-containing flow-through on ice. Discard the RNeasy column.

<u>CAUTION</u> ***Do not discard the final flow-through*****. It now contains the cRNA sample.**

Step 4: Quantify the cRNA <u>using NanoDrop</u>

25. Start the NanoDrop software.

26. Click the Microarray Measurement tab.

27. Before initializing the instrument as requested by the software, clean the sample loading area with nuclease-free water.

28. Once the instrument has initialized, select RNA-40 as the Sample type (use the drop down menu).

29. Blank the instrument by pipetting 1.5µL of nuclease-free water (this can be the same water used to initialize the instrument) and click Blank.

30. Clean the sample loading area with a laboratory wipe. Pipette 1.5µL of the sample onto the instrument sample loading area and click Measure.

31. Print the results. If printing the results is not possible, record the following values:

1. Cyanine 3 or cyanine 5 dye concentration (pmol/µL)
2. RNA absorbance ratio (260 nm/280 nm)
3. cRNA concentration (ng/µL)

32. Determine the yield and specific activity of each reaction as follows:

a) Use the concentration of cRNA (ng/µL) to determine the µg cRNA yield as follows:

$$\frac{(Concentration\ of\ cRNA)\ \text{x}\ 30\mu\text{L}\ (elution\ volume)}{1000} = \mu\text{g of cRNA}$$

b) Use the concentrations of cRNA (ng/µL) and cyanine 3 or cyanine 5 (pmol/µL) to determine the specific activity as follows:

$$\frac{(Concentration\ of\ Cy3\ or\ Cy5)}{(Concentration\ of\ cRNA)}\ \text{x}\ 1000\ = \text{pmol Cy3or5 per}\ \mu\text{g cRNA}$$

33. Examine the yield and specific activity results, see below for recommended values.

Microarray format	Yield (µg)	Specific activity (pmol Cy3/µg cRNA
1-pack	2.5	6
2-pack	1.875	6
4-pack	0.825	6
8-pack	0.825	6

If the yield and the specific activity are less than the appropriate values do not proceed to the hybridization step. Repeat cRNA preparation.

Step 5: Hybridization

Prepare the 10X Blocking Agent

34. Add nuclease-free water to the vial containing lyophilized 10X Blocking Agent supplied with the Agilent Gene Expression Hybridization Kit, (see specific kit for volume to add : large scale kit is 1.25ml, small scale is 500µl)

35. Mix by gently vortexing. If the pellet does not go into solution completely, heat the mix for 4 to 5 minutes at 37°C.

36. Drive down any material adhering to the tube walls or cap by centrifuging for 5 to 10 seconds.

10X Blocking Agent can be prepared in advance and stored at -20°C for up to 2 months. After thawing, repeat the vortexing and centrifugation procedures before use.

Prepare hybridization samples

37. Equilibrate water bath to 60°C.

38. For each microarray, add each of the components as indicated in table 5 below to a 1.5 mL nuclease-free microfuge tube.

39. Mix well but gently on a vortex mixer.

40. Incubate at 60°C for exactly 30 minutes to fragment RNA.

Table 5: Fragmentation mix

Components	**1-pack**	**2-pack**	**4-pack**	**8-pack**
cyanine 3-labeled cRNA	2.5ug	1.875ug	825ng	300ng
cyanine 5-labeled cRNA	2.5ug	1.875ug	825ng	300ng
10X Blocking Agent	50 µL	25 µL	11 µL	5 µL
Nuclease-free water, to bring volume up to	240 µL	120 µL	52.8 µL	24 µL
25X Fragmentation Buffer	10 µL	5 µL	2.2 µL	1 µL
Total Volume	250 µL	125 µL	55 µL	25 µL

41. Add 2x GEx Hybridization Buffer HI-RPM at the appropriate volume, see Table 6 below, to stop the fragmentation reaction.

Table 6: Hybridization mix

Components	**Volumes per hybridization**			
	1-pack	**2-pack**	**4-pack**	**8-pack**
cRNA from Fragmentation Mix	250 µL	125 µL	55 µL	25 µL
2x GEx Hybridization Buffer HI-RPM	250 µL	125 µL	55 µL	25 µL

42. Mix well by careful pipetting. Take care to avoid introducing bubbles. Do NOT mix on a vortex mixer.

43. Spin for 1 minute at room temperature at 13,000 rpm in a microcentrifuge to drive the sample off the walls and lid and to aid in bubble reduction.

44. Place sample on ice and load onto the array as soon as possible.

Prepare the hybridization assembly

45. Load a clean gasket slide into the Agilent SureHyb chamber base with the label facing up and aligned with the rectangular section of the chamber base. Ensure that the gasket slide is sitting flush with the chamber base.

46. Slowly dispense the volume of hybridization sample (see Table 7) onto the gasket well in a "drag and dispense" manner.

47. Slowly place an array "active side" down onto the SureHyb gasket slide, so that the "Agilent"-labeled barcode is facing down and the numeric barcode is facing up. Verify that the sandwich-pair is properly aligned.

Table 7: Hybridization Sample

Components	**Volumes per hybridization**			
Components	**1-pack**	**2-pack**	**4-pack**	**8-pack**
Volume Prepared	500 µL	250 µL	110 µL	50 µL
Hybridization Sample Volume	490 µL	240 µL	100 µL	40 µL

48. Place the SureHyb chamber cover onto the sandwiched slides and slide the clamp assembly onto both pieces.

49. Hand-tighten the clamp onto the chamber.

50. Vertically rotate the assembled chamber to wet the gasket and assess the mobility of the bubbles. If necessary, tap the assembly on a hard surface to move stationary bubbles.

51. Place assembled slide chamber in rotisserie in a hybridization oven set to 65°C. Set your hybridization rotator to rotate at 10 rpm when using 2x GEx Hybridization Buffer HI-RPM.

52. Hybridize at 65°C for 17 hours.

The Gene Expression Wash Buffer 2 needs to be warmed in a 37°C water bath overnight. Make sure that you prepare enough of Wash Buffer 2 the night before you plan to do the microarray wash, see notes below on addition of Triton to buffers before use.

Step 6: Microarray Wash

Add Triton X-102 to Gene Expression wash buffers

This step is optional but highly recommended as the addition of 0.005% Triton X-102 to the Gene Expression wash buffers reduces the possibility of array wash artifacts.
Add the Triton X-102 to *both* Gene Expression wash buffer 1 and 2 when the cubitainer of wash buffer is first opened.
Triton X-102 can be added to smaller volumes of wash buffer as long as the final dilution of the 10% Triton X-102 is 0.005% in the Gene Expression wash buffer solution.

53. Open the cardboard box with the cubitainer of wash buffer and carefully remove the outer and inner caps from the cubitainer.

54. Use a pipette to add 2 mL of the provided 10% Triton X-102 into the wash buffer in the cubitainer.

55. Replace the original inner and outer caps and mix the buffer carefully but thoroughly by inverting the container 5 to 6 times.

56. Carefully remove the outer and inner caps and install the spigot provided with the wash buffer.

57. Prominently label the wash buffer box to indicate that Triton X-102 has been added and indicate the date of addition.

Ensure you prewarm Wash Buffer 2 at 37^{o}C overnight.
Next morning: Wash the microarray slides
Always use clean equipment when carrying out the hybridization and wash steps.

58. Completely fill a dish (#1) with Gene Expression Wash Buffer 1 at room temperature.

59. Fill another dish (#2) with enough Gene Expression Wash Buffer 1 at room temperature to cover a slide rack. Add a magnetic stir bar and place this dish on a magnetic stir plate.

60. Place an empty dish (#3) on the stir plate and add a magnetic stir bar. Do not add the prewarmed (37°C) Gene Expression Wash Buffer 2 until the first wash step has begun.

61. Remove one hybridization chamber from incubator. Check whether bubbles formed during hybridization and if all bubbles are rotating freely.

62. Disassemble each hybridization chamber one at a time.

1. Place the hybridization chamber assembly on a flat surface and loosen the thumbscrew, turning counter clockwise.
2. Slide off the clamp assembly and remove the chamber cover.
3. With gloved fingers, remove the array-gasket sandwich from the chamber base by grabbing the slides from their ends. Keep the microarray slide numeric barcode facing up as you quickly transfer the sandwich to slide-staining dish #1.
4. Without letting go of the slides, submerge the array-gasket sandwich into slide-staining dish #1 containing Gene Expression Wash Buffer 1.

63. With the sandwich completely submerged in Gene Expression Wash Buffer 1, pry the sandwich open from the barcode end only:

1. Slip one of the blunt ends of the forceps between the slides.
2. Gently turn the forceps upwards or downwards to separate the slides.
3. Let the gasket slide drop to the bottom of the staining dish.
4. Remove the microarray slide and place into slide rack in the slide-staining dish #2 containing Gene Expression Wash Buffer 1 at room temperature. Minimize exposure of the slide to air. Touch only the barcode portion of the microarray slide or its edges!

64. Repeat steps step 4 through step 6 for up to seven additional slides in the group. For uniform washing, do up to a maximum of eight disassembly procedures yielding eight microarray slides.

65. When all slides in the group are placed into the slide rack in slide-staining dish #2, stir for 1 minute.

66. During this wash step, remove Gene Expression Wash Buffer 2 from the 37°C water bath and pour into the slide-staining dish #3.

67. Transfer slide rack to slide-staining dish #3 containing Gene Expression Wash Buffer 2 at elevated temperature. Stir for 1 minute.

NOTE The elevated temperature of the second wash step is usually around 31°C due to cooling by the room temperature dish and the rack of arrays.

68. Spin dry each slide for 10 seconds ensuring this is done with the active side facing upwards.

69. Scan slides immediately to minimize the impact of environmental oxidants on signal intensities. If necessary, store slides in a 50ml yellow capped tube wrapped in foil with 200µl 0.1M DTT in the bottom.

Appendix 2

List of genes that are co-regulated with the markers *PcHmp1, PcNpp1* and *PcCdc14*

(extracted from Figure 3.4 B)

PrimaryAccession	ipr Description
Phyca11_8692 (PcHMP1)	
Phyca11_5453	Thioredoxin-like fold
Phyca11_544004	Metallophosphoesterase
Phyca11_19879	
Phyca11_533399	Metallophosphoesterase
Phyca11_504439	
Phyca11_12927	
Phyca11_133687	Pectate lyase, catalytic
Phyca11_132829	
Phyca11_509331	
Phyca11_18679	Ribosomal protein S16
Phyca11_129924	Heat shock protein DnaJ
Phyca11_505845	NmrA-like
Phyca11_550956	Ribosomal protein L11
Phyca11_507156	Necrosis inducing
Phyca11_541134	Heat shock protein 70
Phyca11_557105	
Phyca11_107869	Necrosis inducing
Phyca11_129107	
Phyca11_19251	Proteinase inhibitor I1, Kazal
Phyca11_18443	
Phyca11_16040	Protein of unknown function DUF1754, eukaryotic
Phyca11_576174	Ribosomal protein L7Ae/L30e/S12e/Gadd45
Phyca11_133455	Necrosis inducing
Phyca11_73404	Necrosis inducing
PHYCAscaffold_81_r_177661_176234_4	
Phyca11_108409	Necrosis inducing
Phyca11_105071	
Phyca11_15238	Pectate lyase, catalytic
PHYCAscaffold_51_f_246186_246662_3	
Phyca11_15647	GrpE nucleotide exchange factor
Phyca11_49820	
Phyca11_41509	Ribosomal protein L21
Phyca11_12936	
Phyca11_108012	Pantoate-beta-alanine ligase

Appendix 2 continued

PrimaryAccession	ipr Description
Phyca11_8692 (PcHMP1)	
Phyca11_75839	
Phyca11_4777	Phospholipase D/Transphosphatidylase
Phyca11_17608	Berberine/berberine-like
Phyca11_14279	
Phyca11_120306	Protease inhibitor, Kazal-type
Phyca11_20870	
Phyca11_549549	Ribosomal protein L9
Phyca11_114784	Protein synthesis factor, GTP-binding
Phyca11_571799	AAA ATPase, core
Phyca11_525255	Ribosomal protein L7/L12, C-terminal
Phyca11_100897	Ribosomal protein L17
Phyca11_117300	Biopterin transport-related protein BT1
Phyca11_572091	
Phyca11_14400	Sulphatase
Phyca11_124331	
Phyca11_111706	Porin, eukaryotic type
Phyca11_558787	
Phyca11_112541	60 kDa inner membrane insertion protein
Phyca11_533392	Myb, DNA-binding
Phyca11_115212	Short-chain dehydrogenase/reductase SDR
Phyca11_8098	Ribosomal protein L33
Phyca11_52385	
Phyca11_545078	Glutamyl/glutaminyl-tRNA synthetase, class Ic

PrimaryAccession	ipr Description
Phyca11_11951 (PcNpp1)	
Phyca11_511317	Glycoside hydrolase, family 30
Phyca11_132590	Peptidyl-prolyl cis-trans isomerase, FKBP-type
Phyca11_503352	Diacylglycerol acyltransferase
Phyca11_556109	Peptidase S10, serine carboxypeptidase
Phyca11_512165	
Phyca11_103489	Endonuclease/exonuclease/phosphatase
Phyca11_512163	Cytochrome P450
Phyca11_7454	Peptidyl-prolyl cis-trans isomerase, FKBP-type
Phyca11_545690	Glycoside hydrolase, family 5
Phyca11_14563	
Phyca11_505784	Cytochrome P450
Phyca11_526256	Methyltransferase type 12

Appendix 2 continued

PrimaryAccession	ipr Description
Phyca11_11951 (PcNpp1)	
Phyca11_511318	Glycoside hydrolase, family 30
Phyca11_112865	Glyoxalase/extradiol ring-cleavage dioxygenase
Phyca11_12067	Amidohydrolase 3
PHYCAscaffold_42_r_280110_279883_6	
Phyca11_509055	Gelsolin
Phyca11_532745	
Phyca11_576909	Zinc finger, FYVE/PHD-type
Phyca11_559868	Protein kinase, core
Phyca11_503988	ATPase, V1/A1 complex, subunit E
Phyca11_508469	Flavodoxin/nitric oxide synthase
Phyca11_16644	
Phyca11_509841	C2 calcium-dependent membrane targeting
Phyca11_20969	Alcohol dehydrogenase, zinc-binding
Phyca11_532508	Peptidase S9, prolyl oligopeptidase active site region
Phyca11_120574	Acyl-CoA N-acyltransferase
Phyca11_505789	
Phyca11_13677	Endoribonuclease L-PSP
Phyca11_102996	
Phyca11_6911	Major intrinsic protein
Phyca11_8846	Cyclin-related 2
Phyca11_554050	Gtr1/RagA G protein
Phyca11_8261	
Phyca11_105598	
Phyca11_47441	Rhodanese-like
Phyca11_506742	Crotonase, core
Phyca11_510800	Pleckstrin-like
Phyca11_504715	Multi antimicrobial extrusion protein MatE
Phyca11_131139	FAD dependent oxidoreductase
Phyca11_543332	ABC transporter-like
Phyca11_109739	
Phyca11_124112	
Phyca11_502708	Glutathione S-transferase, C-terminal
Phyca11_15296	
Phyca11_509434	DNA/RNA helicase, DEAD/DEAH box type, N-terminal
Phyca11_9189	
Phyca11_553603	GAF
Phyca11_539519	
PHYCAscaffold_96_f_100470_100751_3	

Appendix 2 continued

PrimaryAccession	ipr Description
Phyca11_11951 (PcNpp1)	
Phyca11_531982	Ubiquitin-activating enzyme, E1
Phyca11_54493	
Phyca11_555004	Ankyrin
Phyca11_507113	ThiamineS
Phyca11_74521	Peptidase M13, neprilysin
Phyca11_57550	Zinc finger, FYVE-type
Phyca11_97709	Glycoside hydrolase, family 3, N-terminal
Phyca11_554070	HEAT
Phyca11_544638	Alpha/beta hydrolase
Phyca11_511213	
Phyca11_505813	
PHYCAscaffold_50_r_103594_102917_6	
Phyca11_563877	ATPase, P-type, K/Mg/Cd/Cu/Zn/Na/Ca/Na/H-transporter
Phyca11_511910	
Phyca11_542166	WD40 repeat
Phyca11_119734	Ankyrin
Phyca11_511032	Peptidase C1A, papain C-terminal
Phyca11_558277	ATPase, P-type, K/Mg/Cd/Cu/Zn/Na/Ca/Na/H-transporter
Phyca11_114678	ATPase, V0 complex, proteolipid subunit C,
Phyca11_553798	Deoxyribonuclease II
Phyca11_547546	
Phyca11_576852	Tetratricopeptide TPR-1
Phyca11_536824	Ribonuclease H
Phyca11_129892	Necrosis inducing
Phyca11_542594	Glycoside hydrolase, family 3, N-terminal
Phyca11_503609	
Phyca11_506531	ATPase, F1/V1/A1 complex, alpha/beta subunit, nucleotide-binding
Phyca11_532835	Delayed-early response protein/equilibrative nucleoside transporter
Phyca11_543076	Xylose isomerase-type TIM barrel
Phyca11_533965	Stem cell self-renewal protein Piwi
Phyca11_559433	Palmitoyl protein thioesterase
Phyca11_503949	20S proteasome, A and B subunits
Phyca11_504195	
Phyca11_503420	Heat shock factor (HSF)-type, DNA-binding

Appendix 2 continued

PrimaryAccession	ipr Description
Phyca11_11951 (PcNpp1)	
Phyca11_547310	Cytochrome P450
Phyca11_548258	
Phyca11_505507	Annexin
Phyca11_526786	
Phyca11_534067	TMS membrane protein/tumour differentially expressed protein
Phyca11_556590	
Phyca11_503881	Ricin B lectin
Phyca11_527410	Major facilitator superfamily MFS-1
Phyca11_505786	Cytochrome P450
Phyca11_111267	FMN-binding split barrel, related
Phyca11_122048	Necrosis inducing
Phyca11_511823	
Phyca11_8758	Isopenicillin N synthase
Phyca11_536100	Initiation factor 2B related
Phyca11_19861	Phox-like
Phyca11_525078	DSS1/SEM1
Phyca11_505505	Annexin
Phyca11_4421	Protein kinase, core
Phyca11_21924	
Phyca11_551684	Zinc finger, RING-type
Phyca11_109567	
Phyca11_538673	
Phyca11_132404	Proteasome maturation factor UMP1
Phyca11_17248	
Phyca11_96835	Proteasome component region PCI
Phyca11_554372	Protein of unknown function DUF580
Phyca11_506337	Stem cell self-renewal protein Piwi
Phyca11_506552	Glucose/ribitol dehydrogenase
Phyca11_525194	
Phyca11_115678	Haloacid dehalogenase-like hydrolase
Phyca11_510020	
Phyca11_574927	20S proteasome, A and B subunits
Phyca11_502609	Electron transfer flavoprotein, alpha subunit, C-terminal
Phyca11_503575	Thioredoxin-related
Phyca11_506536	Aldose 1-epimerase
Phyca11_511621	
Phyca11_108362	Alpha/beta hydrolase
Phyca11_98455	Triosephosphate isomerase
Phyca11_506292	COPI associated
Phyca11_504262	AAA ATPase, core
Phyca11_534296	

Appendix 2 continued

PrimaryAccession	ipr Description
Phyca11_11951 (PcNpp1)	
Phyca11_530385	Crotonase, core
Phyca11_103656	Endonuclease/exonuclease/phosphatase
Phyca11_114788	Peptidase C69, dipeptidase A
Phyca11_534359	
Phyca11_537997	NAD-dependent epimerase/dehydratase
Phyca11_505794	20S proteasome, A and B subunits
Phyca11_534969	
Phyca11_507765	RNA recognition motif, RNP-1
Phyca11_99727	
Phyca11_104510	Ankyrin
Phyca11_503586	Aldo/keto reductase
Phyca11_16336	Glycoside hydrolase, family 1
Phyca11_538005	Short-chain dehydrogenase/reductase SDR
Phyca11_16638	
Phyca11_503741	Alcohol dehydrogenase, zinc-binding
Phyca11_525961	Calcium-binding EF-hand
Phyca11_510153	Peptidase A1
Phyca11_106287	Aldo/keto reductase
Phyca11_505320	
Phyca11_565626	Natural resistance-associated macrophage protein
Phyca11_508065	Calcium-binding EF-hand
Phyca11_21463	Glutathione S-transferase, N-terminal
Phyca11_125034	
Phyca11_538166	Short-chain dehydrogenase/reductase SDR
Phyca11_35423	Ankyrin
Phyca11_547712	Transcription initiation factor IIF, beta subunit
Phyca11_535945	20S proteasome, A and B subunits
Phyca11_509624	Protein kinase, core
Phyca11_510985	Phospholipase D/Transphosphatidylase
Phyca11_122092	Glycolipid anchored surface protein GAS1
Phyca11_545883	Glycoside hydrolase, family 1
Phyca11_504124	B-cell receptor-associated 31-like
Phyca11_123053	Isochorismatase hydrolase
Phyca11_557875	
Phyca11_106667	Ankyrin
Phyca11_14558	
Phyca11_9330	
Phyca11_40265	Peptidase C1A, papain C-terminal

Appendix 2 continued

PrimaryAccession	ipr Description
Phyca11_11951 (PcNpp1)	
Phyca11_508546	
Phyca11_97505	Peptidase T1A, proteasome beta-subunit
Phyca11_529177	Aldehyde dehydrogenase
Phyca11_11043	Glycoside hydrolase, family 3, N-terminal
Phyca11_119208	Zinc finger, DHHC-type
Phyca11_506382	Peptidase T1A, proteasome beta-subunit
Phyca11_39565	MtN3 and saliva related transmembrane protein
Phyca11_528424	Carbohydrate kinase, FGGY
Phyca11_507974	Peptidyl-prolyl cis-trans isomerase, PpiC-type
Phyca11_122315	
Phyca11_511936	Thioredoxin-related
Phyca11_503872	
Phyca11_571712	AAA ATPase, core
Phyca11_36367	Peptidase S28
Phyca11_509547	C2 calcium-dependent membrane targeting
Phyca11_126045	
Phyca11_119587	
Phyca11_97872	20S proteasome, A and B subunits
Phyca11_531311	
Phyca11_5245	Ubiquitin
Phyca11_62759	
Phyca11_576122	Chaperonin clpA/B
Phyca11_507551	Thioredoxin-like
Phyca11_560093	
Phyca11_542145	Isochorismatase hydrolase
Phyca11_8058	Transmembrane transporter protein, chloroquine resistant
Phyca11_572658	Glycoside hydrolase, family 35
Phyca11_109473	Monooxygenase, FAD-binding
Phyca11_568685	Calcium-binding EF-hand
Phyca11_505478	
Phyca11_572181 (572181)	
Phyca11_124496	SET
Phyca11_511117	Peptidyl-prolyl cis-trans isomerase, cyclophilin-type
Phyca11_508386	Rab GTPase activator
Phyca11_511049	
Phyca11_508725	20S proteasome, A and B subunits
Phyca11_504107	Heat shock factor binding 1

Appendix 2 continued

PrimaryAccession	ipr Description
Phyca11_11951 (PcNpp1)	
Phyca11_4600	
Phyca11_508525	
Phyca11_548563	Short-chain dehydrogenase/reductase SDR
Phyca11_525408	Macrophage migration inhibitory factor
Phyca11_527642	Peptidase C1A, papain C-terminal
Phyca11_570162	Choloylglycine hydrolase
Phyca11_559451	Complex 1 LYR protein
Phyca11_547802	Mitochondrial substrate carrier
Phyca11_506766	Urease accessory protein UreF

PrimaryAccession	ipr Description
Phyca11_510939 (CDC14)	
Phyca11_104572	NLI interacting factor
Phyca11_121487	Glutathione S-transferase, C-terminal-like
Phyca11_511517	Protein kinase, core
scaffold_76_161[134756-133872](...	
Phyca11_526800	Globin, subset
Phyca11_510468	
Phyca11_21966	
Phyca11_565932	Sushi/SCR/CCP
Phyca11_550086	Phosphatidylinositol 3- and 4-kinase, catalytic
Phyca11_510473	
Phyca11_561647	HAT dimerisation
Phyca11_529420	
Phyca11_571282	Protein kinase, core
Phyca11_546010	
Phyca11_83926	Protein kinase, core
Phyca11_533011	
Phyca11_563801	Oxysterol-binding protein
Phyca11_566963	
Phyca11_123200	
Phyca11_128667	Acyltransferase 3
Phyca11_130508	Glycoside hydrolase, family 6
Phyca11_556162	Pleckstrin-like
Phyca11_508832	
Phyca11_560479	Glycoside hydrolase, family 43
Phyca11_121523	
Phyca11_535657	
Phyca11_110914	Protein of unknown function Cys-rich
Phyca11_511952	

Appendix 2 continued

PrimaryAccession	ipr Description
Phyca11_510939 (CDC14)	
Phyca11_507758	Sporulation stage II, protein E C-terminal
Phyca11_82762	HAT dimerisation
Phyca11_552080	Alternative oxidase
Phyca11_547218	Peptidase A1
Phyca11_538825	Ankyrin
Phyca11_507351	
Phyca11_100187	ARF/SAR superfamily
Phyca11_530950	
Phyca11_527667	Zinc finger, FYVE-type
Phyca11_127743	
Phyca11_540360	Ankyrin
Phyca11_132828	Peptidase C19, ubiquitin carboxyl-terminal hydrolase 2
Phyca11_546149	
Phyca11_38922	Protein kinase, core
Phyca11_509400	
Phyca11_15378	Cytochrome b5
Phyca11_502934	Protein phosphatase 2C, N-terminal
Phyca11_509900	Phosphoglycerate mutase
Phyca11_506953	Pleckstrin-like
Phyca11_49865	Protein of unknown function Cys-rich
Phyca11_511923	Sterol-binding-like
Phyca11_6021	Zinc finger, PHD-type
Phyca11_126570	Sodium:dicarboxylate symporter
Phyca11_7431	
Phyca11_534810	3'5'-cyclic nucleotide phosphodiesterase
Phyca11_553631	Major intrinsic protein
Phyca11_512065	Basic helix-loop-helix dimerisation region bHLH
Phyca11_60814	
Phyca11_543453	Zinc finger, RanBP2-type
Phyca11_504243	Tubby, C-terminal
Phyca11_20425	
Phyca11_543377	Zinc finger, FYVE-type
Phyca11_507705	Syntaxin, N-terminal
Phyca11_102121	Large-conductance mechanosensitive channel
Phyca11_562644	
Phyca11_46603	GAF
Phyca11_6779	
Phyca11_547501	
Phyca11_547509	
Phyca11_509202	

Appendix 2 continued

PrimaryAccession	ipr Description
Phyca11_510939 (CDC14)	
Phyca11_505246	D111/G-patch
Phyca11_101745	
Phyca11_532826	Necrosis inducing protein-1
Phyca11_507961	Beta-glucan synthesis-associated, SKN1
Phyca11_505108	Zinc finger, RING-type
Phyca11_107310	
Phyca11_131335	Adenylate kinase
Phyca11_569436	Pellino
Phyca11_551085	EGF-like region, conserved site
Phyca11_529130	
Phyca11_557932	
Phyca11_549134	Barwin
Phyca11_19038	Protein of unknown function DUF1336
Phyca11_568946	SNF2-related
Phyca11_508708	Vacuolar sorting protein 9
Phyca11_9322	Adenylyl cyclase class-3/4/guanylyl cyclase
Phyca11_557260	Homeodomain-like
Phyca11_561795	
Phyca11_22122	
Phyca11_557406	D111/G-patch
Phyca11_126161	Calcium-binding EF-hand
Phyca11_574719	Protein phosphatase 2C, N-terminal
Phyca11_507970	
Phyca11_550301	Tubby, C-terminal
Phyca11_552503	
Phyca11_511495	Zinc finger, AN1-type
Phyca11_109358	
Phyca11_510546	High mobility group box, HMG1/HMG2, subgroup
Phyca11_560298	Adenylate/cytidine kinase, N-terminal
Phyca11_558677	Clathrin/coatomer adaptor, adaptin-like, N-terminal
Phyca11_551906	
Phyca11_104501	Phox-like
Phyca11_505238	FAD-dependent pyridine nucleotide-disulphide oxidoreductase
Phyca11_533823	Linker histone, N-terminal
Phyca11_575060	
Phyca11_575616	Protein kinase, core
Phyca11_575575	
Phyca11_507864	Cyclin, N-terminal
Phyca11_510891	Nucleoside phosphorylase

Appendix 2 continued

PrimaryAccession	ipr Description
Phyca11_510939 (CDC14)	
Phyca11_509974	
Phyca11_502908	
Phyca11_107744	SCP-like extracellular
Phyca11_528940	IQ calmodulin-binding region
Phyca11_508111	HECT
Phyca11_560550	
Phyca11_506416	Myosin head, motor region
Phyca11_502811	Phox-like
Phyca11_100770	
Phyca11_507215	
Phyca11_549075	Beta-glucan synthesis-associated, SKN1
Phyca11_510339	
Phyca11_506090	Patatin
Phyca11_510331	
Phyca11_509842	
Phyca11_13559	
Phyca11_11936	
Phyca11_502988	
Phyca11_507432	Ribonucleotide reductase
Phyca11_507869	
Phyca11_508607	
Phyca11_12058	Leucine-rich repeat
Phyca11_505054	Glycoside hydrolase, family 18, catalytic domain
Phyca11_564945	
Phyca11_49298	
PHYCAscaffold_21_r_77725_75368_6	
Phyca11_563404	Peptidase S8 and S53, subtilisin, kexin, sedolisin
Phyca11_550394	
Phyca11_559729	Globin, subset
Phyca11_540977	DNA/RNA helicase, DEAD/DEAH box type, N-terminal
Phyca11_11174	Pleckstrin-like
Phyca11_503783	PDZ/DHR/GLGF
Phyca11_113927	Cytochrome b5
Phyca11_506621	Zinc finger, RING-type
Phyca11_541044	Aminoacyl-tRNA synthetase, class I, conserved site
Phyca11_511415	
Phyca11_502789	C2 calcium-dependent membrane targeting
Phyca11_67599	Ankyrin

Appendix 2 continued

PrimaryAccession	ipr Description
Phyca11_510939 (CDC14)	
Phyca11_512196	
Phyca11_541621	ABC transporter-like
Phyca11_505177	
Phyca11_568700	
Phyca11_19826	Protein of unknown function Cys-rich
Phyca11_559221	
Phyca11_503927	
Phyca11_510017	
Phyca11_8313	
Phyca11_101737	
Phyca11_506991	
Phyca11_530915	Zinc finger, RING-type
Phyca11_106456	HECT
Phyca11_538675	Histone H4
Phyca11_527385	Peptidyl-prolyl cis-trans isomerase, cyclophilin-type
Phyca11_120867	
Phyca11_505638	Protein kinase, core
Phyca11_546674	Leucine-rich repeat
Phyca11_6570	Anticodon-binding
Phyca11_552593	
Phyca11_507392	
Phyca11_574577	Tetratricopeptide TPR-1
Phyca11_77654	Phosphatidylinositol-4-phosphate 5-kinase, core
Phyca11_543599	Protein kinase, core
Phyca11_549115	Pleckstrin-like
Phyca11_503717	
Phyca11_550895	Forkhead-associated
Phyca11_20054	Carbonic anhydrase, eukaryotic
Phyca11_17097	
Phyca11_506932	
Phyca11_569903	
Phyca11_559315	Protein kinase, core
Phyca11_118320	Protein kinase, core
Phyca11_559648	Pleckstrin-like
Phyca11_506606	Calponin-like actin-binding
Phyca11_512034	Brf1-like TBP-binding
Phyca11_131407	Protein kinase, core
Phyca11_98579	
Phyca11_511774	Zinc finger, RING-type
Phyca11_119215	FAD-dependent pyridine nucleotide-disulphide oxidoreductase

Appendix 2 continued

PrimaryAccession	ipr Description
Phyca11_510939 (CDC14)	
Phyca11_103439	Protein-tyrosine phosphatase, dual specificity
Phyca11_572967	
Phyca11_560999	
Phyca11_5907	PDZ/DHR/GLGF
Phyca11_556263	Glycoside hydrolase, family 6
Phyca11_506267	Zinc finger, FYVE-related
Phyca11_563377	Ankyrin
Phyca11_505335	
Phyca11_554376	
Phyca11_573358	
Phyca11_562156	Chitin synthase
Phyca11_511537	
Phyca11_569895	Protein kinase, core
Phyca11_510374	Chorismate synthase
Phyca11_537925	Cytidylyltransferase
Phyca11_559357	Zinc finger, FYVE-type
Phyca11_105191	
Phyca11_552594	
Phyca11_16073	
Phyca11_557253	PDZ/DHR/GLGF
Phyca11_527198	
Phyca11_508836	GAF
Phyca11_555410	WD40 repeat
Phyca11_528890	Diacylglycerol kinase accessory region
Phyca11_551410	Elicitin
Phyca11_507290	
Phyca11_506119	
Phyca11_62706	Zinc finger, RING-type
Phyca11_552194	Glycoside hydrolase, family 5
Phyca11_125676	
Phyca11_506438	
Phyca11_536039	Peptidase M12A, astacin
Phyca11_573300	
Phyca11_49730	
Phyca11_13896	Dpy-30
Phyca11_549322	Leucine-rich repeat, cysteine-containing subtype
Phyca11_78124	Phosphatidylinositol 3- and 4-kinase, catalytic
Phyca11_507826	

Appendix 2 continued

PrimaryAccession	ipr Description
Phyca11_510939 (CDC14)	
Phyca11_12204	
Phyca11_559956	N/apple PAN
Phyca11_506274	Protein kinase, core
Phyca11_34475	IQ calmodulin-binding region
Phyca11_16650	Zinc finger, RING-type
Phyca11_531870	Quinolinate synthetase A
Phyca11_102193	Histone H3
Phyca11_511028	Basic leucine zipper
Phyca11_564059	
Phyca11_122580	Protein phosphatase 2C, N-terminal
Phyca11_547356	
Phyca11_529791	
Phyca11_553345	Protein of unknown function Cys-rich
Phyca11_539393	Cyclin, N-terminal
Phyca11_503496	
Phyca11_529917	WD40 repeat
Phyca11_511072	
Phyca11_43312	Zinc finger, FYVE-type
Phyca11_503280	
Phyca11_539227	Protein phosphatase 2C, N-terminal
Phyca11_36386	Amino acid permease-associated region
Phyca11_575673	
Phyca11_11294	Potassium channel, inwardly rectifying, Kir, cytoplasmic
Phyca11_39946	3'5'-cyclic nucleotide phosphodiesterase
Phyca11_121975	Glycoside hydrolase, family 5
Phyca11_121466	Protein kinase, core
Phyca11_507766	Metallophosphoesterase
Phyca11_507979	Rare lipoprotein A
Phyca11_509421	Pleckstrin-like
Phyca11_503061	RNA recognition motif, RNP-1
Phyca11_509677	
Phyca11_564844	Pleckstrin-like
Phyca11_510000	Protein of unknown function Cys-rich
Phyca11_504393	C2 calcium-dependent membrane targeting
Phyca11_506709	EGF-like
Phyca11_505710	PDZ/DHR/GLGF
Phyca11_556645	
Phyca11_131909	Glycoside hydrolase, catalytic core
Phyca11_40311	Ras GTPase
Phyca11_505129	
Phyca11_509423	Pleckstrin-like

Appendix 2 continued

PrimaryAccession	ipr Description
Phyca11_510939 (CDC14)	
Phyca11_506007	
Phyca11_97368	Centromere protein B, helix-turn-helix
Phyca11_503407	N-6 adenine-specific DNA methylase, conserved site
Phyca11_59357	
Phyca11_503824	ABC transporter-like
Phyca11_508920	
Phyca11_570091	SNF2-related
Phyca11_131759	
Phyca11_544701	Guanylate-binding protein, N-terminal
Phyca11_506413	Phox-like
Phyca11_541266	
Phyca11_102279	
Phyca11_504656	Transcription factor jumonji/aspartyl beta-hydroxylase
Phyca11_132609	
Phyca11_511079	Zinc finger, FYVE/PHD-type
Phyca11_81801	
Phyca11_43331	Zinc finger, CCCH-type
Phyca11_119675	Aldehyde dehydrogenase, conserved site
Phyca11_502599	Mitochondrial substrate carrier
Phyca11_121543	
Phyca11_559353	Exonuclease, RNase T and DNA polymerase III
Phyca11_105184	Major facilitator superfamily MFS-1
Phyca11_506911	
Phyca11_4407	
Phyca11_555049	EGF-like, laminin
Phyca11_533234	
Phyca11_11528	
Phyca11_536161	Vacuolar sorting protein 9
Phyca11_67701	Ankyrin
Phyca11_504359	PA26 p53-induced protein (sestrin)
Phyca11_574276	ABC transporter-like
Phyca11_555166	
Phyca11_563280	GTP cyclohydrolase I
Phyca11_575506	Zinc finger, FYVE/PHD-type
Phyca11_104319	Heat shock protein DnaJ, N-terminal
Phyca11_512103	
Phyca11_528202	Pleckstrin-like
Phyca11_530856	Tubulin
Phyca11_532907	NLI interacting factor
Phyca11_20647	

Appendix 2 continued

PrimaryAccession	ipr Description
Phyca11_510939 (CDC14)	
Phyca11_97233	Ribonucleotide reductase
Phyca11_503223	Guanine-nucleotide dissociation stimulator CDC25
Phyca11_100188	Glycoside hydrolase, family 6
Phyca11_108852	
Phyca11_538372	
Phyca11_544268	SCP-like extracellular
Phyca11_83903	Protein kinase, core
Phyca11_559743	Leucine-rich repeat
PHYCAscaffold_214_r_10698_10306_5	
Phyca11_532832	
Phyca11_122184	
Phyca11_510832	Elicitin
Phyca11_507888	
Phyca11_505235	
Phyca11_128036	ABC transporter-like
Phyca11_16761	
Phyca11_559069	
Phyca11_20926	Zinc finger, FYVE/PHD-type
Phyca11_107676	
Phyca11_14953	CS
Phyca11_527730	Zinc finger, GATA-type
Phyca11_569923	Diacylglycerol acyltransferase
Phyca11_528625	IQ calmodulin-binding region
Phyca11_19132	
Phyca11_502779	SCP-like extracellular
Phyca11_131247	
Phyca11_543671	HAT dimerisation
Phyca11_131042	
Phyca11_572889	Peptidase C19, ubiquitin carboxyl-terminal hydrolase 2
Phyca11_49064	Zinc finger, TAZ-type
Phyca11_130615	Sulphatase
Phyca11_70439	Recoverin
Phyca11_73473	
Phyca11_19784	
Phyca11_542159	Prefoldin
Phyca11_536941	Regulation of nuclear pre-mRNA protein
Phyca11_115958	
Phyca11_506791	Phosphatidylinositol-4-phosphate 5-kinase, core
Phyca11_110956	
Phyca11_132036	

Appendix 2 continued

PrimaryAccession	ipr Description
Phyca11_510939 (CDC14)	
Phyca11_533583	GRIP
Phyca11_509497	Glycoside hydrolase, family 5
Phyca11_573399	
Phyca11_558259	
Phyca11_505935	EGF, extracellular
Phyca11_6905	Protein kinase, core
Phyca11_549844	Tubby, C-terminal
Phyca11_527978	Adaptin ear-binding coat-associated protein 1 NECAP-1
Phyca11_506635	Coactivator CBP, KIX
Phyca11_524955	Smr protein/MutS2 C-terminal
Phyca11_103558	
Phyca11_536708	ABC transporter-like
Phyca11_96237	
Phyca11_505396	Protein kinase, core
Phyca11_49291	Protein kinase, core
Phyca11_577389	Protein kinase-like
Phyca11_503330	
Phyca11_508125	Rubisco LSMT substrate-binding
Phyca11_574924	Diacylglycerol kinase, catalytic region
Phyca11_505820	
Phyca11_545922	Protein kinase, core
Phyca11_126858	
Phyca11_531078	Pleckstrin-like
Phyca11_531142	Peptidase A1
Phyca11_4738	AAA+ ATPase, core
Phyca11_78008	Protein kinase, core
Phyca11_572401	Transcription factor jumonji
Phyca11_555525	Zinc finger, FYVE/PHD-type
Phyca11_561644	
Phyca11_511312	Sodium:dicarboxylate symporter
Phyca11_568171	
Phyca11_537727	Clathrin adaptor, alpha/beta/gamma-adaptin, appendage, Ig-like subdomain
Phyca11_17480	ABC transporter-like
Phyca11_532298	Pleckstrin-like
Phyca11_504468	SNARE associated Golgi protein
Phyca11_556638	
Phyca11_526781	Zinc finger, PHD-type
Phyca11_511282	Protein kinase, core
Phyca11_61640	Protein of unknown function Cys-rich
Phyca11_119500	HAT dimerisation
Phyca11_58571	CD9/CD37/CD63 antigen

Appendix 2 continued

PrimaryAccession	ipr Description
Phyca11_510939 (CDC14)	
Phyca11_43310	Zinc finger, FYVE-type
Phyca11_503703	
Phyca11_535053	Potassium channel, inwardly rectifying, Kir, cytoplasmic
Phyca11_505355	Transcription factor, CBFA/NFYB, DNA topoisomerase
Phyca11_509686	
Phyca11_105572	NADH:flavin oxidoreductase/NADH oxidase, N-terminal
Phyca11_505686	Protein kinase, core
Phyca11_37186	Zinc finger, FYVE/PHD-type
Phyca11_505826	
Phyca11_16110	
Phyca11_541289	
Phyca11_558600	
Phyca11_52304	Zinc finger, CHY-type
Phyca11_123449	DNA breaking-rejoining enzyme, catalytic core
Phyca11_505912	
Phyca11_539610	Ankyrin
Phyca11_546105	
Phyca11_35826	Kinesin, motor region
Phyca11_509585	
Phyca11_107112	Integrase, catalytic core
Phyca11_547885	Zinc finger, RING-type
Phyca11_506290	Protein kinase, core
Phyca11_540554	Mitochondrial import inner membrane translocase, subunit Tim17/22
Phyca11_123193	Protein of unknown function Cys-rich
Phyca11_537582	
Phyca11_506907	
Phyca11_547373	Protein kinase, core
Phyca11_505072	
Phyca11_528843	Kinesin, motor region
Phyca11_111720	
Phyca11_569924	
Phyca11_506134	
Phyca11_553501	Myb, DNA-binding
Phyca11_510367	
Phyca11_105943	
Phyca11_119130	
Phyca11_509572	
Phyca11_525407	Longin-like

Appendix 2 continued

PrimaryAccession	ipr Description
Phyca11_510939 (CDC14)	
Phyca11_20197	
Phyca11_119549	Multi antimicrobial extrusion protein MatE
Phyca11_19300	
Phyca11_11491	RIO kinase
Phyca11_125983	Kinesin, motor region
Phyca11_572766	
Phyca11_530562	C2 calcium-dependent membrane targeting
Phyca11_113099	TATA-box binding
Phyca11_112700	MORN motif
Phyca11_546768	Armadillo
Phyca11_560991	Acyltransferase 3
Phyca11_504431	
Phyca11_510199	RNA recognition motif, RNP-1
Phyca11_575859	Tubulin
Phyca11_532077	Basic helix-loop-helix dimerisation region bHLH
Phyca11_533774	Peptidase C19, ubiquitin carboxyl-terminal hydrolase 2
Phyca11_536781	Glycosyl transferase, family 48
Phyca11_550557	Pleckstrin-like
Phyca11_551304	Armadillo-type fold
Phyca11_6903	Di-copper centre-containing
Phyca11_535685	WD40 repeat
Phyca11_39602	MCM
Phyca11_507024	Zinc finger, FYVE/PHD-type
Phyca11_544054	DNA repair nuclease, XPF-type/Helicase
Phyca11_533453	BRCT
Phyca11_510840	
Phyca11_566695	Zinc finger, PHD-type
Phyca11_12070	Pleckstrin-like
Phyca11_509410	Protein kinase, core
Phyca11_507023	Prefoldin
Phyca11_126839	Phosphatidylinositol 3- and 4-kinase, catalytic
Phyca11_528365	
Phyca11_509106	Terpenoid synthase
Phyca11_509108	
Phyca11_80918	GAF
Phyca11_543173	
Phyca11_510654	
Phyca11_548162	Myosin head, motor region

Appendix 2 continued

PrimaryAccession	ipr Description
Phyca11_510939 (CDC14)	
Phyca11_131045	ARF/SAR superfamily
Phyca11_105728	
Phyca11_536099	CENP-B protein
Phyca11_103174	Zinc finger, AN1-type
Phyca11_569112	
Phyca11_510994	WD40 repeat
Phyca11_558907	Protein of unknown function DUF907, fungi
Phyca11_11220	Sodium:dicarboxylate symporter
Phyca11_546185	Zinc finger, CCCH-type
Phyca11_560917	Radical SAM
Phyca11_509590	
Phyca11_511473	
Phyca11_50766	
Phyca11_511023	GPCR, rhodopsin-like
Phyca11_505481	Choline/ethanolamine kinase
Phyca11_19285	Aminotransferase, class V/Cysteine desulphurase
Phyca11_4547	
Phyca11_504787	Ribonucleoside-triphosphate reductase, adenosylcobalamin-dependent
Phyca11_551908	Phosphatidylinositol-4-phosphate 5-kinase, core
Phyca11_15665	
Phyca11_128113	C2 calcium-dependent membrane targeting
Phyca11_530272	
Phyca11_50846	Glycoside hydrolase, family 6
Phyca11_510870	Pleckstrin-like
Phyca11_10826	Dynein heavy chain
Phyca11_554171	
PHYCAscaffold_1_r_2050121_20495...	
Phyca11_507636	
Phyca11_6236	Calcium-binding EF-hand
Phyca11_571595	
Phyca11_5469	
Phyca11_36040	Peptidase S10, serine carboxypeptidase
Phyca11_511275	Tubulin
Phyca11_10542	FAD-dependent pyridine nucleotide-disulphide oxidoreductase
Phyca11_125534	
Phyca11_509773	Tubulin binding cofactor C
Phyca11_508997	bZIP transcription factor, bZIP-1

Appendix 2 continued

PrimaryAccession	ipr Description
Phyca11_510939 (CDC14)	
Phyca11_505827	Protein of unknown function DUF221
Phyca11_536390	
Phyca11_104265	
Phyca11_506220	DNA/RNA helicase, DEAD/DEAH box type, N-terminal
Phyca11_534471	Clathrin adaptor, sigma subunit/coatomer, zeta subunit
Phyca11_505071	Voltage-dependent potassium channel
Phyca11_571095	Lysine exporter protein (LYSE/YGGA)
Phyca11_132286	
Phyca11_561476	
Phyca11_116290	
Phyca11_100811	Target SNARE coiled-coil region
Phyca11_503047	SGS
Phyca11_534123	Pleckstrin-like
Phyca11_11736	Vesicle transport v-SNARE
Phyca11_509120	
Phyca11_113740	
Phyca11_540842	Protein kinase, core
Phyca11_18434	
PHYCAscaffold_55_r_249313_247433_4	
Phyca11_575024	
Phyca11_572387	Zinc finger, PHD-type
PHYCAscaffold_568_r_1948_1547_4	
Phyca11_503318	NAD(P)-binding
Phyca11_509041	
Phyca11_125015	
Phyca11_545044	Rieske [2Fe-2S] region
Phyca11_564159	Peptidase A22B, signal peptide peptidase
Phyca11_548149	DNA/RNA helicase, DEAD/DEAH box type, N-terminal
Phyca11_512206	MCM
Phyca11_527865	Oxidoreductase, N-terminal
Phyca11_506548	MFS general substrate transporter
Phyca11_116405	
Phyca11_121780	Phox-like
Phyca11_12852	
Phyca11_508253	SGS